Pauline Zimmermann

Electrochemical Oxidation of Landfill Leachate on Boron-Doped Diamond Anodes

Master's thesis in Environmental Engineering
Supervisor: Thomas Meyn
May 2019

Master's thesis

NTNU
Norwegian University of Science and Technology
Faculty of Engineering
Department of Civil and Environmental Engineering

NTNU
Norwegian University of
Science and Technology

University of Stuttgart
Germany

NTNU
Norwegian University of Science and Technology
Department of Civil and Environmental Engineering

University of Stuttgart
Germany
Institute for Sanitary Engineering, Water Quality and Solid Waste Management

Master's Thesis

ELECTROCHEMICAL OXIDATION OF LANDFILL LEACHATE ON BORON-DOPED DIAMOND ANODES

Submitted by
Pauline Zimmermann

Trondheim, 31/05/2019

Examiner: Prof. Dr. rer. nat. habil. Jörg Metzger
Supervisor: Assoc. Prof. Thomas Meyn

I hereby certify that I have prepared this thesis independently, and that only those sources, aids, and advisors that are duly noted herein have been used and/or consulted. I further agree that this thesis is made accessible for scientific purposes by the library of the Department of Hydraulic and Environmental Engineering of the Norwegian University of Science and Technology (Publication according to §6 Abs. 1 UrhG). I agree that contents may be cited according to §52 UrhG.

Trondheim, 03/06/2019

Pauline Zimmermann

Abstract

In this work, electrochemical oxidation of landfill leachate on boron-doped diamond anodes was studied. The study is collocated in a broader research project that aims at establishing a treatment scheme for removing organic pollutants from a landfill leachate collected at a municipal landfill in Northern Norway. A laboratory plant with an electrode surface of 70 cm^2 was used. The reactor was operated in batch mode with a feed stream of 15 L. The limiting current density that results from the reactor hydraulics was estimated by studying the anodic oxidation of potassium ferrocyanide with linear sweep voltammetry. A limiting current density of 18.13 A/m^2 was obtained at a flow rate of 300 L/h and 30.72 A/m^2 at a flow rate of 600 L/h, respectively. The corresponding values for the limiting current are 127 mA at 300 L/h and 215 mA at 600 L/h. Preliminary experiments were conducted with potassium indigotrisulfonate as a model substance to study the performance of the reactor and to adjust treatment conditions. The degradation of potassium indigotrisulfonate followed first order reaction kinetics with $k_1 = 0.02315\ min^{-1}$ and $k_2 = 0.03017\ min^{-1}$ for applied currents of 300 mA and 1 A, respectively. Complete elimination was achieved after 180 min and 120 min, respectively. The cumulative energy consumption for complete elimination of potassium indigotrisulfonate was 4 Wh for I = 300 mA and 14 Wh for I = 1 A, showing that the current efficiency decreases for intensities significantly above the limiting current.

A 2^3 full factorial design of experiments was established to assess the influence of current intensity, pH and temperature on the treatment efficiency. A high and a low level were defined for every influencing factor: T (4 °C, 20 °C), pH (5, 10) and I (110 mA, 320 mA). The criteria for evaluation of treatment efficiency were the degradation of COD, TOC and ammonium as well as the evolution of nitrate during the treatment. Statistical analyses suggested that in the range of tested conditions, only the pH had a significant influence on the treatment efficiency. COD and TOC concentrations decreased slightly during 4 hours of treatment at pH 5 with a maximum removal of 11 % for COD and 13 % for TOC. At pH 10, no removal of organic matter could be ascribed to electrochemical processes. In contrast, ammonium degradation was more pronounced at pH 10 with a maximum of 25 %. Nitrate generation fluctuated strongly for both levels of pH and ranged from 14 to 94 %.
Because of the poor elimination of organic matter achieved under the tested conditions, an additional experiment was run at I = 7 A. Eliminations of 42 % COD, 28 % TOC and 3 % ammonium-nitrogen were obtained. Nitrate-nitrogen evolution was 54 %. The cumulative energy consumption was 303.8 Wh after 240 min of treatment.

Kurzzusammenfassung

Gegenstand der vorliegenden Arbeit ist die elektrochemische Oxidation von Deponiesickerwasser mit bordotierten Diamantelektroden. Die Arbeit fand ihm Rahmen eines Projekts statt, in dessen Mittelpunkt die Entwicklung einer Methode zur Reduktion der organischen Belastung in Deponiesickerwasser steht. Das verwendete Sickerwasser entstammt einer Deponie in Nord-Norwegen. Die Experimente wurde in einem Reaktor im Labormaßstab durchgeführt, mit einer Elektrodenfläche von 70 cm^2 und einem Batch-Volumen von 15 L. Die sich aus der Reaktorhydraulik ergebende Grenzstromdichte wurde anhand der elektrochemischen Oxidation von Kaliumferrocyanid ermittelt.
Für einen Durchfluss von 300 L/h ergab sich eine Grenzstromdichte von 18,13 A/m^2 und für einen Druchfluss von 600 L/h eine Grenzstromdichte von 30,72 A/m^2. Der entsprechende Grenzstrom beträgt 127 mA für 300 L/h und 215 mA für 600 L/h. Vorversuche mit der organischen Modellsubstanz Kaliumindigotrisulfonat wurden durchgeführt, um die Oxidationseffizienz des Reaktors zu evaluieren und die Behandlungsparameter bestmöglich einzustellen.
Der Abbau folgte einer Reaktionskinetik 1. Ordnung mit den entsprechenden Reaktionskonstanten k_1 = 0,02315 min^{-1} und k_2 = 0,03017 min^{-1} für die Stromstärken 300 mA und 1 A. Der vollständige Abbau des Kaliumindigotrisulfonats war bei einer Stromstärke von 1 A nach 120 Minuten der elektrochemischen Oxidation erreicht. Bei einer Stromstärke von 300 mA war die Testsubstanz nach 180 Minuten vollständig abgebaut. Die vollständige Oxidation beanspruchte einen kumulativen Stromverbrauch von 14 Wh für I = 1 A und 4 Wh für I = 300 mA. Es wurde deutlich, dass eine Stromstärke nahe des Grenzstroms maßgeblich für die Energieeffizienz ist.

Eine faktorielle Versuchsplanung wurde durchgeführt, um den Einfluss der Parameter Stromstärke, pH und Temperatur auf die Effizienz der elektrochemischen Oxidation zu evaluieren. Jedem der Einflussfaktoren wurde ein hoher und ein niedriger Wert zugeschrieben: T (4 °C, 20 °C), pH (5, 10) und I (110 mA, 320 mA). Die Effizienz der Behandlung wurde auf Grundlage der Faktoren COD-, TOC- und Ammonium-Abbau sowie Nitrat-Entwicklung bewertet. Die statistische Auswertung offenbarte, dass unter den getesteten Bedingungen einzig der pH eine statistisch signifikante Auswirkung auf die Oxidationseffizienz hatte. Für pH 5 betrug der maximale COD-Abbau 11 % und der maximale TOC-Abbau 13 %. Bei einem pH von 10 konnte keine Elimination von Organik auf elektrochemische Prozesse zurückgeführt werden. Ammonium-Stickstoff wurde hingegen bei pH 5 nicht abgebaut. Bei pH 10 betrug die maximalen Stickstoff-

Elimination 25 %. Der Abbau von Nitrat-Stickstoff unterlag in saurer und in basischer Lösung starken Schwankungen und reichte von 14 bis 94 %.
Wegen des geringen Abbaus organischer Substanz unter den getesteten Bedingungen wurde ein zusätzliches Experiment mit einer Stromstärke von 7 A durchgeführt. 42 % COD, 28 % TOC und 3 % Ammonium-Stickstoff wurden abgebaut und 54 % Nitrat-Stickstoff entstand. Der kumulative Energieverbrauch betrug 303,8 Wh nach 240 Minuten elektrochemischer Oxidation.

Contents

List of Figures

List of Tables

List of Abbreviations

•OH	Hydroxyl Radicals
AOP	Advanced Oxidation Process
Abs	Absorbance
BDD	Boron-Doped Diamond
BPA	Bisphenol A
COD	Chemical Oxygen Demand
Cl^-	Chloride
DoE	Design of Experiments
EAOP	Electrochemical Advanced Oxidation Process
EO	Electrochemical Oxidation
EU-LoPS	List of Priority Substances, EU
$FeCl_3$	Iron(III)-chloride
H_2O_2	Hydrogen Peroxide
HPLC	High-Performance Liquid Chromatography
I	Current
I_{lim}	Limiting Current
LSV	Linear Sweep Voltammetry
Milli-Q	Ultrapure Milli-Q® water
N-LoPS	Norwegian List of Priority Substances
NH_3	Ammonia
NH_4	Ammonium

NH_4-N	Ammonium Nitrogen
NO_2	Nitrite
NO_3	Nitrate
NO_3-N	Nitrate Nitrogen
NaOH	Sodium Hydroxide
O_2	Oxygen
O_3	Ozone
PI	Potassium Indigotrisulfonate
SHE	Standard Hydrogen Electrode
T	Temperature
THM	Trihalomethane
TOC	Total Organic Carbon
i_{lim}	Limiting Current Density
k_m	Mass Transfer Coefficient

1. Introduction

Water has become a scarce and valuable resource in the industrialized world, where waste water is produced in nearly every sector. In order to address the need of our society for clean water, effective treatment of aqueous waste streams is imperative. Leachates from municipal landfills arise as a consequence of rainwater percolation through the waste, decomposition of organic waste and its inherent water content (Cabeza et al., 2007c). The result is a foul-smelling aqueous waste that typically holds a high concentration of persistent and eco-toxic organic contaminants, as well as nitrogen compounds, heavy metals, xenobiotics and inorganic salts. In consequence, leachate poses serious risk to aquatic organisms and public health when infiltrating surface and groundwater (Urtiaga et al., 2009).

The leachate collected at SHMIL Åremma Landfill in Mosjøen, Norway, is currently discharged into the neighboring fjord, without undergoing previous treatment to reduce its contaminant load. Therefore, within the scope of a wider project, a treatment scheme was developed taking into account the specific conditions of the landfill site and characterizations of the effluent. The combination of those two factors dictates some essential requirements for the treatment scheme. Concerning the site specifics, a major challenge is the cold climate in Northern Norway, reflecting in leachate temperatures between 4 °C and 8 °C in the course of the year, as well as the restricted available space of about 50 m^2 for installing a treatment plant. With a view to the leachate characteristics, major challenges arise from the high variability of its amount, composition and concentration of compounds, low biodegradability, and presence of recalcitrant, eco-toxic substances.

Having these prerequisites in mind, biological treatment is not viable as the leachate temperature is too low for respective microorganisms and the leachate generally features low biodegradability. Common physical-chemical methods often fail to remove persistent organic compounds and require high amounts of chemicals. Therefore, electrochemical oxidation (EO) has gained interest in the field of leachate treatment, as it has been showing high effectiveness in the elimination of persistent pollutants while no addition of chemicals is needed. Other advantages of EO include the use of simple equipment, easy operation, robustness and amenability to automation. Moreover, a prominent benefit for its application in landfill leachate treatment is its high versatility regarding the amount of effluent treated, the wide range of concentrations as well as treatment settings like temperature and pH.

EO is a process based on effluent electrolysis in an electrolytic cell, where strong oxidants are generated at the anode surface and attack organic compounds in the effluent. With the only mandatory input being electrical energy, EO enjoys the reputation of being an environment-friendly technology. Energy demands could furthermore be met by using the methane gas naturally evolving on a landfill as energy source. Moreover, depending on the chosen treatment scheme, EO treatment plants have a rather low space requirement.
EO can lead to the complete mineralization of organic compounds; however in leachate treatment, often a partial oxidation is sufficient to reduce toxicity. With CO_2 and water being the main output, EO presents a final solution without facing the problem of contaminants shifting from one phase to another (Martínez-Huitle and Ferro, 2006).

Landfill leachate is a complex, multicomponent mixture of various pollutants, making the prediction of its behavior during the treatment process difficult. Competitive reactions may occur and different species may interact creating complex scenarios. Therefore, a detailed study of chemical properties of the leachate and the influence of relevant treatment parameters on the EO is mandatory in order to establish an effective treatment scheme. A variety of influencing factors like pre-treatment methods, anode material, temperature, pH, current density and present electrolytes, can considerably effect the performance (Anglada et al., 2009b).

The present work aims at evaluating the influence of the parameters temperature (T), pH and applied current (I) on the EO treatment of the landfill leachate generated at SHMIL Åremma Landfill. The results contribute to the elaboration of effective operating conditions, that guarantee a safe disposal of the discharge while promoting an economical use of energy and other resources.
The leachate is treated in a laboratory plant with a batch feed of 15 L and an electrode surface of 70 cm^2. The electrode material is boron-doped diamond (BDD).

The experimental part of this work can be subdivided into two fractions: First, suitable operating levels for pH, T and I have to be identified, and second, the importance and magnitude of the influencing factors are evaluated applying a factorial design of experiments.In order to fulfill the first part, the practicability of operating the treatment plant with the chosen settings is assessed, e.g. adaptions are made to facilitate the operation under desired conditions.
One level of pH is given by the inherent characteristic of the pretreated leachate (approx. pH 10). The other setting (pH 5) is taken from suggestions in literature. The lower value for T is chosen to be 4 °C, which is remarkably low in comparison with temperatures applied in similar studies. One aim of this work is to verify that EO can be used in cold northern climate without the need to preheat the water. This rather extreme setting is compared to the upper value of 20 °C, which is a setting often chosen in comparable research projects. The identification of appropriate settings for I is a cru-

cial task when implementing an EO treatment, and demands preliminary experiments. The current dictates the transport mechanisms prevailing in the cell and therefore has a strong influence on the reaction rate and mechanism as well as the specific energy consumption. A limiting current (I_{lim}) can be identified, at which the mass transport of organic compounds equals the rate of electron transfer at the electrode surface. At that current, pollutants reaching the anode surface are oxidized immediately and the current efficiency is close to 100 %. Exceeding this level, secondary reactions arise that lower the current efficiency. Therefore, in electrochemistry it is desired to work close to I_{lim}, where a reasonable share of elimination rates and energy efficiency can be yielded. I_{lim} is highly influenced by the reactor design, e.g. the hydraulic characteristics (Schmidt, 2003). A mathematical model as well as a potentiostatic experiment are employed in order to estimate I_{lim}. To validate the results, a test series with textile dye (potassium indigotrisulfonate) is established, wherein the oxidizing efficiency in terms of elimination and energy consumption is assessed at different current densities. Furthermore, the removal rate of the dye diluted in landfill leachate is compared to the removal rate using sodium sulfate as supporting electrolyte, to reassure the good electrolyte properties of the leachate.

Once the operating conditions are specified and the reactor is adjusted to meet the correspondent standards, a factorial experimental design is established to evaluate the importance and magnitude of the three chosen influencing factors (T, pH, I) on the EO of the real leachate.
For each factor, two operating levels are chosen, a high and a low one. In consequence, eight combinations of settings for temperature, pH and current are tested. The evaluation relates to the degradation of Total Organic Carbon (TOC), Chemical Oxygen Demand (COD) and ammonium-nitrogen (NH_4-N) as well as the evolution of nitrate-nitrogen (NO_3-N). A statistical analysis is employed to identify the significance of factors and derive further research demands.
In addition, the evolution of free chloride during the EO treatment is traced. Chlorine species are strong oxidants that can enhance the organics elimination rate but also promote the generation of unwanted chlorinated byproducts. Therefore, when treating chloride-containing wastewaters, it is essential to monitor the evolution of harmful byproducts.

2. Characteristics and Quality of Landfill Leachate

2.1. Landfill Leachate

Sanitary landfills are still a wide-spread method for the ultimate disposal of solid wastes. Through precipitation and degradation processes of organic compounds in the waste, a foul-smelling effluent known as landfill leachate is produced. Surface water percolates quite easily through the layers of a landfill because of the heterogeneous nature of solid wastes and different compaction densities. By passing through the solid wastes, the water leaches soluble compounds and degradation products from the refuse, accumulating organic and inorganic contaminants. The composition of landfill leachate as well as its grade of contamination can be subject to high variations, emanating from a wide range of influencing factors such as type of wastes, precipitation rate, moisture content, landfill design and operation age (Ozkaya, 2005).
Pollutants commonly found in sanitary landfill leachate can be classified into four main groups: (1) dissolved organic matter including volatile fatty acids and more recalcitrant material such as humic and fulvic acids, (2) inorganic ions like ammonium, chloride, potassium and sodium, (3) heavy metals and (4) xenobiotic organic compounds originating from industry and households (e.g. aromatic hydrocarbons, phenols and pesticides) in low concentrations (Moreira et al., 2015). Depending on rainfall conditions, the color of leachate varies from black to brown. Decomposition of solid wastes in a landfill occurs through combined physico-chemical and biological processes. Changes in volume, size and components account to the physical processes while biological processes include decomposition of organic compounds by bacteria, fungi and other micro-organisms(Kurniawan, 2012). The biological decomposition of landfilled waste can be divided into four mayor stages: (1) an initial aerobic phase, (2) an anaerobic acid phase, (3) an initial methanogenic phase and (4) a stable methanogenic phase. Due to depletion of oxygen, aerobic decomposition only lasts for a few weeks. Then, anaerobic processes take over and dominate until the total decomposition of organics, which may take over 50 years (Kjeldsen et al., 2002). Landfill leachate can be categorized according to the life span of the treatment plant into young, intermediate and stabilized, resulting in differences in pH and compound concentrations. Table 2.1 summarizes the characteristics for the different stages of landfill leachate.
Young leachate is characterized by high levels of BOD and COD as well as a high

Table 2.1.: Classification of landfill leachate (Kurniawan, 2012; Deng and Englehardt, 2007).

Type of leachate	Young	Intermediate	Stabilized
Age of landfill [years]	< 1	$1 - 5$	> 5
pH	< 6.5	$6.5 - 7.5$	> 7.5
BOD/COD	> 0.5	$0.1 - 0.5$	< 0.1
COD [g/L]	> 15	$3 - 15$	< 3
NH_3-N [mg/L]	< 400	NA	> 400
TOC/COD	< 0.3	$0.3 - 0.5$	> 0.5
Kjeldahl nitrogen [g/L]	$0.1 - 2$	NA	NA
Heavy metals [mg/L]	> 2	< 2	< 2
Chloride (Cl^-)[mg/L]	200-3000	NA	100-400

BOD/COD ratio, underlining the good biodegradability of leachate compounds in the early stage. Volatile fatty acids represent the biggest part of biodegradable organic compounds to be found in this type of leachate.
With proceeding age, organic compounds get degraded by micro-organisms such as methane-forming bacteria, breaking down the acids into methane and CO_2 with hydrogen. This transformation leads to a rise in pH above 7 and to a lower biodegradability of organic compounds in the leachate. The stabilized leachate, which is dominated by anaerobic decomposition processes, is commonly characterized by high concentration of ammonia (NH_3-N), moderate concentrations of COD and a drop of BOD/COD ratio below 0.1 (Kurniawan, 2012).

There are several treatment options for sanitary landfill leachates: In the young stage, leachate can be effectively treated with biological approaches, including anaerobic and aerobic processes. However, for leachates featuring a low BOD/COD ratio or high concentration of toxic metals, these processes are unsuitable. Hence, physical-chemical approaches are the common choice for pre-treatment or full treatment of leachates. They include flocculation/precipitation, activated adsorption, membrane technologies and chemical oxidation (Deng and Englehardt, 2007).

2.2. Legal Situation in Norway

Regulations on landfills in Norway are adapted to the legislation of the European Union. The *Council Directive 1999/31/EC of April 26 1999 on the landfill of waste* (in Norwegian *Deponidirektivet*) builds an important framework. Therein, regulations for the collection and treatment of leachate can be found. However, no generally valid threshold values are given for the discharge of landfill leachate. Instead, regulations on

water quality of leachate are subject to the national governments. Threshold values should be derived from the characteristics of the disposed waste. Therefore, local governments are encouraged to establish suitable regulations according to the individual conditions found for each landfill site (European Council, 1999).
In Norwegian law, the *Guidelines on risk assessment of landfills* contain threshold values for diffuse emissions of 42 parameters like TOC, Total-N, Total-P and metals. However, there are no thresholds defined which apply directly to the quality of leachate to be discharged into the receiving water body. The *Guidelines on leachate monitoring* set up an annual sampling program with 24 parameters for leachate and 16 parameters for sediment, but again, threshold values for discharge of leachate are not given (Harstad, 2006).

This brief check-up on the legal situation regarding the treatment of landfill leachate reveals a lack of legal regulations, especially threshold values, for the discharge into water bodies.There is, however, a directive in European law referring to the general water quality of water bodies. In this directive, the so called *List of Priority Substances* (*EU-LoPS*) is published. It contains threshold values for 33 substances that are hazardous to ecosystems and human health. By law, these threshold values are not to be exceeded in water bodies (European Parliament and Council of the European Union, 2012). This directive applies to concentrations in water bodies, not to the leachate per se. The effect of leachate pollution is dependent on size and hydrodynamics of the receiving water body. Nevertheless, the *EU-LoPS* indicates on which compounds to focus when assessing the potential environmental harmfulness of the leachate and for implementing a treatment scheme. The list and corresponding threshold values are given in Appendix A.
The Norwegian government established an additional *Norwegian List of Priority Substances* (*N-LoPS*), that refers to emissions of over 30 substances believed to be especially harmful to the environment, due to high persistence, bio-accumulation, serious long-term health effects or high ecotoxicity. The set aim is to reduce the emission of these substances to zero by the year 2020. For now, the list represents a suggestion only, without legal liability (The Norwegian Environment Agency, 2018). The list is added in Appendix A.

2.3. Location and further Description of SHMIL Åremma Landfill

Søndre Helgeland Miljøverk IKS (SHMIL) is an intermunicipal waste company located near the city of Mosjøen (Municipality Vefsn, Province Nordland) in Northern Norway. Its location in Norway is specified in Figure 2.1. SHMIL was founded in 1995 to safeguard the owner municipalities' obligations in the area of waste treatment. The eleven owner municipalities count a total of approximately 41,000 inhabitants.

The landfill is approved for receiving non-hazardous domestic wastes as well as contaminated masses. Methane gas outlets can be used for energy supply.
As for now, the leachate produced in SHMIL Årmenna Landfill is collected and discharged into the neighboring Vefsnfjord untreated (SHMIL IKS, 2019).
Potential stricter regulations in the future and a rise in environmental awareness provoke the need for a treatment scheme to reduce the environmental impact on ecosystems and human health.

Figure 2.1.: Location of SHMIL Åremma Landfill in Norway (Google Maps, 2019).

The landfill has an elevation range from 70 - 80 m above sea level. Figure 2.2 shows the monthly average precipitation and temperature in Mosjøen. The respective values are listed in Table 2.2. With an average yearly precipitation of 1996 mm, the climate in Mosjøen can be classified as wet according to the Köppen-Geiger climate classification (Michael and Munt, 2012). The season with the highest average monthly precipitations lasts from September to March with the highest value of 247 mm in October. April to August are the dryer months with the least average precipitation of 91 mm in May.
The yearly average temperature is 5.4 °C. The warmest month of the year is August with an average temperature of 13.9 °C. Lowest temperatures are reached in January with an average of -1.6 °C.

The amount of precipitation and its monthly variation is an important factor as it strongly influences the amount and grade of dilution of the landfill leachate. The difference in average monthly precipitation between the wettest month October and the driest month May accounts to 156 mm.

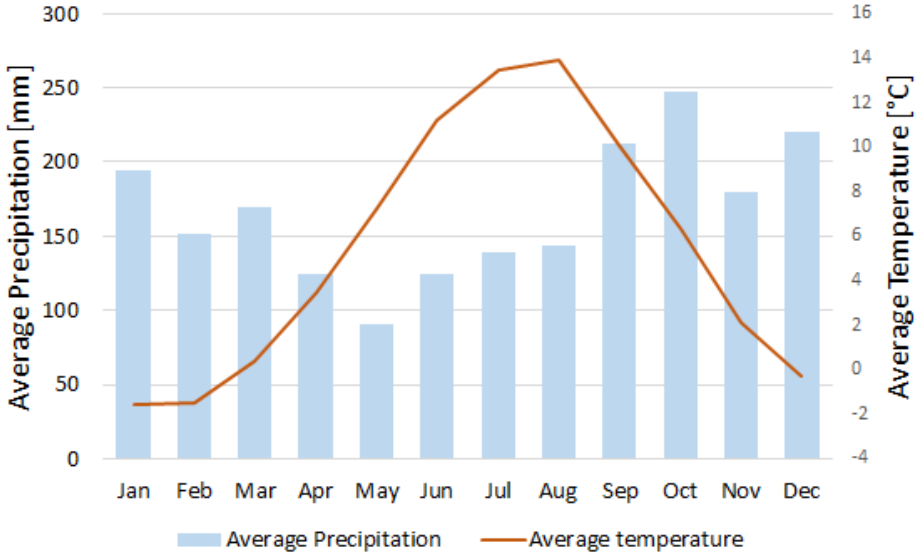

Figure 2.2.: Average monthly precipitation and temperature in Mosjøen, Norway (1982-2012), modified after Merkel (2013).

Table 2.2.: Average monthly precipitation (P) and temperature (T) in Mosjøen, Norway (1982-2012) (Merkel, 2013).

Month	Jan	Feb	Mar	Apr	May	Jun	Jul	Aug	Sept	Oct	Nov	Dec
P [mm]	194	151	169	124	91	125	139	144	212	247	180	220
T [°C]	-1.6	-1.5	0.4	3.5	7.2	11.2	13.5	13.9	10.1	6.3	2.1	-0.3

The amount of leachate produced at SHMIL Åremma Landfill is highly variable. Within a monitoring program from 2006 to 2015, the daily leachate volume ranged from around 30 m^3/d measured in August 2012 to approx. 500 m^3/d in March 2007. For these measurements, leachate was collected at one specific day during the month.

2.3.1. Pretreatment on-site

A physio-chemical pretreatment scheme for the collected landfill leachate was elaborated and realized in a pilot plant on-site. It consists of aeration, precipitation and coagulation-flocculation. In the first tank, the leachate is aerated through a pipe. This step aims at the oxidation of organic compounds which often prevail in their reduced

forms in leachate due to the predominant anaerobic conditions in landfills. The oxidation of these easily oxidized compounds as a pretreatment step promises a more efficient treatment of more recalcitrant compounds with EO.
A pH around 11 is adjusted by dosing sodium hydroxide (NaOH). The addition of NaOH has two purposes: (1) At alkaline pH, ammonia-nitrogen (NH_3-N) prevails in its undissociated form and can move into the air phase during aeration. This process is known as ammonia stripping. As NH_3-N is a compound known to accumulate in landfill leachate, this pretreatment step is imperative to avoid competition with COD removal during the EOP; (2) NaOH is an effective agent for heavy metal precipitation (Kurniawan, 2012).
In the fast-mixing tank, iron(III)-chloride ($FeCl_3$) is added as an coagulant to promote particle growth and therefore sedimentation. High turbulence keeps the solid particles in suspense and enhances the reaction with $FeCl_3$. The subsequent step is a slow-mixing tank to promote flocculation, followed by a lamella clarifier for solid/liquid separation. The inlet is located at half of the depth of the tank. Solids sink to the bottom and evacuate through a sludge outlet. The clear liquid phase discharges through a hole at the top of the clarifier.
The last column of Table 2.3 summarizes physio-chemical properties of the pre-treated leachate.

2.3.2. Water Quality Data

In order to assess the water quality of the leachate produced at SHMIL Årmenna Landfill, relevant parameter were measured over a period of 9 years, from 2006 to 2015. In total, 51 samples were taken and statistically analyzed. During a field trip in October 2018, values for the raw leachate were measured, as well as values after pretreatment in the pilot plant described above. A sample of the pre-treated leachate was sent to Trondheim Kommune Analysesenteret for further analyses. The mean values for some characteristic parameters are shown in Table 2.3, along with the measured values for the leachate collected in October 2018.
By comparing the characterizing parameters for the raw leachate to the classification for landfill leachate given in Table 2.1, SHMIL Årmenna Landfill Leachate can be classified as intermediate to stabilized. This is indicated by the neutral pH, the low BOD_5/COD ratio of 0.1 and the TOC/COD ratio between 0.3 (mean values 2006 - 2015) and 0.5 (October 2018). The low BOD_5/COD ratio suggests that the biodegradability of the leachate is very low and therefore biological treatment is no option. In total, the organic load is rather low and fits to the characterization of stabilized leachate. In contrast, the nitrogen pollution of the leachate is high, as can be derived from the Total-N/COD ratio of 0.5. A large proportion of nitrogen is present in the form of NH_4-N.
The BOD_5/COD ratio of 0.8 obtained for the pre-treated leachate collected in October 2018 is surprisingly high and indicates the biodegradability of young leachate.

Table 2.3.: Characterizing parameters for SHMIL Årmenna Landfill Leachate. Mean 2006-2015: includes mean values from 51 samples taken during 9 years. Oct '18 raw: measured values for the raw leachate during the field trip 2018. Oct '18 pre-treated: measured values for the pre-treated leachate during the field trip 2018, or after the field trip by an external laboratory for inputs marked with (*).

Parameter	Mean 2006-2015	Oct '18 raw	Oct '18 pre-treated
pH	6.8	7.0	10.6
Conductivity [mS/m]	257.1	121.0	484.0
Turbidity [NTU]	NA	40.10	7.39
COD [mg/L]	211.5	61.6	53.0 (51.0*)
BOD_5 [mg/L]	20.7	NA	42.0*
BOD_5/COD	0.1	NA	0.8
TSS [mg/L]	86.56	26.14	15.63
TOC [mg/L]	59.5	31.0	22.45
TOC/COD	0.3	0.5	0.4
Total-P [mg/L]	0.55	NA	NA
Total-N [mg/L]	102.2	NA	40.8
Total-N/COD	0.5	NA	0.77
NH_4-N [mg/L]	95.15	28.4	25.3 (32.4*)
NH_3-N [mg/L]	NA	NA	4.94*
Chloride [mg/L]	NA	NA	118*
Sulfate [mg/L]	NA	NA	28.8*
Fluoride [mg/L]	NA	NA	3.04*
Phosphate [μg/L]	NA	NA	26.0*

The concentrations for COD, total suspended solids (TSS), TOC and NH_4-N measured in October 2018 are significantly below the mean values for 2006 to 2015. This can be ascribed to the fact that October is the month with the highest average precipitation of the year. Therefore, the leachate has a high dilution index. This also reflects in a lower conductivity of the raw leachate. However, after pretreatment in the pilot plant, the conductivity is about four times higher than in the raw leachate. This is due to the addition of $FeCl_3$ as a coagulant in the pretreatment plant, although the biggest portion of Fe^{2+} and Fe^{3+} precipitates and is disposed in the sludge. The conductivity of 484 mS/m is sufficient for electrochemical treatment without further addition of electrolytes. The pH is neutral in the raw leachate. After pre-treatment, the pH is alkaline due to the addition of NaOH.
The elimination rate for COD is about 15 %, for TOC around 30 % and for NH_4-N approximately 10%. TSS are reduced by around 60 % and the turbidity decreases by approximately 80 %. The rather low elimination of organic matter and NH_4-N em-

phasize the difficulties involved in treating this type of aqueous solution expected to include various persistent compounds.

The raw leachate samples taken during 2006 and 2015 were further tested for alkaline earth metals, heavy metals, polycyclic aromatic hydrocarbons (PAHs), BTEX (Benene, Toluene, Ethylbenzene, Xylene), herbicides and hydrocarbons as well as some other parameters including acute toxicity. The results can be consulted in Appendix A. It can be concluded, that the overall grade of pollution is rather low in this leachate compared to leachate characterizations found in literature (Harstad, 2006). However, 16 of the priority substances from the *EU-LoPS* and three additional ones listed on the *N-LoPS* have been detected in the leachate. Therefore, the treatment should aim at the removal of specific hazardous and recalcitrant organic compounds, like PAHs and BTEX. These compounds usually need to be oxidized in order to mineralize them or, at least, to increase their degradability.
Furthermore, the share of nitrogen compounds, mainly NH_4-N, is remarkably high and therefore NH_4-N should also be regarded during the treatment. The third relevant group of pollutants identified for SHMIL Årmenna Landfill Leachate are metals, including heavy metals. In general, their concentrations are low but some of them are classified as priority substances (Gröhlich, 2015). However, heavy metals are sufficiently reduced by chemical precipitation in the pretreatment plant.

Table 2.4.: Concentrations of organic target substances in the pretreated leachate.

Substance	Concentration (μg/L)	*EU-LoPS*	*N-LoPS*
BPA	8.4		x
Sum PAH16	0.62	x	x
Naphthalene	0.549	x	
Acenaphthene	0.054		
Fluorene	0.021		
Sum BTEX	1.49		
Benzene	<0.2	x	
Toluene	<1.0		
Ethylbenzene	0.44		
o-Xylene	0.25		
m/p-Xylene	0.80		

A sample of the pretreated leachate was sent to an analytical laboratory (ALS Laboratory Group Norway AS) and tested for PAHs, BTEX and bisphenol A (BPA), as those are compounds identified to be relevant for the treatment of the leachate. The results are shown in Table 2.4. The table furthermore gives information which of the listed compounds and cumulative parameters are mentioned in the *EU-LoPS* and *N-LoPS*, marked with an (x).

3. Theoretical Background

3.1. Electrochemical Advanced Oxidation Processes

As described in Chapter 2.1, landfill leachates are highly complex effluents that feature high variability in composition and concentrations. Further characteristics are a low BOD/COD ratio and the presence of recalcitrant and toxic compounds. Therefore, biological abatement is often not feasible and physical-chemical methods are preferred. In this context, so called advanced oxidation processes (AOPs) are of high relevance. AOPs are based on the in-situ production of hydroxyl radicals (•OH), that present high reactivity towards most organics. In fact, with a standard redox potential of $E^0(\bullet OH/H_2O) = 2.80$ V/SHE (measured against standard hydrogen electrode (SHE)), hydroxyl radicals are the second strongest oxidants known after fluorine and are able to degrade even highly recalcitrant organics. In consequence, AOPs allow the total mineralization of organic pollutants or, at least, their transformation to harmless products and present a complete solution rather than only a phase separation with the problem of final disposal still remaining.
The most common AOPs are hydrogen peroxide (H_2O_2) with Ultraviolet-C (UVC) radiation, ozone (O_3) and ozone based processes, titanium dioxide based processes and Fenton's reaction based methods (Moreira et al., 2017). Advanced oxidation approaches involving ozone or chlorine dioxide are not always effective and transportation as well as storage of reactants pose cost and safety issues. Electrochemical advanced oxidation processes (EAOPs) are a subcategory of AOPs that present a promising alternative for the treatment of complex effluents, as no addition of chemicals is needed and electricity is the only mandatory consumable (Martínez-Huitle and Ferro, 2006). Three key techniques can be summarized for advanced electrochemical treatment of waste waters (Moreira et al., 2017):

- **Electrochemical Oxidation**, where organics are oxidized directly at the anode surface by electron transfer or indirectly by •OH from the anode surface or oxidizing agents like active chlorine, O_3, persulfates and H_2O_2 from the bulk solution,
- **Electrochemical Oxidation with electrogenerated** H_2O_2, where anodic oxidation is combined with cathodic electrogeneration of H_2O_2,
- **electro-Fenton**, where Fe^{2+} is added to the bulk solution in order to induce the so called Fenton's reaction, which results in the generation of the oxidizing

agent H_2O_2. Further developments of this technique are the photoelectro-Fenton and solar photoelectro-Fenton processes, where artificial light or natural sunlight provides irradiation to enhance the reaction.

The major advantages of EAOPs are:

- **Environmental compatibility** because the main reagent is the electron, which is produced in-situ and regarded as clean. Wastewaters like landfill leachate often exhibit medium to high salinity, which is conjoined to high conductivity and make the addition of further electrolytes obsolete,
- **Versatility** in terms of nature and concentration of pollutants to be treated, treatment conditions like pH and temperature as well as volume of effluent,
- **Energy efficiency** in comparison to non-electrochemical approaches like incineration due to applicability at room temperature and efficient design of reactors to reduce power losses through inhomogeneous current distribution, voltage drop and side reactions and
- **Amenability to automation** of the inherent process variables like electrode potential and cell current.

Furthermore, EO holds some advantages over the other EAOPs, bein no requirement of addition of chemicals or feeding of O_2 (as in Fenton processes), no tendency to produce secondary pollution and fewer accessories required (Martínez-Huitle and Ferro, 2006).

Downsides to electrochemical approaches are high operation costs due to the high energy consumption and expensive anode material, potential formation of recalcitrant byproducts, limitations in the long term stability and activity of electrode material and inherent procedural limitations. Latter generate mainly from the heterogeneous nature of electrochemical processes, where the reactions take place at the interphase of an electronic conductor (the electrode) and an ion conduction medium (the electrolyte). Therefore, the rate of mass transfer of target compounds to the interphase and the size of specific electrode area limit the performance of electrochemical processes (Jüttner et al., 2000).

3.2. Electrochemical Oxidation

3.2.1. Fundamentals

Electrochemistry describes chemical reactions that involve electron transfer through an outer conductor circuit. In consequence, one reaction partner is always given by an electrode receiving or releasing electrons. That means, in electrochemistry not only mass and energy balance need to be considered but also charges, i.e. electrical current

flow. Inside the reactor, the charge is carried by ions in mostly liquid electrolytes. The electrolyte also carries the reactants and products of the electrochemical reaction and is furthermore where up- or downstream chemical reactions take place. Figure 3.1 illustrates a simple composition for an electrochemical reactor.

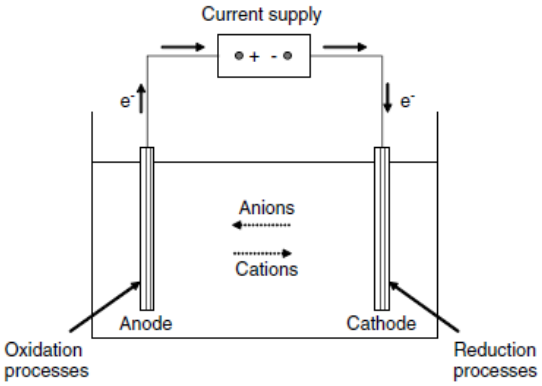

Figure 3.1.: Scheme of an electrochemical reactor (Anglada et al., 2009a).

Control variables for electrochemical cells are the potential, the current and the resistance. When applying a current, charge is carried through the outer electrical circuit by electrons and through the electrolyte by ions. The cell potential becomes a function of the applied current.
The equilibrium potential is the potential that prevails when no current is applied to the cell. By inducing a potential different from the equilibrium one, electrochemical reactions are commenced, forcing a transfer of charges between electrode and electrolyte. The difference between the electrode potential when applying a current and the equilibrium potential is called overpotential. It is defined by Equation 3.1. In order to promote oxidation processes, the cell potential needs to be higher than the equilibrium potential:

$$\eta = \varphi - \varphi_0 \tag{3.1}$$

where:

$$\begin{aligned} \eta &= \text{overpotential} \\ \varphi &= \text{applied potential} \\ \varphi_0 &= \text{equilibrium potential} \end{aligned}$$

When applying a positive overpotential, the anode absorbs electrons from the reactants (Red) present in the electrolyte, oxidizing them according to Equation 3.2:

$$\text{Red} \longrightarrow \text{Ox} + \text{ne}^- \tag{3.2}$$

where:

Red, Ox = ions or neutral compounds
n = number of transferred electrons per reactive particle

In electrochemistry, the current flow through the electrodes is expressed as current density, referring it to the electrode area:

$$i = \frac{I}{A} \tag{3.3}$$

where:

i = current density	$[Acm^{-1}]$
I = applied current	$[A]$
A = electrode area	$[cm]$

Whenever an electrode is immersed in an electrolyte, a boundary layer builds up. In this boundary layer electrochemical reactions take place. It is therefore also called reaction layer. With an inevitable need for the involvement of two phases in electrochemistry (the solid electrodes and the aqueous electrolyte), electrochemical reactions are inherently heterogeneous. Figure 3.2 depicts the physical-chemical processes that can occur in the reaction layer during EO.

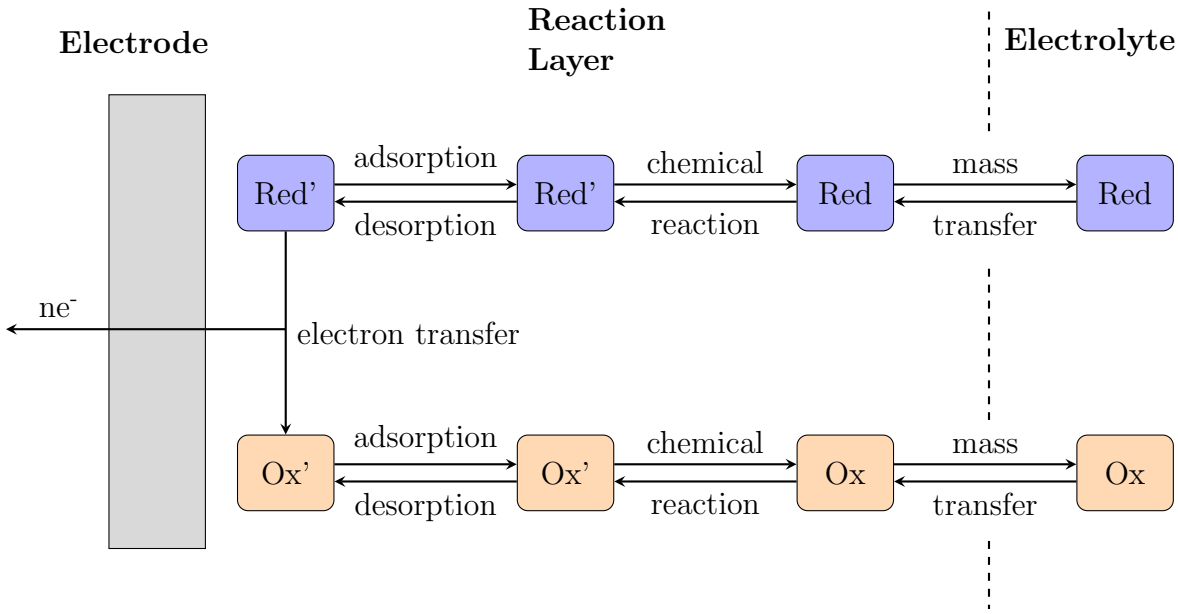

Figure 3.2.: Possible physical-chemical processes in the boundary layer between electrode and electrolyte during EO, modified after Schmidt (2003).

In the course of EO treatment, the concentration of the target compound decreases in the reaction layer. New molecules have to be transported from the inner of the electrolyte towards the electrode surface constantly to keep the reaction ongoing. Meanwhile, the oxidized compounds have to be removed from the reaction layer. Two controlling mechanisms can be distinguished for EO; the reaction rate, or more precisely the electron transfer at the anode surface itself and the rate of transport of reactants and products through the electrolyte.
The applied current dictates which of the two controlling regimes is effective in each individual setup, as further described in Chapter 3.2.4.

3.2.2. Electrode Material

The electrode material is an important parameter in EO as different materials promote different oxidation mechanisms leading to varying intermediates. The nature of electrode material has a strong influence on the selectivity as well as the efficiency of the EO process (Martínez-Huitle et al., 2004). Main requirements for electrode materials are high stability in the electrolysis medium, low cost and high activity toward organic oxidation whereas the activity toward secondary reactions such as oxygen evolution should be low (Panizza, 2010).

Previous studies showed that some anodes favor the partial and selective oxidation of pollutants, while others favor complete combustion to CO_2 (Comninellis, 1994). On grounds of this observation, a model for the oxidation of organics at metal oxide electrodes with simultaneous oxygen evolution was proposed, distinguishing between so called active and non-active electrode materials. For both materials, the first step is the discharge of water molecules, leading to the formation of adsorbed hydroxyl radicals on the electrode surface (M), according to Eq. 3.4:

$$\mathrm{MO}_x + \mathrm{H_2O} \longrightarrow \mathrm{MO}_x(\bullet\,\mathrm{OH}) + \mathrm{H^+} + \mathrm{e^-} \tag{3.4}$$

The further steps differ for active and non-active electrode materials:

1. **Active electrodes**
   For these materials, higher oxidation states are available on the electrode surface, leading a path to interactions of the adsorbed hydroxyl radicals with the anode. Higher oxides may be formed on the anode surface according to Eq. 3.5:

   $$\mathrm{MO}_x(\bullet\,\mathrm{OH}) \longrightarrow \mathrm{MO}_{x+1} + \mathrm{H^+} + \mathrm{e^-} \tag{3.5}$$

   Subsequently, the surface redox couple MO_{x+1}/MO_x can act as mediator in the selective oxidation of organics according to Eq. 3.6:

   $$\mathrm{MO}_{x+1} + \mathrm{R} \longrightarrow \mathrm{MO}_x + \mathrm{RO} \tag{3.6}$$

2. **Non-active electrodes**
   These materials do not promote the formation of higher oxides, but allow non-selective oxidation of organics (R) via hydroxyl radicals, according to Eq. 3.7:

$$\mathrm{MO}_x(\bullet\,\mathrm{OH}) + \mathrm{R} \longrightarrow \mathrm{MO}_x + \mathrm{mCO}_2 + \mathrm{nH}_2\mathrm{O} + \mathrm{H}^+ + \mathrm{e}^- \tag{3.7}$$

   These mechanisms may result in the complete combustion to CO_2.

For both mechanisms, competitive side reactions can occur, such as oxygen evolution. However, in the EO mechanism on active electrodes, the hydroxyl radicals are chemisorbed at the electrode surface whereas for non-active electrodes, they are physisorbed. In consequence, the interaction with the electrode surface is stronger for active electrodes. As a general rule, the electrochemical activity toward oxygen (O_2) evolution rises with the strength of interaction between hydroxyl radicals and anode surface, while the chemical reactivity toward organics oxidation decreases. In conclusion, higher potentials can be applied when working with non-active electrodes, without facing a decrease in EO efficiency due to oxygen evolution. In addition, larger $\bullet OH$ concentrations have been found to occur on non-active electrodes than on active ones (Comninellis, 1994).

Table 3.1 shows the oxygen evolution potential for selected common anode materials. Typical active anodes are irridium dioxide (IrO_2), ruthemium dioxide (RuO_2), platinum (Pt) and other carbon based electrodes. Their potential for O_2 evolution is usually below 1.8 V/SHE.
Examples for non-active anode materials are lead dioxide (PbO_2), tin dioxide (SnO_2) and BDD. With an O_2 evolution potential between 2.2 and 2.6 V/SHE, the BDD anode is the most potent non-active anode known and therefore enjoys great popularity in the application of EAOPs (Moreira et al., 2017).

Table 3.1.: Potential for O_2 evolution at common anode materials, modified after Moreira et al. (2017).

Anode material	Potential for O_2 evolution (V/SHE)
RuO_2	1.4-1.7
IrO_2	1.5-1.8
Pt	1.6-1.9
Graphite	1.7
PbO_2	1.8-2.0
SnO_2	1.9-2.2
BDD	2.2-2.6

3.2.2.1. Boron-Doped Diamond Anodes

BDD anodes consist of a boron-doped diamond film maintained on a silicon substrate. Boron provides the required electrical conductivity (WaterDiam, 2015).
BDD anodes have widely been used for EO processes due to their outstanding qualities such as stability up to high anodic potentials and high overpotential for oxygen evolution. Furthermore, BDD electrodes have a high corrosion stability in strong acidic media (Polcaro et al., 2003; Fernandes et al., 2015).
In comparison with other electrode materials, BDD anodes achieve high organic oxidation rates and great current efficiencies (Anglada et al., 2009a). This is believed to be mainly a result of the weak adsorption of hydroxyl radicals to the anode surface, leading to high reactivity towards organics oxidation (Panizza and Martinez-Huitle, 2013).
Figure 3.3 shows the cyclic voltammogram of BDD electrodes compared to platinum electrodes in 1 M sulfuric acid (H_2SO_4) solution. It can be seen that BDD electrodes have a wide working window, which can range from -1.5 V in cathodic polarization to 3 V in anodic polarization. This range allows the operation at exceptionally high potentials compared to other electrode materials, promoting the generation of a multitude of active compounds that benefit the EO treatment (WaterDiam, 2015).

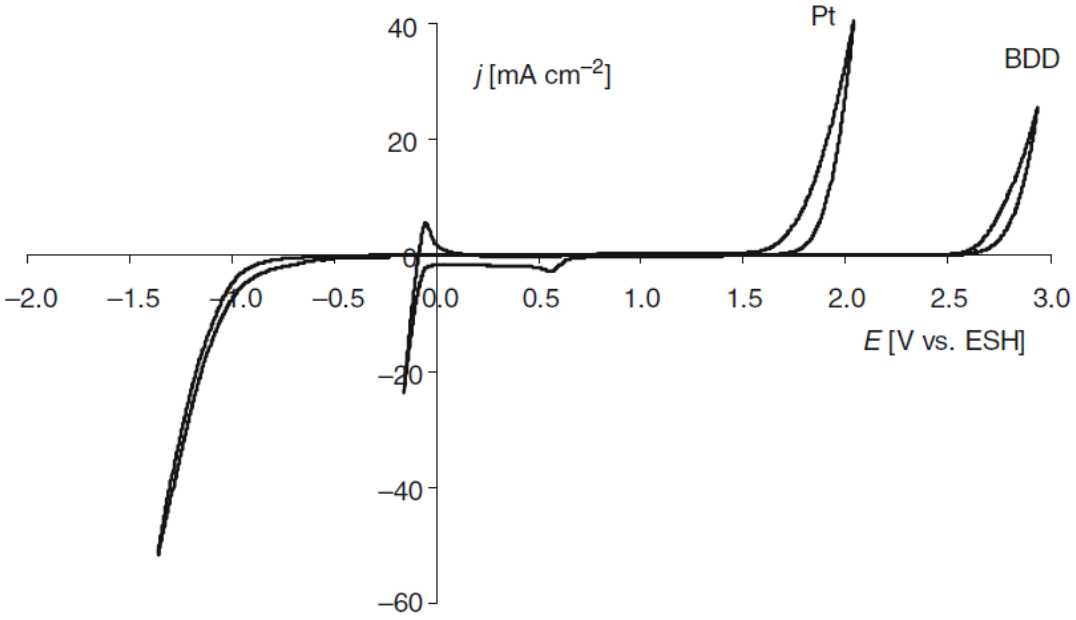

Figure 3.3.: Cyclic voltammograms for BDD and platinum electrodes in 1 M H_2SO_4 solution (Kapalka et al., 2010).

Due to their outstanding properties, BDD anodes have been used in many EO applications and shown effective for complete mineralization of several phenolic compounds

(Sun et al., 2012; Rabaaoui et al., 2013; Rodrigo et al., 2001; Pereira et al., 2012; Murugananthan et al., 2008), industrial wastewater from a fine chemicals plants (Cañizares et al., 2006b), olive mill wastewaters (Chatzisymeon et al., 2009) and landfill leachate (Cabeza et al., 2007a).

However, there are some downsides to the application of BDD electrodes for EO. Apart from high material and manufacturing costs, the possible evolution of chlorinated byproducts is a major drawback. Reactive chlorine can be produced during EO on BDD electrodes when treating chlorine containing waters. While active chlorine enhances organic matter removal, it can also form organochlorine intermediates, such as trihalomethanes (THM). These compounds are resistant towards further oxidation and some are toxic (Wu et al., 2016).

3.2.3. Direct and Indirect Oxidation

Two pathways for EO of organics have been reported and are schematized in Figure 3.4:

1. **direct oxidation**, where the electron transfer takes place directly at the electrode surface, through adsorption of reactants and intermediates. Oxidation is promoted by hydroxyl radicals forming at the anode surface. No other compounds are involved in this oxidation mechanism (Martínez-Huitle and Panizza, 2018). The two steps required for direct oxidation are diffusion of pollutant from the bulk solution to the electrode surface and subsequently their oxidation. Direct oxidation can again succeed via two different pathways (Anglada et al., 2009a):
   - **electrochemical conversion**, which only partially oxidizes organic compounds:
   $$\mathrm{R} \longrightarrow \mathrm{RO} + \mathrm{e}^- \tag{3.8}$$
   - **electrochemical combustion**, where organic compounds are transformed into water, carbon dioxide and other inorganic substances:
   $$\mathrm{R} \longrightarrow \mathrm{CO_2} + \mathrm{H_2O} + \mathrm{Salts} + \mathrm{e}^- \tag{3.9}$$
2. **indirect oxidation**, where electroactive compounds such as chlorine/hypochlorite and persulfate are generated at the electrode surface and function as mediators for the electron transfer from the anode to the target compounds. For indirect oxidation, the main reaction stages occur in the solution bulk rather than directly at the anode surface. Therefore, electrode fouling is avoided by this mechanism (Martínez-Huitle and Panizza, 2018). The indirect oxidation mechanism plays an important role in EO of landfill leachate, most commonly mediated by chlorine, which forms strong oxidants and is a ubiquitous compound in wastewater (Deng and Englehardt, 2007).

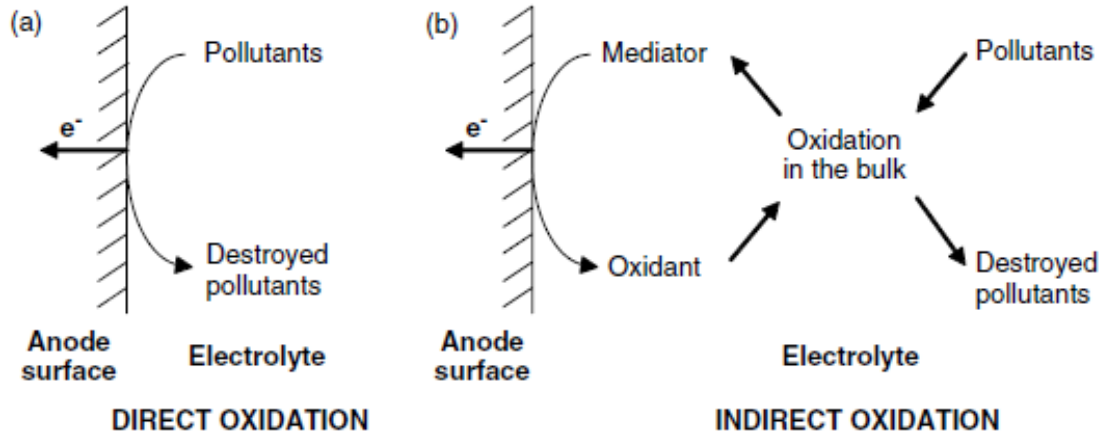

Figure 3.4.: Schematic description of EO via (a) direct and (b) indirect pathways (Anglada et al., 2009a).

3.2.4. Limiting Current Density

The limiting current density (i_{lim}) defines the intensity at which the rate of electron transfer at the anode equals the diffusion rate of organics into the boundary layer. At this current, all molecules reaching the anode surface are theoretically oxidized immediately. The concentration of elements carrying electrical charges is near zero at the anode surface and the current efficiency is 100 %. The current density does not rise any more when increasing the overpotential. According to previous studies ((Rodrigo et al., 2001), (Panizza et al., 2001b), (Panizza et al., 2001a)), two regimes can be distinguished based on the applied current (schematized in Figure 3.5):

1. $i < i_{lim}$
   With the applied current being lower than the limiting one, the electrolysis is under current control. The charge transfer from electrode to active compounds in the electrolyte is the rate-determining step. The transport of active compounds to the boundary layer has no influence on the voltage-current-behavior (Schmidt, 2003). Working with a current below the limiting one, the instantaneous current efficiency is close to 100 %. The degradation of organic matter proceeds linearly with time and intermediates are formed (Panizza et al., 2008).

2. $i > i_{lim}$
   When working with a current higher than the limiting one, the transport of active compounds and charge carriers to the electrode, e.g. to the electrode/electrolyte interphase, is the rate-determining step. The electrolysis is under mass transfer control. In this case, the current density is determined by the particle current density of the particles to be oxidized. i_{lim} does not accelerate with further increase of the over-potential anymore (Schmidt, 2003). The instantaneous current

efficiency sinks under 100 % because secondary reactions such as oxygen evolution start to arise. The organics degradation follows an exponential trend. A complete combustion of organic matter to CO_2 can be achieved (Panizza et al., 2008).

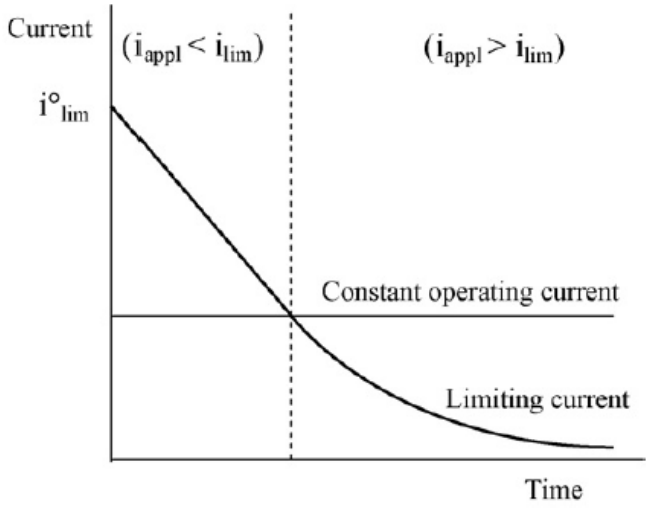

Figure 3.5.: Course of i_{lim} over time during EO at a constant operating current. The vertical dashed line indicates the transition between the two operating regimes, from current control to mass transfer control (Panizza et al., 2008).

As i_{lim} depends on the concentration of target compounds in the effluent, its level sinks in the course of the treatment and a shift in oxidation regimes can occur.

The limiting current density can be increased by two methods (for a given electrode area and effluent volume):

1. Higher concentration of electrochemically active compounds
2. Higher mass transfer coefficient k_m

The first option is not desirable as it implies further addition of chemicals. In contrast, increasing k_m is a feasible and realistic approach. k_m is correlated to the diffusion coefficient of electrochemically active substances and inversely proportional to the thickness of the reaction layer. The diffusion coefficient, in turn, is correlated to the mobility of compound in the electrolyte, which increases with temperature. However, k_m is usually enhanced by minimizing the reaction layer. In order to do so, convective mass transport is promoted by either stirring the electrolyte inside the reactor, letting the electrolyte pass the electrodes or moving the electrodes themselves. k_m is further enhanced when the electrolyte flow through the electrodes is turbulent. When moving

the electrolyte passed the electrodes at a defined flow rate, the conditions of convective mass transport are known and can be described mathematically (Schmidt, 2003).

3.2.4.1. Empirical Determination of the Limiting Current Density

The limiting current density for a given setup can be calculated by implying a simple mathematical model proposed by Kapalka et al. (2010), that links i_{lim} directly to the concentration of organic matter:

$$i_{lim} = nFk_mC_{org} \tag{3.10}$$

where:

$$\begin{aligned} i_{lim} &= \text{limiting current density} && [Am^{-2}] \\ n &= \text{number of electrons exchanged during EO} && [\text{-}] \\ F &= \text{Faraday constant} && [C \cdot mol^{-1}] \\ k_m &= \text{mass transfer coefficient} && [ms^{-1}] \\ C_{org} &= \text{concentration of organics in solution} && [mol \cdot m^{-3}] \end{aligned}$$

Three assumptions underlie this model:
(1) Adsorption of the organic compound at the electrode surface can be neglected,
(2) The diffusion coefficient D is equal for all compounds,
(3) The electrochemical oxidation of organic compounds via BDD electrodes is a fast reaction which is controlled by mass transport of organics to the electrode surface.

With mass transport assumed as main driver for the reaction, the chemical nature of the organic reactants does not influence the oxidation rate and can be neglected.

In order to estimate the mass transfer coefficient, a set of dimensionless equations is applied. They are derived from similitude theory and make use of experimentally established constants and exponents. These equations include (Schmidt, 2003):

– **Sherwood number Sh**, that represents the ratio of mass transfer and diffusion

$$Sh = \frac{\bar{k_m}d_h}{D} \tag{3.11}$$

where:

$$\begin{aligned} \bar{k_m} &= \text{average mass transfer coefficient} && [ms^{-1}] \\ d_h &= \text{hydraulic diameter} && [m] \\ D &= \text{molecuar diffusivity of compounds} && [m^2s^{-1}] \end{aligned}$$

The Sherwood number can also be calculated through the following universal equation, fitting the parameter a, b and c to the particular case of application:

$$Sh = K \cdot Re^a \cdot Sc^b \cdot \Gamma^c \tag{3.12}$$

where:

K = constant for flow conditions [-]
Re = Reynolds number [-]
Sc = Schmidts number [-]
Γ = geometric number [-]

When using Eq. 3.12 to calculate the Sherwood number, Eq. 3.11 can be applied to calculate k_m.
The experimentally identified values for the fitting-parameters for turbulent flow through plane-parallel electrodes are as followed: K = 0.023; a = 0.8; b = 0.33 and c = 1.

– **Reynolds number Re**, which is the ratio of inertial forces to viscous forces within a fluid

$$Re = \frac{\rho \cdot d_{hyd} \cdot Q}{A_{flow} \cdot \mu} \tag{3.13}$$

where:

ρ = density of the fluid $[kg\,m^{-3}]$
d_{hyd} = hydraulic diameter $[m]$
Q = flow rate $[Lh^{-1}]$
A_{flow} = throughflow area $[m^2]$
μ = dynamic viscosity of the fluid $[m^2 s^{-1}]$

The flow-through area for a rectangular duct can be calculated with Eq. 3.14:

$$A_{flow} = bh \tag{3.14}$$

where:

b = inner electrode gap $[m]$
h = electrode diameter $[m]$

With the electrodes being circular, their diameter can be calculated through their area $A_e = \pi(h/2)^2$.

The hydraulic diameter for a rectangular duct is calculated as follows:

$$d_{hyd} = \frac{4A_{flow}}{P} = \frac{4A_{flow}}{2(h+b)} = \frac{2A_{flow}}{h+b} \tag{3.15}$$

where:

$$P = \text{wetted perimeter} \qquad [m]$$

If the width of the duct is significantly smaller than the height ($b << h$), b can be erased from the denominator in Eq. 3.15.

– **Schmidt number**, defined as the ratio of momentum diffusivity (kinematic viscosity) and mass diffusivity:

$$Sc = \frac{\nu}{D} = \frac{\mu}{\rho \cdot D} \tag{3.16}$$

where:

$$\begin{aligned} \nu &= \text{kinematic viscosity} & [m^2 s^{-1}] \\ D &= \text{molecular diffusivity} & [m^2 s^{-1}] \\ \mu &= \text{dynamic viscosity} & [kg(m*s)^{-1}] \\ \rho &= \text{density of the fluid} & [kgm^{-3}] \end{aligned}$$

3.2.5. Experimental Determination of Mass Transfer Coefficient

k_m is a crucial factor for describing the macrokinetics in the reactor, as it determines the maximum possible current density in the cell.
Apart from estimating k_m by a theoretical model, it can also be determined experimentally by means of Linear Sweep Voltammetry (LSV). This method is known under the name diffusion limiting current technique. Fixed current-voltage characteristics, also called polarization curves, are generated under well-defined hydrodynamic conditions. A fixed potential range is scanned from a lower to an upper voltage limit. A predefined parameter, most commonly the concentration of electrochemically active compounds, is varied. For each variation the corresponding polarization curve is measured by means of a potentiostat. Typical plots of current versus applied potential at different concentrations are shown in Figure 3.6 on the left. They feature a plateau region which indicates the limiting current. The characteristic plot results from the transition from current control to mass transfer control, as described in Chapter 3.2.4. Starting at the equilibrium potential, no current is measured. When increasing the voltage gradually, a rising number of electrons are transferred from the reactants to the anode, leading to a concomitant increase in current. When reaching the point where mass transfer of reactants into the reaction layer equals the rate of electron transfer, the current does not respond to further increase of potential anymore, as the current density is at its maximum. Therefore, the polarization curves show a plateau region, indicating the limiting current for each individual concentration of active compound. When the

overpotential is high enough to induce oxygen evolution, the polarization curve rises again.
The graph on the right side of Figure 3.6 shows the limiting current values as a function of respective concentrations of active compound. A straight line is obtained. From the slope, k_m is calculated according to Eq. 3.10 (Schmidt, 2003). Subsequently, k_m can be engaged to calculate i_{lim} for the landfill leachate, again with Eq. 3.10, applying the respective organic concentration.

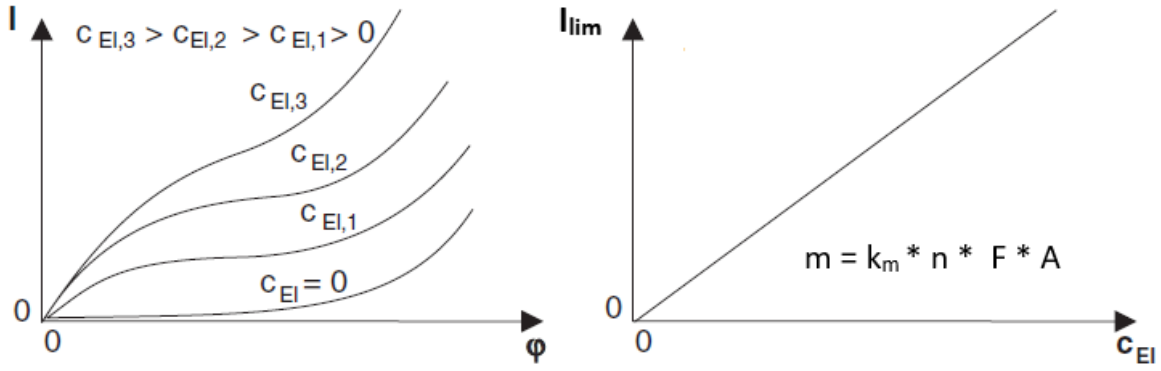

Figure 3.6.: Scheme of current-voltage characteristics obtained for different concentrations of electrochemically active compounds, modified after Schmidt (2003).

This experiment also enables a quick check regarding the influence of various parameters, such as temperature and flow rate, on the mass transfer coefficient. A well studied model reaction for determining k_m is the anodic oxidation of potassium ferrocyanide ($K_4Fe(CN)_6$) to potassium ferricyanide ($K_3Fe(CN)_6$) in sodium hydroxide (Chatzisymeon et al., 2009), (Cañizares et al., 2006a).

3.3. Influencing Factors

In this work, the influence of three parameters on the performance of EO of landfill leachate is investigated. These parameters are pH and temperature of the treated water as well as the applied current. In the following, findings from previous studies on the influence of the chosen factors are summarized.

– **pH**

  Different aspects have to be considered when evaluating the influence of the solution pH on oxidation efficiency.
  First, it should be noted that the solution pH defines the oxidative power of the hydroxyl radicals formed at the anode, according to the Nernst equation:

$$E^0(\bullet OH_{aq}/H_2O) = 2.59 - 0.059\,pH \tag{3.17}$$

where 2.59 V is the redox potential of $\bullet OH_{aq}/H_2O$ at pH 0 at standard condition. It is easy to see that the oxidative power of •OH lowers with the rise of pH (Wu et al., 2016).
Wu et al. (2016) found, that for EO of BPA, the difference in TOC removal efficiency for alkaline and acidic conditions is not as significant as it is for other tested electrode materials. They attribute this observation to an improvement of mass transfer at alkaline conditions due to ionization of BPA. With a dissociation constant (pK_a) between 9.6 and 10.2, deprotonation reactions take place in strongly alkaline solution. Bisphenolate anions form and are drawn to the anode surface by electric potential or attacked by mediators. This effect of mass transfer enhancement at high pH offsets the higher oxidation power of •OH at acidic conditions.
Second, the formation of carbonate (CO_3^{2-}) and hydrocarbonate (HCO_3^-) is promoted by alkaline conditions. These species are known to be effective •OH scavengers and are likely to be present in landfill leachate (Anglada et al., 2011). They are furthermore products of alkaline solution of CO_2, which is a main product of EO (Wu et al., 2016). It is favorable to work at acidic conditions, considering that hydroxyl radicals are the main drivers for organic oxidation on BDD anodes. Moreover, free chlorine, that forms at the anodes when chlorine-containing solutions are oxidized, is more reactive when it is present as hypochlorous acid ($HOCl$) rather than as its alkaline equivalent hypochlorine ions (OCl^-) (Anglada et al., 2011).

Anyhow, when revising existing literature with regard to the influence of solution pH on EO, ambiguous findings have been published.

Cañizares et al. (2004, 2005) studied EO of 4-nitrophenol and several phenolic aqueous wastes on BDD electrodes. They report higher removal efficiencies when working at acidic pH. This observation is ascribed to a higher extend of polymerization and enhanced formation of organic intermediates at alkaline conditions.

Fernandes et al. (2015) state that EO efficiency for landfill leachate at Pt/Ti electrodes rises with increasing pH, with the highest applied pH being 9. One benefit from operating at alkaline pH is that nitrogen is likely to be transformed into nitrogen gas whereas at low pH organic and ammonium nitrogen is oxidized to nitrates. Furthermore, it is reported that acidic conditions favor the formation of chloramines. With more byproducts being formed, the specific energy consumption was found to be higher at low pH.

Murugananthan et al. (2008) studied the oxidation of BPA on BDD anodes and report that the removal rate of BPA and TOC increases with pH. At pH 10, BPA

was removed completely after three hours of electrolysis whereas at pH 2 and 6, it took five hours to eliminate BPA; applying the same current, temperature and initial BPA concentration. They explain the higher removal efficiency at pH 10 with the fact that BPA exists predominantly in its ionized form in this regime, as mentioned above. It is further argued that an electrolysis at strongly acidic pH is less efficient in TOC removal due to neutralization of •OH by H+.

– **Temperature**

The influence of temperature on EO has not been of major interest in past studies. Literature research shows that in most studies on EO treatment of wastewater temperatures around 20 °C were employed (Martínez-Huitle and Ferro, 2006; de Oliveira Campos, 2018; Cabeza et al., 2007b; Urtiaga et al., 2009; Muruganan-than et al., 2008). One of the perks of EO treatment is its applicability at a wide range of temperature. In electrochemisty, working at ambient temperature is desired to reduce energy consumption and consequently operation costs.

However, a rise in temperature is believed to have a positive impact on removal efficiency. Sahiri (1995) reported that an increase in temperature is associated with enhanced mobility of chemical compounds, which is concomitant to a rise in the diffusion coefficient. Cañizares et al. (2006b) studied the influence of temperature on removal efficiency in the EO of effluent from a fine chemicals plant, employing temperatures of 25°C, 40°C and 60°C. They found that the removal efficiency increased with temperature but argue that the temperature does not have a major affect on direct oxidation processes, as the diffusion coefficient is not expected to be greatly modified in the range of temperature studied. They do, howsoever, imply that the rate of indirect oxidation by electrogenerated reagents is significantly improved by temperature. Anglada et al. (2010a) studied EO of landfill leachate at laboratory scale, operating at 10°C, 20°C and 40°C. They report that the mass transfer coefficient enhances with temperature and ascribed this finding to enhancement of diffusivity.

Moreira et al. (2015) did extensive studies on the application of EAOPs for the treatment of landfill leachate and suggest an optimal working temperature of 20 °C for the EO on BDD anodes. de Oliveira Campos (2018) reported a removal of more than 97 % of organic matter from petrochemical effluent in a pre-pilot reactor operating at 25°C using BDD anodes.

No literature was found on the application of EO for landfill leachate at a temperature as low as 4 °C, as intended in this work.

– **Applied Current**

The current density is a parameter often discussed in studies about EO, because it determines the reaction rate and the current efficiency for a given setup. Therefore, this variable has been modified in most works investigating on influencing

parameters for EO. As a general rule, the oxidation rate rises with the applied current, but the current efficiency decreases (when operating under mass transfer control). The higher the current density, the faster the electron transfer from the anode to the compounds in the solution, but the higher the side reactions like oxygen evolution. In electrochemistry, the goal is to work close to the limiting current as, in this range the best ratio of organics removal and current efficiency is yielded (Schmidt, 2003).

3.4. Response Factors

To monitor the chemical reactions proceeding during EO of landfill leachate, a group of parameters is measured. Those factors and their importance for wastewater and its electrochemical treatment are introduced in the following.

– **Total Organic Carbon**

The total organic carbon (TOC) is a common bulk parameter to measure the overall pollution of drinking, surface and wastewaters. It indicates the concentration of the totality of organic compounds present in a sample. In order to identify the TOC of a sample, the organic substance is oxidized to CO_2 through incineration or wet-chemically by oxidizing agents. The released CO_2 is measured and determines the overall organic load in the sample (Koppe and Stozek, 1990).

– **Chemical Oxygen Demand**

The Chemical Oxygen Demand (COD), likewise the TOC, is a bulk parameter widely used for estimating organic concentrations in waters. The information given by COD measurement is the amount of O_2 needed to completely oxidize organic compounds in the sample to CO_2 and H_2O. Strong oxidizing agent are used to oxidize organic compounds present in a sample. As the TOC does not deliver information on the oxidizablitity of detected carbons and the amount of needed oxygen to reduce them, the ratio of COD to TOC gives valuable insights on the nature of organic compounds in the analyzed sample (e.g. on the presence of alcohols, proteins, etc.). Therefore, a shift in COD/TOC ratio can reveal ongoing chemical processes during wastewater treatment. Some inorganic compounds, like NO_2^-, are included in the COD and interfere with the measurement of organics concentration (Gujer, 2007).

– **Ammonium**

Ammonium (NH_4) is a ubiquitous compound of wastewater. It leads to oxygen depletion in water bodies due to microbial processes that induce its oxidation to nitrate and nitrite. Therefore, NH_4 should be removed before discharging wastewater. The chemical equilibrium between ammonium and ammonia (NH_3) is a function of pH:

$$NH_4{}^+ \longleftrightarrow NH_3 + H^+ \tag{3.18}$$

If the pH exceed a value of approximately 9.3, NH_3 concentration exceeds NH_4 concentration. NH_3 is gaseous and is highly toxic to fish.
Organic nitrogen, that prevails in its reduced forms, is transformed mainly to NH_4 during the removal of organic substances. Nitrogen compounds can be converted to elementary nitrogen, which is gaseous and consequently leaks into the atmosphere (Gujer, 2007).

– **Nitrate**

Nitrate (NO_3) is the highest oxidized form of nitrogen. In the presence of O_2, nitrogen is accumulated as NO_3. In the course of oxidation, NO_2^- is an intermediate. Alike NH_3, NO_2^- is toxic to fish and should be removed before releasing effluents into water bodies (Gujer, 2007).

– **Free Chlorine**

Chlorides are a common substance found in wastewater. Because of their ubiquitous appearance and the strong oxidizing properties of active chlorine, it is widely employed for EO of wastewater. Active chlorine can be produced anodically forming gaseous chlorine, hypochlorous acid or hypochlorite ions, according to Eq. 3.19 - 3.21 (Martínez-Huitle and Panizza, 2018):

$$2\,Cl^- \longrightarrow Cl_2 + e^- \tag{3.19}$$

$$Cl_2 + H_2O \longrightarrow HOCl + e^- + Cl^- \tag{3.20}$$

$$HOCl \longrightarrow H^+ + OCl^- \tag{3.21}$$

Apart from enhancing the EO of organic compounds, active chlorine has been found to trigger ammonium oxidation (Cabeza et al., 2007b). However, EO through active chlorine can lead to the formation of chlorinated byproducts. In fact, several sources agree on that especially when treating chloride-containing effluents on BDD anodes, the formation of perchlorate (ClO_4) and chlorinated organic compounds is promoted (Anglada et al., 2011; Li and Ni, 2012; Donaghue and Chaplin, 2013). This is a problematic finding, as ClO_4 features a resistance to further oxidation and its consumption poses several health risks such as carcinogen potential (Urbansky and Schock, 1999; Urbansky, 2002).
Murugananthan et al. (2008) studied the influence of different supporting electrolytes for EO of BPA on BDD anodes and report that, when using Na_2SO_4 and $NaNO_3$ as supporting electrolyte, the organics removal efficiency is significantly higher than when using NaCl. The comparably poor performance of NaCl was attributed to formation of chlorinated organic byproducts which are more resistant to further oxidation.

4. Experimental Part

In this chapter chemicals, instruments and methods applied in the experiments and analyses carried out in the frame of this study are specified. Test records are given for the conducted experiments. The landfill leachate referred to in this work was collected at SHMIL Åremma Landfill in Mosjøen, Norway. The experiments were carried out in the Drinking Water Laboratory and in the Water Analysis Laboratory at the Department for Civil and Environmental Engineering of the Norwegian University of Science and Technology (NTNU).

4.1. Sampling and Storing of Landfill Leachate

The landfill leachate was collected in October 2018 from the municipal landfill site SHMIL Åremma. The raw leachate was initially treated on-site by a physical-chemical process, as described in Chapter 2.3.1. Around 600 L of pre-treated leachate were bottled in a 1 m^3 plastic container and transported to the laboratory facilities in Trondheim. At the Department of Civil and Environmental Engineering at NTNU, the leachate was bottled in 10 and 20 L plastic containers and stored in a cooling chamber at 2 to 4 °C, for stabilization. Before feeding leachate samples from the containers into the tank of the EO reactor, the containers stirred to homogenize compound concentrations.

4.2. Electrochemical Reactor

Experiments are conducted in a *DiaClean*® single-compartment electrolytic flow-cell manufactured by WaterDiam Sarl in Switzerland. The *DiaClean*® unit is embedded in a treatment plant, that connects the cell to a leachate feed tank and a power supply, as can be seen in Figure 4.1. The respective flux scheme is given in Figure 4.2.

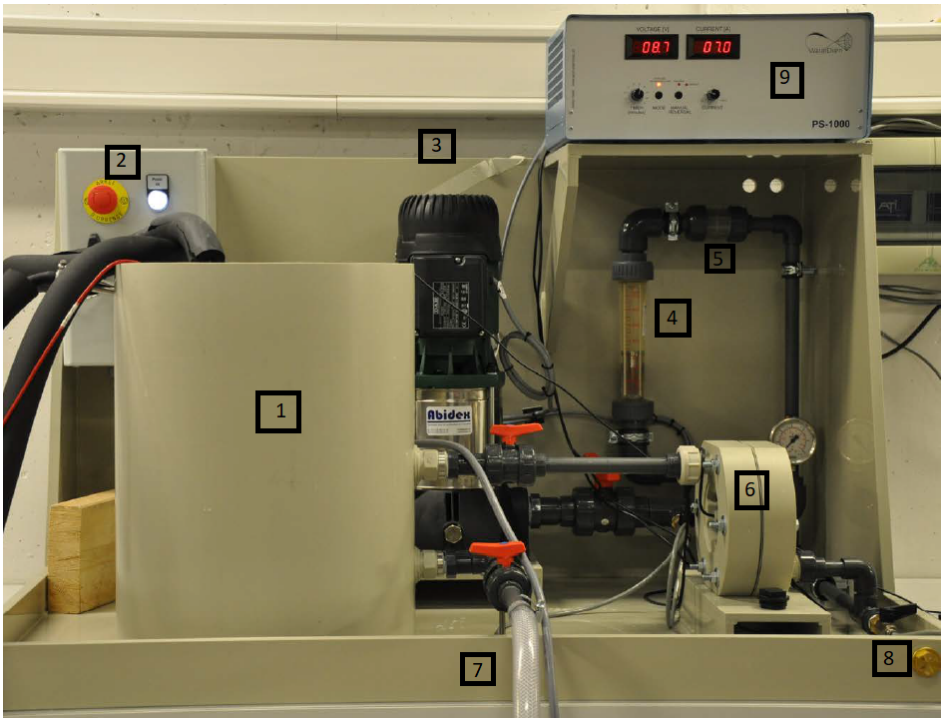

Figure 4.1.: Treatment Plant, with (1) feed tank, (2) power supply for pump, (3) centrifugal pump, (4) flow-meter, (5) filter, (6) electrolytic flow-cell, (7) tank-outlet, (8) sample port and (9) power supply for electrolytic cell.

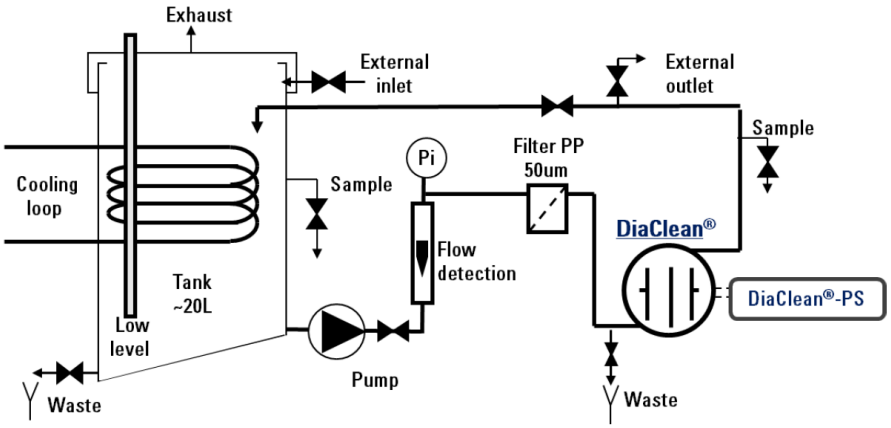

Figure 4.2.: Flux scheme of the treatment plant (WaterDiam, 2015).

In the following, the individual components of the treatment plant are further specified. The numeration refers to the labels given in Figure 4.1:

(1) **Feed Tank**
The feed tank enables the storage of up to 20 L of fluid. The tank material is polypropy-

lene (PP), which is inert and thus does not interact with the fluid. A lid can be put on the tank, which has a hole in it to permit the evacuation of gases produced during the electrolysis, measurement of the solution temperature and pH and their maintenance within the treatable range (below 35 °C). An outlet permits effluent transportation to the electrolytic cell via the centrifugal pump. After passing the cell, the leachate is carried back into the tank. A draining valve (7) is located at the bottom of the tank, to enable the discharge of the effluent into a container.

(2) **Power Supply for the Pump**
The power supply provides the pump with 25 A and 230 V. If the flow-rate sinks below a minimum value, the pump is emergency-stopped to prevent dry working of the system.

(3) **Centrifugal Pump**
To enable the recirculation of the batch feed, a vertical multi-level centrifugal pump is applied. The pump model KVC 20/50 M provided by DAB Pumps Germany GmbH is used. The maximal pump rate is 4800 L/h and the pumping head is 27.4 m.

(4) **Flow-meter**
The flow-meter is installed between the pump and the electrolytic cell, to control the flow rate. Inside the plexiglass cylinder floats a metallic cone that indicates the flow rate on a scale from 100 to 1000 L/h. A low level sensor defines the minimum level for the flow rate and cuts the power supply when the feed stream drops to this threshold.

(5) **Filter**
Before entering the *DiaClean*® unit, the solution is transmitted through a filter that retains particles bigger than 50 μm to prevent the hydraulic canals in the compartment from getting blocked.

(6) **Electrolytic Cell**
The *DiaClean*® single-compartment electrolytic flow-cell consists of two circular electrodes. BDD on silicon is the material used for both electrodes. The electrodes are manufactured by NeoCoat SA. The area of each electrode is 70 cm^2. The electrode gap is 1 mm. The silicon support has a thickness of 2 mm and a resistivity of 100 mΩcm. The BDD film is 2 to 3 μm thick and contains a boron concentration of 500 to 1000 ppm. The cell is crossed by an electric stream as well as an hydraulic stream. The connection to the poles of the power supply defines which electrode is used as a cathode and which as an anode. Switching the cable connections, e.g. for each experimental run, provides for equal erosion. The hydraulic stream enters at the bottom of the cell through an O-ring. It then proceeds vertically through the cell and exits at the top. The vertical upstream flow enhances the evacuation of produced gases.
To preserve their functionality, all parts of the cell that get in contact with the effluent are kept in polypropylene or elastomer (Viton).

(7), (8) **Valves**
Valve (7) is used to open the drain of the tank and release the effluent. Valve (8) can be operated to take samples. It is located between the filter and the electrolytic cell. Another sampling port can be found between filter and pump. In the same location, a valve with an orange handle (see Figure 4.1) can be manipulated to adjust the flow rate.

(9) **Power Supply for the Electrolytic Cell**
Two different DC power supplies are used for the EO experiments. The *DiaClean*® PS-1000 works in a range from 0.6 to 20 A. The ES 0300 by Delta Elektronika is used for small current values up to 450 mA. The power supplies deliver a continuous current, that is specified by the user. The voltage is floating and fitted to the current value. The maximum potential for the electrolytic cell is 12 V. For the *DiaClean*® PS-1000, a reversal mode can be chosen. When applying this mode, the polarity of the electrodes is interchanged with a tunable frequency (5 - 70 min). Thereby, both electrodes are fretted equally and their life cycle is extended. Similarly, when working with the ES 0300, the poles are interchanged after each experimental run.

Refrigerated Circulator
Continuous pumping of the effluent and electrochemical processes lead to fluctuations in temperature. To cool the effluent down and keep the temperature constant during the experimental runs, a spiral coil is immersed in the tank, circulating a refrigerating fluid. For this use, the F25-ME Refrigerated/Heating Circulator by Julabo GmbH is applied. A Pt100 External Sensor is immersed in the bath fluid, measuring the external temperature of the effluent in the reactor. In accordance, the internal temperature of the refrigerating fluid is adjusted to cool the effluent down to the desired working temperature, i.e. to maintain the temperature constant. The refrigerating fluid (Thermal H10 distributed by Julabo GmbH) can be cooled down to approx. -20 °C. For optimization of the temperature control, a set of parameters can be adjusted to fit the application at hand:

- Xp_{ext} describes in which approximation to the setpoint the cooling capacity is reduced, so that the temperature reaches the setpoint slowly, without exceeding it. The possible range for Xp_{ext} is 0.1 to 99.9. A level of 0.7 is applied in this work.

- Tv_{ext} can be adjusted to minimize the transient time. If high overshooting of the setpoint is observed, the Tv_{ext} level is too low. Excessive values for Tv_{ext} manifest themselves in instabilities and oscillations. The possible range for Tv_{ext} is 0 to 999. A level of 45 is chosen in this work.

- Tn_{ext} defines the reset time for a proportional regulation. An insufficient value may cause instabilities, whereas excessive values prolongate the compensation

process unnecessarily. The possible range for Tn_{ext} is 3 to 9999. A level of 720 is applied in this work.

Neoprene covers are installed around the tubes that connect the spiral coil to the Julabo Refrigerating Circulator and around the tank to prevent heating effects through interaction with the ambient air.

To cool the leachate down to 4 °C, an additional cooler is needed. In that case, the C1G Refrigerated Immersion Cooler distributed by Grant Instruments Ltd is used. The internal temperature is set to 0 °C. This device does not dispose of a sensor to measure the effluent temperature. The temperature control is still performed by the Julabo Refrigerated Circulator.

4.3. Chemicals and Measuring Instuments

In the following, all **chemicals** used in the experiments conducted in the frame of this work are listed:

– **Potassium indigotrisulfonate**, by Sigma-Aldrich, CAS Number: 67627-18-3, Empirical Formula: $C_{16}H_7K_3N_2O_{11}S_3$, Molecular Weight: 616.72 g/mol, Structural Formula: see Figure 4.3.

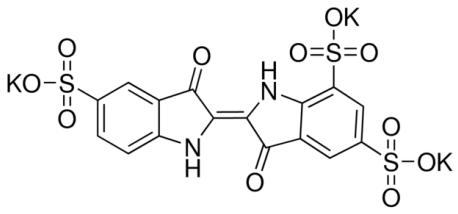

Figure 4.3.: Structural formula of potassium indigotrisulfonate (Sigma-Aldrich, 2019).

– **Potassium hexacyanoferrate(II) trihydrate**, by Sigma-Aldrich, CAS Number: 14459-95-1, Linear Formula: $K_4Fe(CN)_6 \cdot 3\,H_2O$, Molecular Weight: 422.39 g/mol.

– **Potassium hexacyanoferrate(III)**, by Sigma-Aldrich, CAS Number: 13746-66-2, Linear Formula: $K_3Fe(CN)_6$, Molecular Weight: 329.24 g/mol.

– **Sodium hydroxide**, by Sigma-Aldrich, CAS Number: 1310-73-2, Linear Formula: NaOH, Molecular Weight: 40.00 g/mol.

– **Sodium sulfate**, by Sigma-Aldrich, CAS Number: 7757-82-6, Linear Formula: Na_2SO_4, Molecular Weight: 142.04 g/mol.

- **ortho-Phosphoric acid, 85%**, by Merck KGaA, Article Number: 100573.
- **Milli-Q® water**, by Merck KGaA, purified water Type 1.

Table 4.1 contains a list of all **measuring instruments** that are used in the analysis of experiments conducted in the frame of this study and that are not already specified elsewhere.

Table 4.1.: Measuring instruments.

Type of Device	Manufacturer	Model
UV/Vis Spectrophotometer	PerkinElmer	Lambda 650
Total Organic Carbon Analyzer	TeleDyne Tekmar	Apollo 9000
Potentiostat	Gamry Instruments	Reference 600
Portable Spectrophotometer	Hach-Lange GmbH	DR1900
pH and ORP Meter	Hach-Lange GmbH	Sension+ PH 31 GLP
Microprocessor Conductivity Meter	WTW	LF 537
Analytical Balance	Sartorius AG	A200S

For determining the concentrations of follow-up parameters during the EO treatment, a set of **cuvette-tests** provided by Hach-Lange GmbH are employed. They are specified in the following:

- **COD**
  COD concentrations are analyzed with the Cuvette-Test LCK 314. It is applicable in a working range of 15 to 150 mg/L O_2. Potassium dichromate is used to oxidize organic compounds in the sample. The digestion solution contains sulfuric acid and mercuric sulfate. A sample volume of 2 mL is needed for the analysis. The sample is heated to 149 °C for 2 hours in the LT200 Thermostat by Hach-Lange GmbH, then cooled at room temperature for one hour. The absorbance is measured at a wavelength of 694 nm. The cuvettes are stored at room temperature (Hach Lange GmbH, 2014).
- **NH_4-N**
  For the determination of NH_4-N concentration, Cuvette-Test LCK 303 is used. It is applicable in a working range of 2.0 to 47.0 mg/L NH_4-N. The colorimetric analysis is based on the reaction of NH_4-N with hypochlorite and salicylate ions to indophenol blue at pH 12.6. Sodium nitroprusside is used as a catalyst. A sample volume of 200 μL is needed for the analysis. The final absorbance is reached after 15 minutes and can be determined photometrically at a wavelength of 694 nm. The cuvettes are stored in a refrigerator at 2 to 8 °C (STEP Systems GmbH, 2000; Hach Lange GmbH, 2019).

– **NO_3-N**
Cuvette-Test LCK 339 is applied to determine NO_3-N concentrations. The working range of this test is 0.23 to 13.5 mg/L. The colorimetric analysis is based on the reaction of NO_3-N with 2.6-dimethylphenol to 4-nitro-2.6-dimethylphenol in sulphuric and phosphoric acids. The product gives the solution a yellow color, which is more intense at higher concentrations of NO_3-N. A sample volume of 1 mL is needed for the analysis. The final absorbance is reached after 15 minutes and can be determined photometrically at a wavelength of 370 nm. The cuvettes are stored at room temperature (Hach Lange GmbH, 1995).

– **Free Chlorine**
The concentration of hypochlorous acid and hypochlorite is determined by means of the USEPA DPD Method. The working range of this test is 0.1 to 8.00 mg/L Cl_2. An indicator powder containing N,N-diethyl-p-phenylenediamine (DPD) is added to the sample. Free chlorine immediately reacts with DPD to form a pink color, which is proportional to the chlorine concentration. The sample volume needed for this analysis is 5 mL. Color intensity is measured using the POCKET Colorimeter by Hach-Lange GmbH (Hach Lange GmbH, 2018). The first leachate sample, taken at t = 0 min, is used for calibration.

4.4. Design of Experiments

To assess the significance of the tested influencing parameters for the EO process, a design of experiments (DoE) is applied for statistical analysis. For that purpose, the software Minitab 18 is used. A 2^3 (three influencing parameters with two values each) full factorial design is performed to investigate on the effect of the independent variables pH, temperature and current. Each variables is ascribed a high and a low level, which are specified in Table 4.2. Each experiment is repeated once, resulting in a total of sixteen experiments required. The run order is randomized to reduce bias of the results by uncontrolled interference. The results obtained are evaluated in terms of concentrations of COD, TOC, $NH_4 - N$ and $NO_3 - N$. Analyses involve the estimation of average effect, main effects of each individual variable as well as their two and higher order interaction effects based on a multiple linear regression model. Effects that fall below the standard error are considered insignificant.

Table 4.2.: Independent variables of the 2^3 factorial design of experiments.

Level of Value	pH	Temperature (°C)	Current (mA)
-	5	4	110
+	10	20	320

To visualize the significance of the different factors, a **Pareto chart** is generated. It

shows the absolute values for the standardized effects in descending order. To standardize the effects, t-statistics are used with the underlying null hypothesis that the effect is 0. The statistical significance of the tested factors is indicated by a reference line, using a confidence level of 95 %. If the absolute value of a factor exceeds the level indicated by the reference line, the factor can be considered as statistically significant at a significance level of $\alpha = 0.05$. Subsequently, variation of this factor is associated to changes in the response factors.

Residual plots are consulted to check the model and the underlying assumptions on normality. Four different kinds of residual plots are generated by Minitab 18 (Minitab Inc., 2017):

- The **Normal Probability Plot** verifies a normal distribution of the residuals by displaying them against their expected values. The plot should approximately follow a straight line.
- The **Histogram** shows the distribution of residuals for all observations and reveals skewed data and outliers.
- The **Residual vs. Fits Plot** is used to check the residuals for constant variance. The points should be randomly distributed on both sides of 0, without recognizable patterns.
- The **Residual vs. Order Plot** is applied to ensure that the residuals are not correlated with each other. Displaying the residuals in time order should not show a trend or pattern; they should fall randomly around the center line.

4.5. Experimental Procedure

In this section, the procedure adopted during the three experimental series conducted in the frame of this study are explained in detail.

4.5.1. Linear Sweep Voltammetry

To determine k_m for the hydraulics of the reactor, the diffusion limiting current technique as described in Chapter 3.2.5 is applied. Two settings for the flow rate are tested and compared: 300 L/h and 600 L/h.
The redox couple $K_4Fe(CN)_6/K_3Fe(CN)_6$ is used and the oxidation of Fe^{2+} to Fe^{3+} at the anode is followed by potentiostatic measurements. 2:1 mixtures of $K_4Fe(CN)_6$ (as potassium hexacyanoferrate(II) trihydrate) and $K_3Fe(CN)_6$ (as potassium hexycyanoferrate (III)) in different concentrations ranging from 4 to 24 mM $K_4Fe(CN)_6$ are employed and polarization curves are recorded. The exact molecular concentrations and corresponding masses of $K_4Fe(CN)_6$ and $K_3Fe(CN)_6$ are given in Table 4.3.

Table 4.3.: Molecular concentrations and corresponding masses of $K_4Fe(CN)_6$ and $K_3Fe(CN)_6$ for the LSV experiment.

Polarization Curve	$c_{K_4Fe(CN)_6}$ (mM)	$m_{K_4Fe(CN)_6}$ (g)	$c_{K_3Fe(CN)_6}$ (mM)	$m_{K_3Fe(CN)_6}$ (g)
1	4	22.100	2	9.876
2	8	44.201	4	19.752
3	12	66.301	6	29.628
4	16	88.402	8	39.504
5	24	132.602	12	59.256

The electrodes of the *DiaClean*® electrolytic cell are connected to the correspondent cell cables of the Reference 600 Potentiostat. One cell is defined as working electrode. It is connected to the blue and the green cell cable. The other electrode functions as reference/counter electrode and is connected to the red and the white cell cable. Gamry software (Gamry Framework and Gamry Echem Analyst) is used to write the correspondent scripts for recording the polarization curves and analyzing the data. A scan rate of 100 mV/s and a scan interval from -0.5 to 3.5 V are applied.

NaOH is used as supporting electrolyte. 300 g NaOH pellets are diluted in 3 L of Ultrapure Milli-Q® water (Milli-Q). The reactor tank is filled with 12 L of Milli-Q and the NaOH solution is added, summing up to 15 L 0.5 M NaOH solution in the tank. A blank curve is recorded for $c_{K_4Fe(CN)_6} = 0\,mM$, for both Q = 300 L/h and Q = 600 L/h.

For each polarization curve, the correspondent weighted samples of $K_4Fe(CN)_6$ and $K_3Fe(CN)_6$ are prepared. A flow rate of 300 L/h is adjusted and the weighted samples for Polarization Curve 1 are added to the tank. When $K_4Fe(CN)_6$ and $K_3Fe(CN)_6$ are dissolved, the polarization curve is recorded. Subsequently, the flow rate is adjusted to 600 L/h and again a polarization curve is recorded. The second pair of weighted samples is added and dissolved. The added masses of $K_4Fe(CN)_6$ and $K_3Fe(CN)_6$ correspond to the mass difference needed for Polarization Curve 1 and Polarization Curve 2. Polarization Curve 2 is recorded for both flow rates. This procedure is repeated for all polarization curves.

The current-voltage characteristics show a plateau region which indicates the limiting current. The limiting current values for each polarization curve are applied as a function of the correspondent $K_4Fe(CN)_6$ concentrations. A straight line is obtained and k_m is calculated from the slope.

When finishing the experimental run, the effluent is discharged through the outlet valve. The filter is removed and rinsed; then build in again. To clean the reactor, 15 L of Milli-Q are filled in the tank and recirculated for about 10 minutes. This procedure

is repeated two times.

4.5.2. Electrochemical Oxidation Experiments with Potassium Indigotrisulfonate

Preliminary experiments are conducted with potassium indigotrisulfonate (PI) as a model organic substance. PI is a textile dye of deep blue color. Its concentration can be tracked via absorbance measurement using UV-Vis spectrophotometry.

In a first set of experiments, the dye degradation in leachate is compared to the dye degradation in 0.05 M Na_2SO_4 solution at a flow rate of 300 L/h. 15 L of effluent (leachate or Na_2SO_4 solution) are spiked with 50 mg/L PI. Experiments are performed at 100 mA and 7 A.

In a second set of experiments, the rate of dye degradation in leachate is analyzed for different current intensities at 4 °C and 600 L/h. The leachate is spiked with 50 mg/L PI.

To spike the effluent with PI, a solution of 750 mg PI in 0.5 L Milli-Q is prepared. For the experiments in 0.05 M Na_2SO_4 solution, 14.5 L Milli-Q are filled in the reactor tank and 106.53 g Na_2SO_4 are added. For the experiments in leachate, 14.5 L of leachate are filled in the tank. The dye solution is added. The desired temperature and flow rate are adjusted. pH and conductivity are measured continuously in the reactor tank. Once the setpoint for temperature is reached, the first sample is taken and the power is switched on immediately after sampling. The *DiaClean*® PS-1000 power supply is used for I = 7A and I = 1 A. The polarity reversal function is enabled to switch polarities of the electrodes every 30 minutes. The ES 0300 power supply is used for I = 100 mA and I = 300 mA. The polarities of the electrodes are switched for each run by switching the cable connections. Every 20 minutes, a sample volume of approximately 10 mL is discharged from the sample port into a 20 mL beaker glass. 5 mL are pipetted into a glass tube containing thiosulfate as inhibitor to stabilize the sample. The remaining sample volume is loaded back into the tank. pH, temperature, potential and conductivity for every time step are noted down in a test protocol. The test protocols can be found in the supplementary material.

After the experiments, the reactor is cleaned as described in Chapter 4.5.1.
The samples are diluted 1:5 with Milli-Q, using 25 mL flasks. The dilution is needed to degrade the dye concentration down to the linear range of absorbance measurement. The Lambda 650 UV/Vis spectrophotometer is used to determine the absorbance of the samples at a wavelength of 600 nm, which is the absorbance maximum of PI. The measurement is started with the last taken sample which has the lowest dye concentration. In this way, interference through carry-over of concentrations from one sample to

the next is minimized. The silica glass cuvette is rinsed three times with Milli-Q after each measurement.

Calibration curves are prepared to find the linear correlation between absorbance and dye concentration. Standards with concentrations from 0.1 to 10 mg/L PI are employed. Blank samples are taken, measuring the absorbance of effluent without PI added. The calibration curves are given in Figure 4.4. The correspondent data is given in Table 4.4.

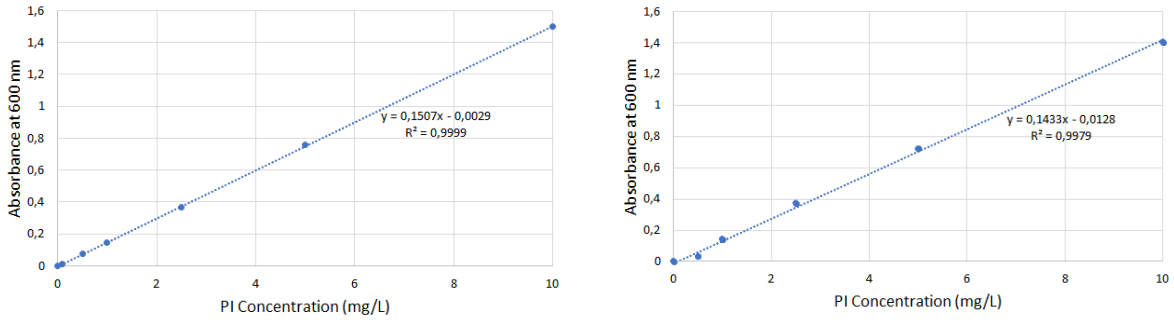

(a) Calibration Curve in Milli-Q (b) Calibration Curve in Leachate

Figure 4.4.: Calibration curves for the determination of PI concentrations through absorbance measurements in (a) Milli-Q and (b) leachate.

Table 4.4.: Standard concentrations of PI and corresponding absorbance (Abs) at $\lambda = 600$ nm.

C_{PI} (mg/L)	0	0.1	0.5	1.0	2.5	5.0	10.0
$Abs_{\text{Milli-Q}}$	0.0004	0.0127	0.0730	0.1428	0.3682	0.7588	1.5013
$Abs_{Leachate}$	0.0003	-	0.0352	0.1436	0.3736	0.7224	1.4041

The equations for the linear trendlines given in Figure 4.4 are inversed to obtain the PI concentration as a function of the absorbance:

$$c_{\text{PI,Milli-Q}} = 6.6357 \cdot Abs + 0.0192 \quad (mg/L) \tag{4.1}$$

$$c_{\text{PI,Leachate}} = 7.0472 \cdot Abs + 0.0197 \quad (mg/L) \tag{4.2}$$

The concentration for samples in Na_2SO_4 solution is calculated by Eq. 4.1. Eq. 4.2 is applied to determine PI concentration in leachate. To evaluate the degradation efficiency, normalized concentration profiles of PI are produced.

The correspondent rate constants (k) are calculated for the concentration profiles. Curves with a constant slope are best described by zero order reaction kinetics. The

linear trend suggests that no concentration term affects the rate of reaction. An exponential trend, in contrast, suggests that k is directly proportional to the concentration of the reactant ([A]). The reaction is described by first order kinetics. Table 4.5 summarizes the rate laws needed to calculate the rate constant k for zero and first order reactions (Upadhyay, 2006):

Table 4.5.: Rate laws for zero and first order chemical reactions (Upadhyay, 2006).

Reaction Order	Rate Law	Integrated Rate Law
Zero Order	$-d[A]/dt = k_0$	$[A] = [A]_0 - k_0 t$
First Order	$-d[A]/dt = k_1[A]$	$[A] = [A]_0 \cdot e^{-k_1 t}$

The integrated rate law can be used to calculate k:

$$k_0 = 1/t \cdot ([A]_0 - [A]) \tag{4.3}$$

$$k_1 = 1/t \cdot ln([A]_0/[A]) \tag{4.4}$$

k is calculated for every time step t between two measurements and a final average is built.

Additionally, a kinetic model previously proposed by Cabeza et al. (2007c) for the removal of organic matter in landfill leachate on BDD anodes is applied to evaluate its applicability to the study at hand. The model is described by Equation 4.5 and assumes that the oxidation of organic matter takes place mainly at the electrode surface and that the limiting step is the organics transfer from the electrolyte to the anode:

$$C_{org} = C_{org,0} \cdot exp[-(\frac{A \cdot k_m}{V})] \cdot t, \tag{4.5}$$

where A is the anode area and V is the treated volume.

As electric energy is the main consumable of EO processes, it is important to monitor the energy consumption. A useful method is to illustrate the cumulative energy consumption as a function of removal rates. This plot allows to compare current efficiencies regarding elimination rates for different applied currents.

The electrical work (W) consumed in an electric circuit for moving charge against the electric field forces at constant levels of current and voltage (U) can be expressed with Eq. 4.6 (Schmidt, 2003):

$$\Delta W = U \cdot I \cdot \Delta t \tag{4.6}$$

The cumulative energy consumption is evaluated for every experimental run of this series and presented as a function of the correspondent PI elimination.

4.5.3. Electrochemical Oxidation of Landfill Leachate

To evaluate the influence of the factors pH, T and I on the efficiency of EO treatment of real leadchate, a factorial design of experiments is established as described in Chapter 4.4. Each factor is assigned a low and a high level. For pH, the high level (approx. pH 10) is given by the inherent pH of the pre-treated leachate. The low level (pH 5) is suggested by literature (Anglada et al., 2011; Vlyssides, 2003)). For temperature, the aim is to evaluate the treatability of the leachate at low levels, being 4 °C a good average for leachate temperatures in winter. The high level of 20 °C is a common setting in EO of landfill leachate (Cabeza et al., 2007b; Urtiaga et al., 2009; Anglada et al., 2010b)) and is therefore chosen as a reference point. As for the applied current, the aim is to have one value below and one value above the limiting current. The high level of 320 mA corresponds to approximately 1.5 I_{lim}. The low level of 110 mA corresponds to approximately 0.5 I_{lim}.

The run order is suggested by the Minitab 18 software and is based on a random distribution to minimize data bias. A list of the settings for each experiment and the run order are given in Appendix B.

A fixed flow rate of 600 L/h is applied in all runs. The batch volume of leachate is 15 L. pH and conductivity are measured continuously throughout the experimental runs. For those experiments where the effluent's inherent pH is adjusted to acidic conditions, the appropriate amount of 85 % ortho-Phosphoric acid is added. For those experiments where the effluent is cooled down to 4 °C, the C1G Refrigerated Immersion Cooler is applied. The experiment is initiated once the setpoints for T and pH are reached. After the first sample is taken, the power supply ES 0300 is switched on immediately and the time is taken. During the first hour, samples are taken every 20 minutes. Starting from minute 60, the sampling frequency is set to 30 minutes. The last sample is taken after 240 minutes. A sample volume of approximately 100 mL is discharged from the sample valve into a 200 mL beaker glass. pH, temperature and conductivity are noted for every sample time. The cuvette-tests for determination of NH_4-N and NO_3-N concentrations are prepared and the absorbance is measured after 15 minutes. The Portable Spectrophotometer DR1900 by Hach-Lange is used, which is pre-programmed for determining the concentrations of Hach-Lange cuvette-tests. The COD cuvette-test is prepared and disposed in the LT200 Thermostat, where it is heated for 2 hours at 149 °C. The COD test is cooled down at room temperature for another hour, after which the COD concentration is determined in the Spectrophotometer DR1900. Free chlorine is measured using indicator powder. The first sample is used to calibrate the POCKET Colorimeter. 5 mL of sample are pipetted into the dedicated cuvette, one sachet of indicator powder is added, the cuvette is closed and shook for 20 seconds. The concentration of HOCl and OCl^- is determined with the colorimeter. 40mL-glasses for TOC measurement are filled with sample and acidified

with ortho-phosphoric acid. The samples are given to the Water Analysis Laboratory at the Department for Civil and Environmental Engineering, NTNU, where the TOC concentrations are determined.

After each experimental run, filter and tank are rinsed as described in Chapter 4.5.1. The cable connections of the power supply to the electrolytic cell are switched for each run to erode both electrodes equally.

Protocols documenting the measured data for each of the 16 experimental runs are attached in the supplementary material. The measured data is read into the Minitab 18 Software for statistical analysis. The corresponding Minitab file containing regression models for all factors is likewise attached in the supplementary material.

5. Results

5.1. Limiting Current Density

Two methods are applied to determine the limiting current density for the given reactor hydraulics; an empirical model and an experimental approach.

5.1.1. Empirical Determination of the Limiting Current Density

The model presented in Chapter 3.2.4.1 is implemented to estimate i_{lim} for EO of organic compounds in SHMIL Åremma Landfill Leachate. The values for the parameters used in Eq. 3.10 to 3.16 are given in Table 5.1. The molecular diffusivity needs to be estimated, as it is not known for the landfill leachate. In this study, the molecular diffusivity of BPA is employed, as it is an organic compound which has been detected in the landfill leachate and is a target to EO. For Eq. 3.15 the width of the duct is neglected because it is significantly smaller than the height.

Table 5.1.: Parameters used in Eq. 3.10 - 3.16 for empirical estimation of i_{lim}.

Parameter	Symbol	Unit	Value
Exchanged electrons	n	[-]	4
Concentration of organics in solution	C_{org}	$mol \cdot m^{-3}$	1.51
Hydraulic diameter	d_{hyd}	m	$2 \cdot 10^{-3}$
Molecular diffusivity of BPA	D_{BPA}	$m^2 s^{-1}$	$5.89 \cdot 10^{-10}$
Faraday constant	F	$C \cdot mol^{-1}$	96485.33
Density of water	ρ	$kg \cdot m^{-3}$	998.29
Flow rate	Q	$L \cdot h^{-1}$	600
Flow-through area	A_{flow}	m^2	$9.44 \cdot 10^{-5}$
Electrode area	A_e	m^2	0.007
Electrode diameter	h	m	$9.44 \cdot 10^{-2}$
Inner electrode gap	b	m	$1 \cdot 10^{-3}$
Dynamic viscosity of water	μ	$kg(m \cdot s)^{-1}$	$1.002 \cdot 10^{-3}$

Table 5.2 provides the results obtained through Eq. 3.10 to 3.13 and 3.16 when inserting the values given in Table 5.1.

Table 5.2.: Results obtained through Eq. 3.10 to 3.13 and 3.16

Parameter	Symbol	Equation	Unit	Value
Schmidt number	Sc	3.16	-	1704
Reynolds number	Re	3.13	-	3517
Sherwood number	Sh	3.12	-	184.1
Mass transfer coefficient	k_m	3.11	ms^{-1}	$5.42 \cdot 10^{-5}$
Limiting current density	i_{lim}	3.10	Am^{-2}	31.68

By multiplying the limiting current density with the electrode surface, the limiting current is obtained:

$$I_{lim} = i_{lim} A_e = 0.222\, A$$

5.1.2. Experimental Determination of the Limiting Current Density

For the determination of k_m, the diffusion limiting current technique as described in Chapter 3.2.5 and Chapter 4.5.1 is applied. The experiment is performed at two different flow rates to evaluate the influence of the flow rate on the limiting current density. At 300 L/h, the flow through the electrolytic cell is laminar ($Re = 1758$). The polarization curves for this experiment can be seen in Figure 5.1. Applying a flow rate of 600 L/h, a turbulent flow ($Re = 3517$) arises in the cell. The corresponding polarization curves are depicted in Figure 5.3. For the experiment at 600 L/h no curve is obtained at a $K_4Fe(CN)_6$ concentration of 24 mM.
For both flow rates, the plateau region can be observed approximately between 1.5 and 3 V. It was decided to select the current value at 2.5 V for each run to determine the limiting current. Figures 5.2 and 5.4 show the limiting current plotted against the corresponding concentration of $K_4Fe(CN)_6$ for 300 L/h and 600 L/h, respectively. In both cases, a good linear fit can be observed and k_m is calculated from the slope. Table 5.3 summarizes the values for the limiting current and the respective mass transfer coefficient for each concentration of $K_4Fe(CN)_6$. The average k_m values are calculated from the experimental data, resulting in an average k_m of $3.10 \cdot 10^{-5}$ for a flow rate of 300 L/h and $5.26 \cdot 10^{-5}$ for 600 L/h. i_{lim} for the oxidation of organic matter in the leachate is determined by applying $\bar{k_m}$ and the initial COD concentration to Eq. 3.10, resuling in:

$$i_{lim,300L/h} = 18.13 \quad A/m^2$$
$$i_{lim,600L/h} = 30.72 \quad A/m^2$$

i_{lim} is multiplied by the anode area to obtain the limiting current of 127 mA for 300 L/h and 215 mA for 600 L/h.

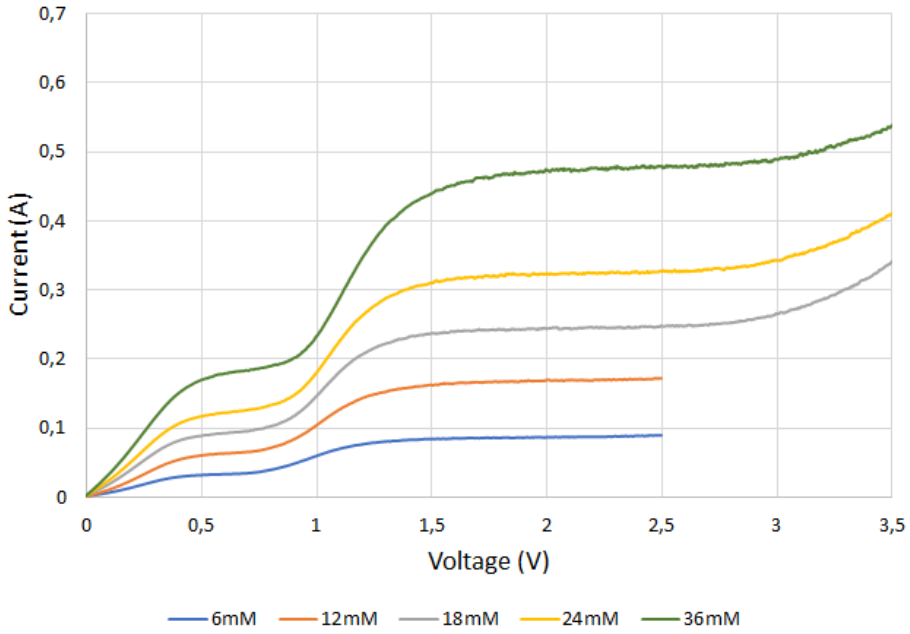

Figure 5.1.: Polarization curves for different molar concentrations of potassium ferrocyanide at Q = 300 L/h.

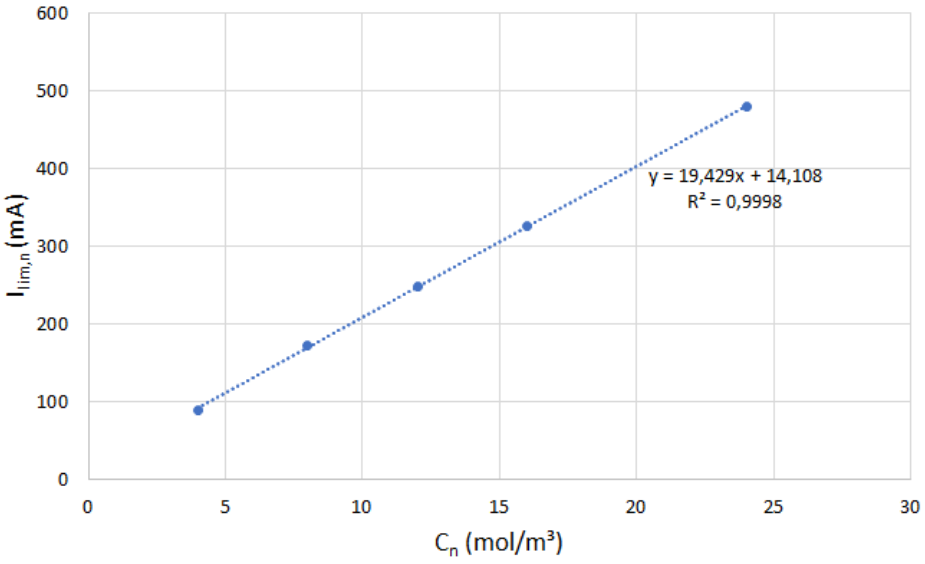

Figure 5.2.: Limiting current as a function of potassium ferrocyanide concentration for Q = 300 L/h.

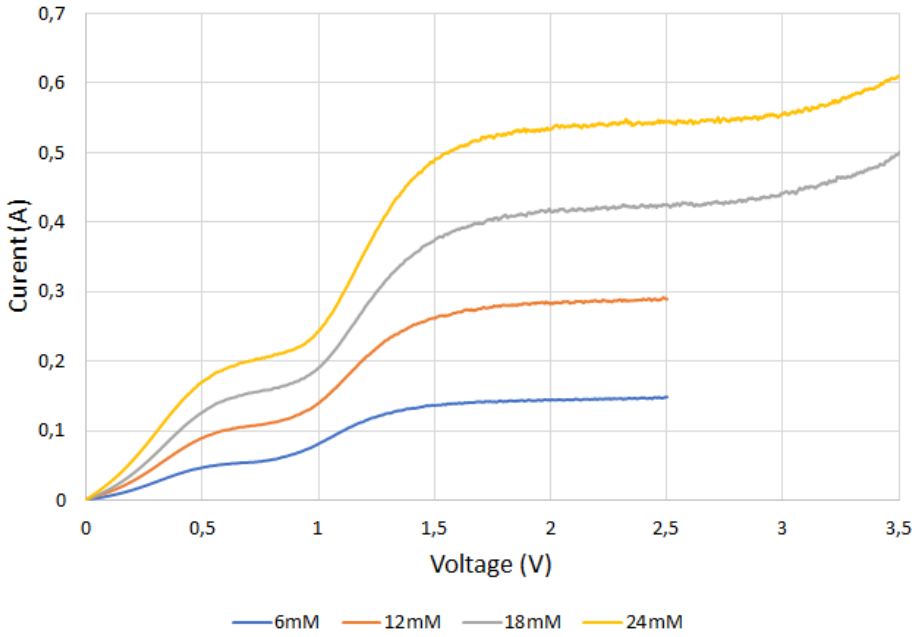

Figure 5.3.: Polarization curves for different molar concentrations of potassium ferrocyanide at Q = 600 L/h.

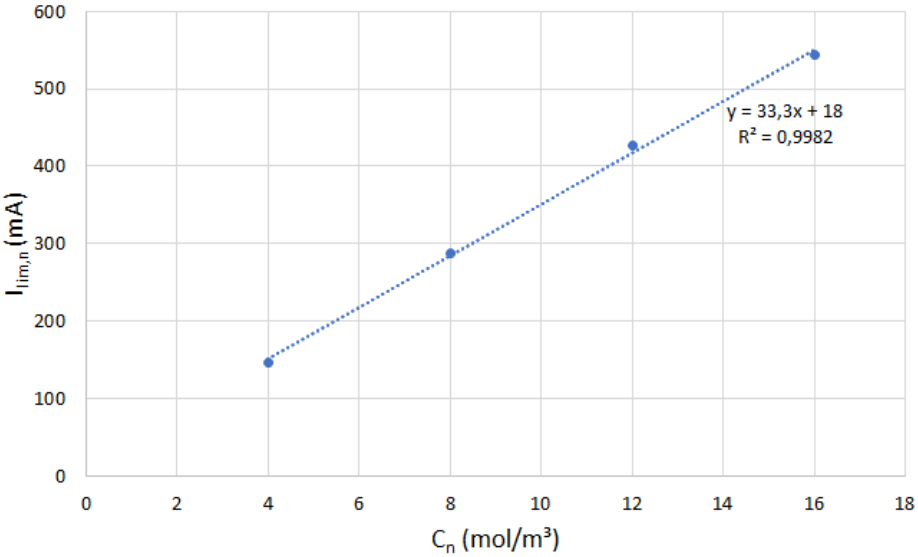

Figure 5.4.: Limiting current as a function of potassium ferrocyanide concentration for Q = 600 L/h.

Table 5.3.: Limiting current and mass transfer coefficient for different molar concentrations of potassium ferrocyanide.

$c_{K_4Fe(CN)_6,n}$ (mM)	$I_{lim,n}$ (mA)		$k_{m,n}$ ($10^{-5}\cdot$ m/s)	
	300 L/h	600 L/h	300 L/h	600 L/h
4	89	146	3.29	5.4
8	172	288	3.18	5.33
12	248	426	3.06	5.26
16	326	544	3.02	5.03
24	479	-	2.96	-
$\bar{k_m}$			3.10	5.26

5.2. Electrochemical Oxidation of Potassium Indigotrisulfonate

Figure 5.5 shows the normalized concentration profiles of PI degradation in Na_2SO_4 solution and in landfill leachate for the applied currents of (a) 100 mA and (b) 7A at a flow rate of 300 L/h. The blue dots show the degradation curves in sodium sulfate solution, likewise the gray dots in landfill leachate. Furthermore, the model predictions obtained through the application of Equation 4.5 are compared to the experimental data recorded in this study.
Both curves obtained at I = 100 mA are best fitted with zero order reaction kinetics. The coefficients of determination (R^2) for the respective extrapolated linear trends are specified in Table 5.4, along with the values for k calculated according to Equation 4.3. The curves obtained at I = 7 A show first order reaction characteristics, therefore Equation 4.4 was applied to calculate k. The respective values for k and R^2 are likewise listed in Table 5.4.

Figure 5.6 depicts the cumulative energy consumption for the performed experiments as a function of PI elimination. In Na_2SO_4 solution, about 1.5 Wh of energy are consumed during 4 hours of treatment at 100 mA, yielding a PI elimination of 24 %. In Leachate, 1.2 Wh are consumed, yielding 36 % of PI removal after 3 hours of oxidation.
At a current intensity of 7A, PI is degraded completely from the leachate after 2 hours of treatment with a total energy consumption of approx. 180 Wh. For the same treatment duration, PI elimination yields 49 % in Na_2SO_4 solution, consuming around 120 Wh of energy.

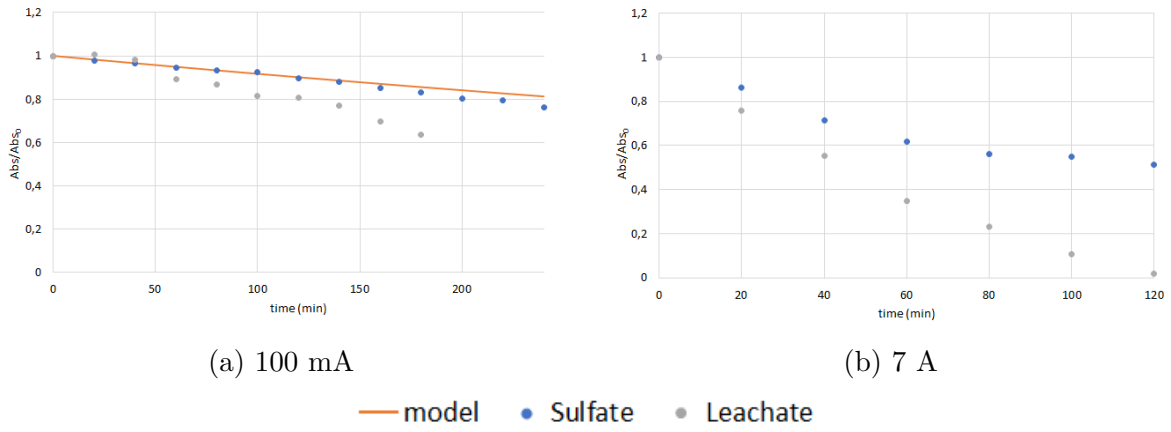

(a) 100 mA (b) 7 A

Figure 5.5.: Normalized concentration profiles of PI degradation at 300 L/h in 0.05 M Na_2SO_4 solution and in landfill leachate for (a) 100 mA and (b) 7A, compared to the model assumption. The experiments in Na_2SO_4 solution are run at a temperature of 20 °C, the experiments with landfill leachate at 4 °C.

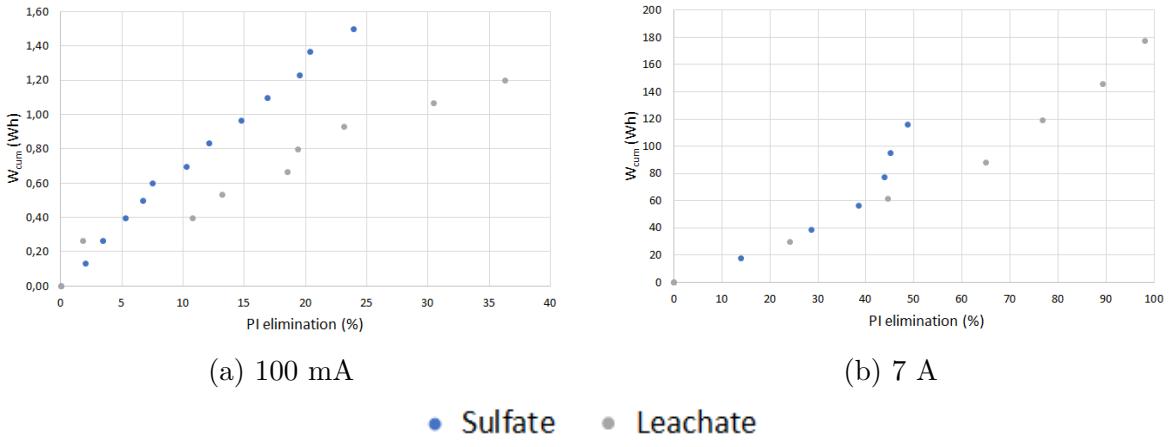

(a) 100 mA (b) 7 A

Figure 5.6.: Cumulative energy consumption as a function of PI elimination at 300 L/h in 0.05 M Na_2SO_4 solution and in landfill leachate for (a) 100 mA and (b) 7A. The experiments in Na_2SO_4 solution are run at a temperature of 20 °C, the experiments with landfill leachate at 4 °C.

Table 5.4.: Reaction constants and coefficients of determination for the degradation of PI in Na_2SO_4 and in landfill leachate at 300 L/h.

I	100 mA		7 A	
	Na_2SO_4	Leachate	Na_2SO_4	Leachate
k	$1.60027{\cdot}10^{-7} \cdot \frac{M}{min}$	$2.25763 \cdot 10^{-7} \cdot \frac{M}{min}$	$0.00553\ min^{-1}$	$0.03211\ min^{-1}$
R^2	0.9896	0.9695	0.8891	0.9361

Figure 5.7 shows normalized concentration profiles for PI oxidation in landfill leachate operating at 4 °C with a flow rate of 600 L/h for different applied currents. The curves show a good fit for first order reaction kinetics. k was calculated according to Equation 4.4. The corresponding values as well as R^2 for the extrapolated exponential curves are listed in Table 5.5. It can be observed, that k enhances with the applied current.

Figure 5.8 shows the cumulative energy consumption as a function of PI removal for the different applied currents. At 100 mA, 41 % of PI is eliminated after 200 minutes of treatment, consuming close to 1.5 Wh. For both 300 mA and 1 A, complete elimination of PI is achieved. The treatment duration is 3 hours at 300 mA, consuming around 4 Wh of energy. For I = 1A, 14 Wh are consumed during 2 hours of EO.

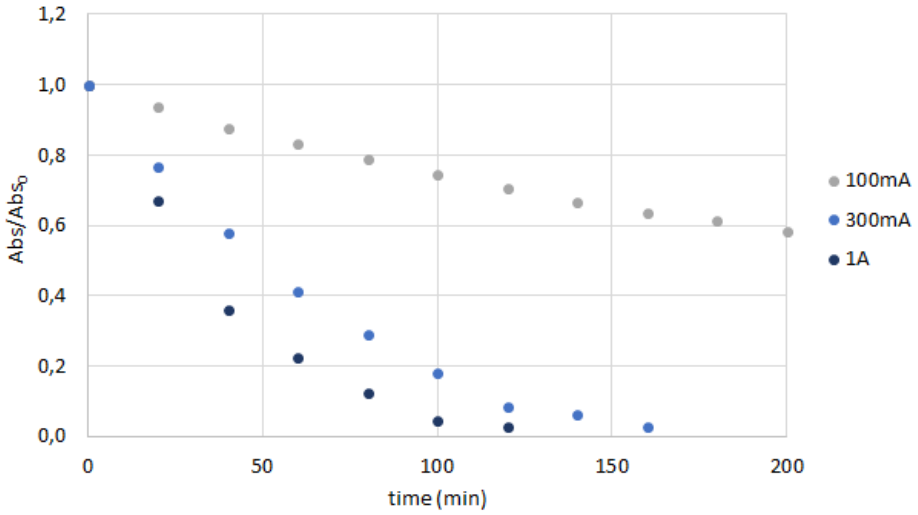

Figure 5.7.: Normalized concentration profiles of PI for EO in landfill leachate at 4 °C and 600 L/h applying different currents.

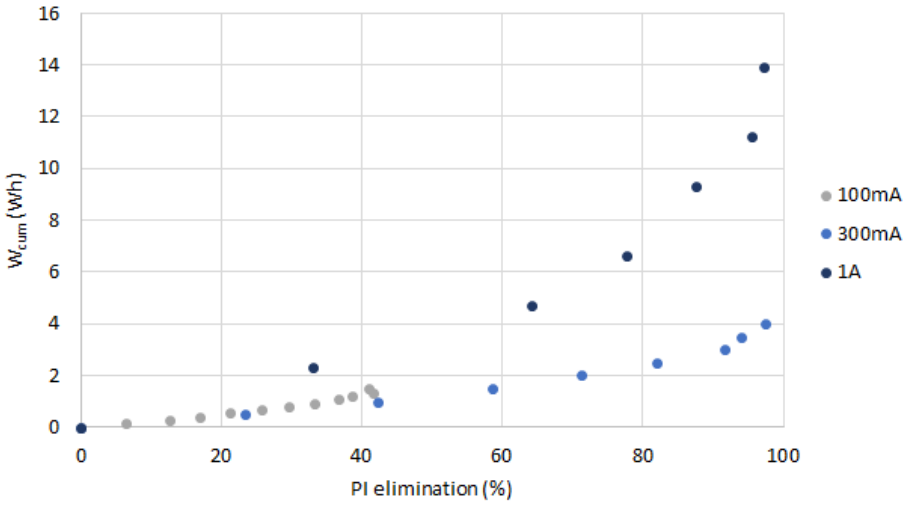

Figure 5.8.: Cumulative energy consumption as a function of PI elimination in landfill leachate at 4 °C and 600 L/h for different currents.

Table 5.5.: Reaction constants and coefficients of determination for the degradation of potassium indigotrisulfonate in landfill leachate at different currents for Q=600L/h and T=4°C.

I	100 mA	300 mA	1 A
k (min^{-1})	0.00239	0.02315	0.03017
R^2	0.9957	0.9674	0.9857

5.3. Factorial Design Experiments

5.3.1. Statistical Analysis

The software Minitab 18 is used to analyze the statistical importance of the influencing factors as described in Chapter 4.4. Pareto charts are generated to show the magnitude and importance of effects of the three factors pH, T and I. Residual plots are used to check the model for normal distribution and validate underlying assumptions. In Figure 5.9 and Figure 5.10, the Pareto chart and residual plots for the response factor TOC are given. For the other response factors, the respective charts can be consulted in Appendix C.

The red line in the Pareto chart for TOC removal indicates the minimum absolute value for the standardized effects to be of significant importance, which is 2.447. The only factor exceeding this threshold is the pH. The effects of temperature and current, as well as all higher interactions of variables, are below the threshold value for significant importance. Similarly, this can be concluded for COD and NH_4-N.
NO_3-N evolution is significantly influenced by pH, current and the interaction of pH

and temperature in descending order.

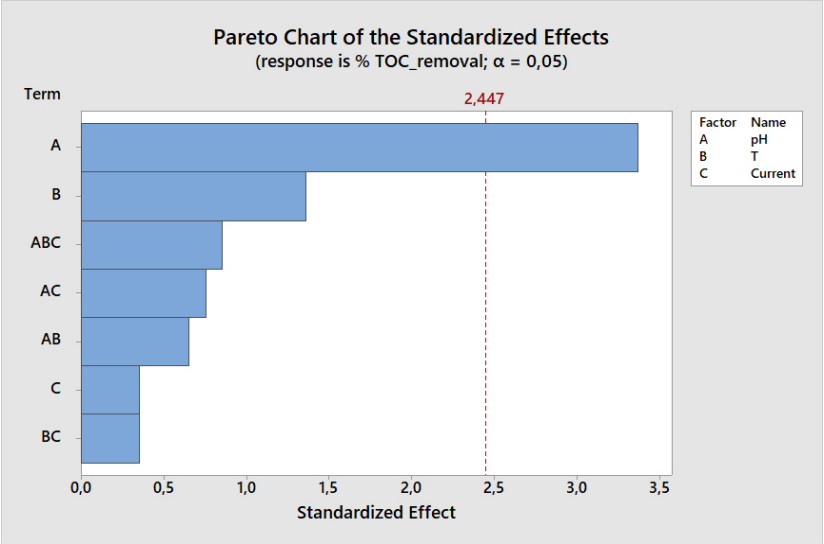

Figure 5.9.: Pareto chart for TOC.

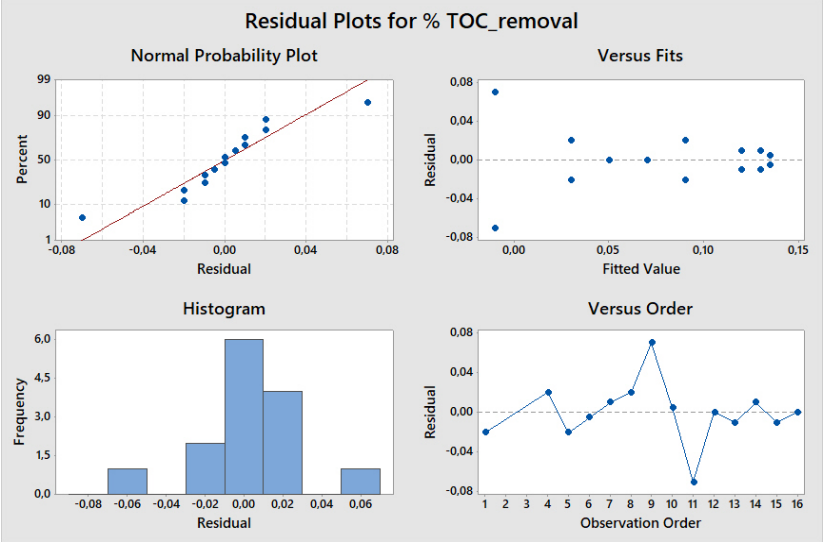

Figure 5.10.: Residual plots for TOC.

The normal probability plot approximately follows a straight line and therefore encourages the assumption of normal distribution. The points lying away from the line imply a distribution with outliers. The histogram displayed in Figure 5.10 similarly shows the presence of some outliers, indicated by the two bars on the far left and far right that show distance to the other bars. For all response factors, a similar pattern can be seen in the histograms. Skewness, as indicated by a long tail in one direction, is not suggested by the pattern. Again, this observation refers to all response factors. The

residual vs. fits plot suggests constant variance of the residuals but again outlines the existence of some outliers, indicated by data points lying far away from zero.

The residual vs. order plots show a random distribution around the center line for all response factors and therefore confirm the independence of the residuals from one another.

5.3.2. Evaluation of Response Factors

As the pH is the only influencing factor of statistical importance, the factorial design experiments are interpreted by comparing the evolution of response factors at the different pH levels. Each experiment is replicated once. In Figures 5.11 to 5.18 mean values of total degradation e.g. evolution of the response factors during the 4 hours of EO treatment are depicted. The ratio of final and initial concentration is analyzed. The error bars on each column indicate the degree of dispersion between the two equal runs.

Two additional experiments are performed to help interpret the results: One at pH 5, T = 20 °C and I = 7 A and one at pH 10, T = 20 °C and I = 0 A. The experiment with no current applied elucidates which effects may occur independently from the applied current. The experiment at 7 A is performed to have evidence of the system behavior when a current significantly higher than the estimated limiting current is applied.

Figures 5.11 and 5.12 show the extent of total TOC degradation during 4 hours of oxidation at pH 5 and pH 10, respectively. For pH 5, the ratio of final and initial TOC concentration ranges from 9 % to 13 % for the different settings. At I = 7 A the total removal rate reaches 28 %.
At pH 10, the removal rate ranges from 3 % to 7 % for the different settings. Operating the reactor without applying any current resulted in a TOC degradation of 6 %. Only one setting from this series includes the averaged results of two runs. Three runs are excluded from the evaluation because of strong oscillation in the measured values.

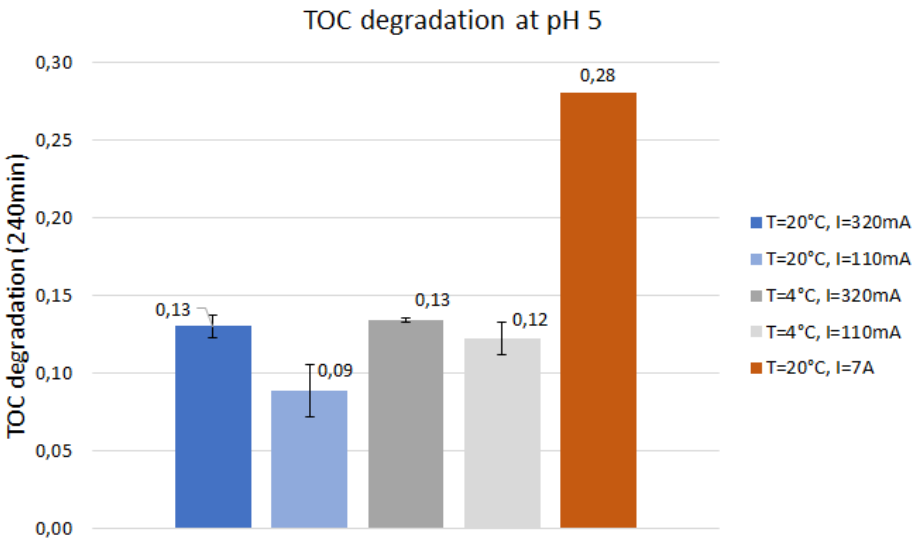

Figure 5.11.: Total degradation of TOC at pH 5 for different settings of temperature and current.

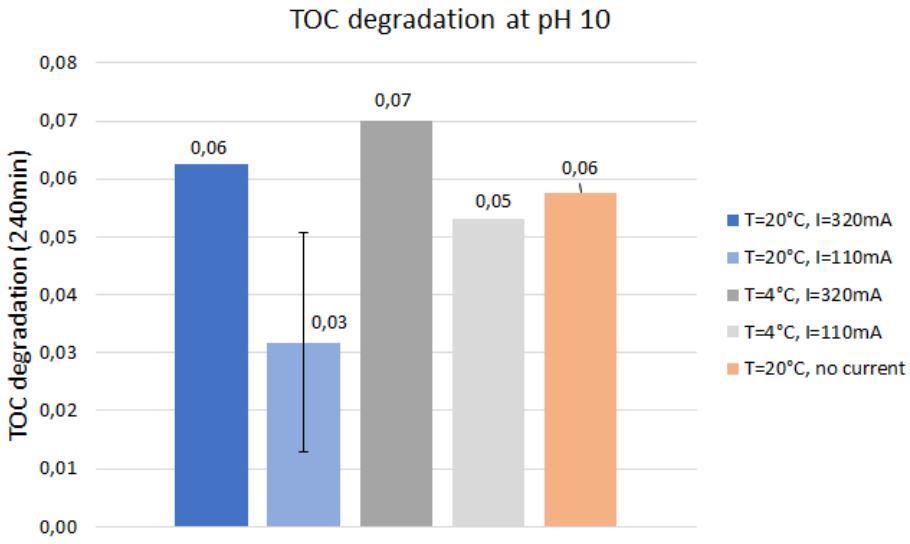

Figure 5.12.: Total degradation of TOC at pH 10 for different settings of temperature and current.

Figures 5.13 and 5.14 show the rate of total COD degradation during 4 hours of oxidation at pH 5 and pH 10, respectively. For the setting pH = 10, T = 20 °C and I = 110 mA, COD was only measured in the second run. Therefore, there is no error bar on the respective column.
For operation at pH 5, COD removal ranges from 5 % at 4 °C and 110 mA to 11 % at 20 °C and 110 mA. The variance in COD degradation for the different settings is small, as well as the removal rate per se. The two experiments at 20 °C yield slightly

higher removals as compared to the two experiments at 4 °C. The COD removal for an applied current of 7 A is 42 %.
In contrast, the experiments run at pH 10 all show negative values for COD degradation, meaning that COD increases instead of being degraded. The two runs at 4 °C and 320 mA show an especially high COD evolution of 14 % in average. The COD upgrowth observed for the other settings moves in the small range from 4 % to 5 %. When no current is applied, the COD evolution equally amounts to 5 %.

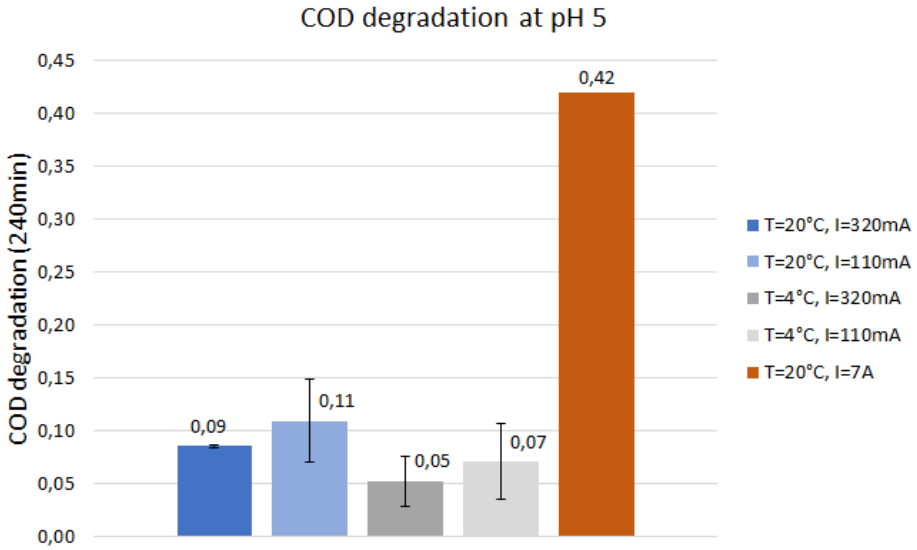

Figure 5.13.: Total degradation of COD at pH 5 for different settings of temperature and current.

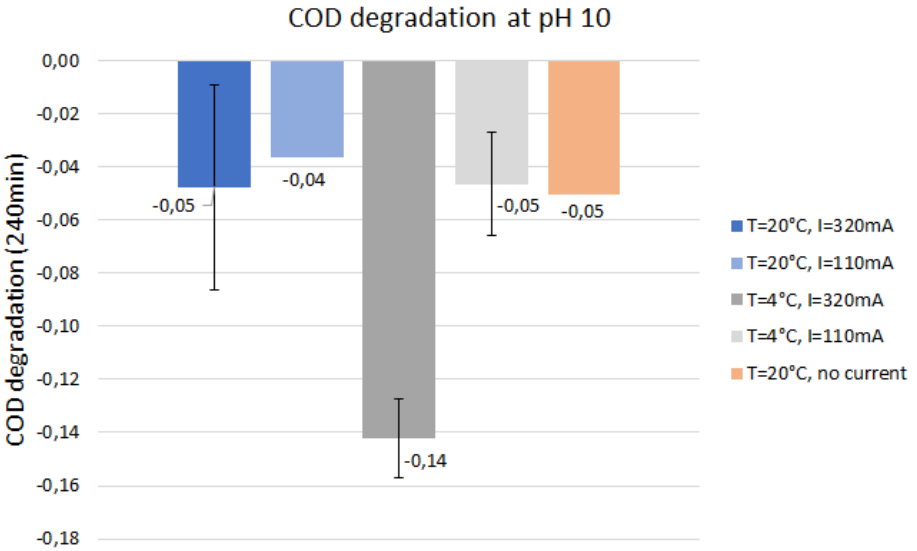

Figure 5.14.: Total degradation of COD at pH 10 for different settings of temperature and current.

Figures 5.15 and 5.16 show the rate of total NH_4-N degradation during 4 hours of oxidation at pH 5 and pH 10, respectively.

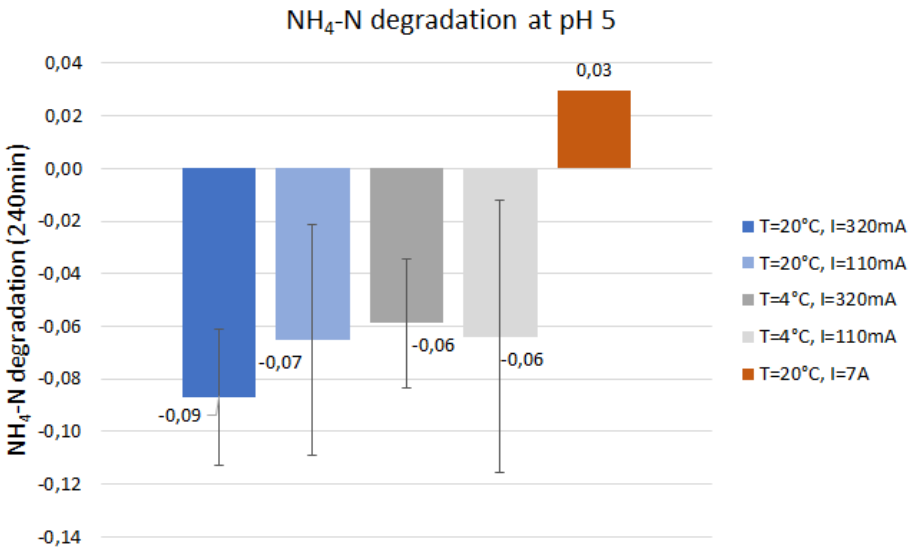

Figure 5.15.: Total degradation of ammonium at pH 5 for different settings of temperature and current.

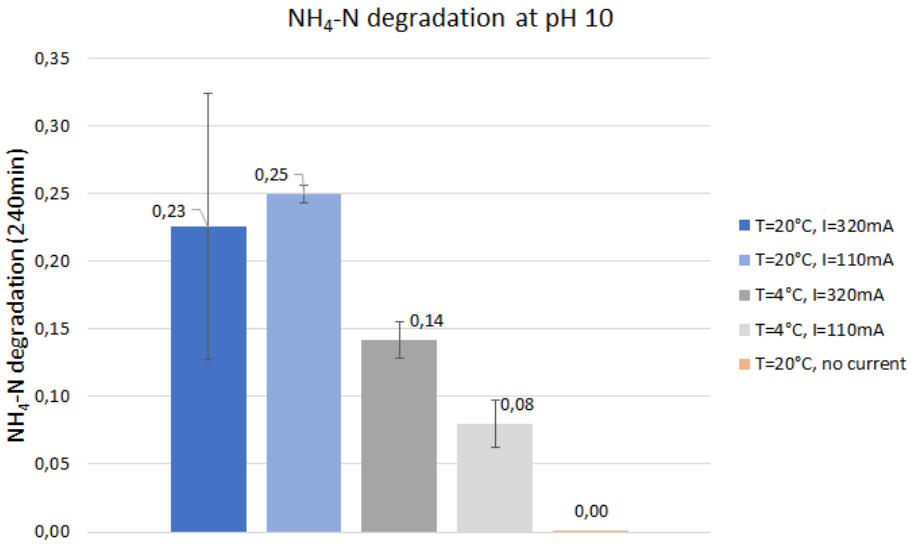

Figure 5.16.: Total degradation of ammonium at pH 10 for different settings of temperature and current.

It can be observed that for pH 5 the value for NH_4-N degradation is negative for all settings, implying that NH_4-N was generated rather than degraded. The mean values range from 6 % NH_4-N evolution for the two experiments at 4 °C to 9 % NH_4-N

evolution for the experiment at 20 °C and 320 mA. In contrast, when applying a current of 7 A, a slight degradation of 3 % of NH_4-N is achieved.
The experiments at pH 10 all yield a positive value for the percentage of degradation, meaning that ammonium is actually removed. For operating at 4 °C, around 10 % of NH_4-N is eliminated. At 20 °C, average removal of over 20 % is achieved for both applied currents. The run without applied current showed neither removal nor evolution of NH_4-N.

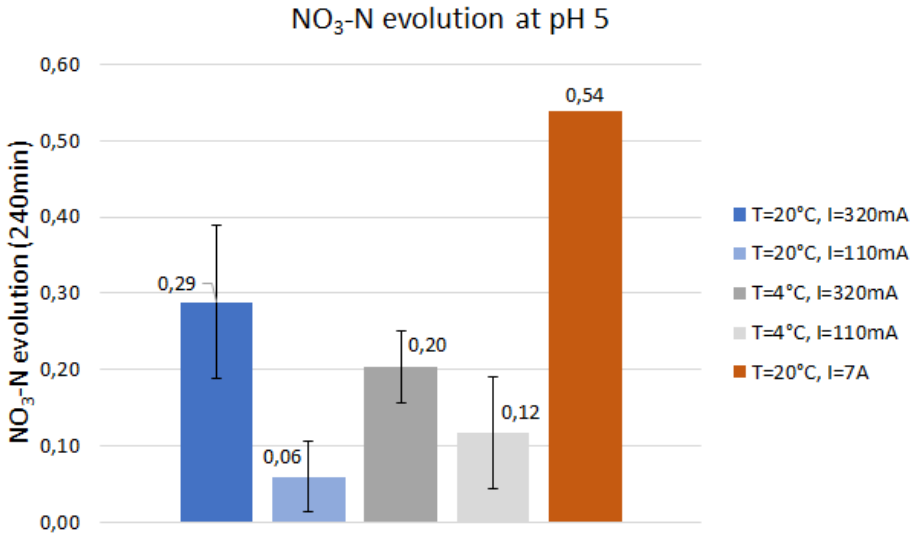

Figure 5.17.: Total evolution of nitrate during EO at pH 5 for different settings of temperature and current.

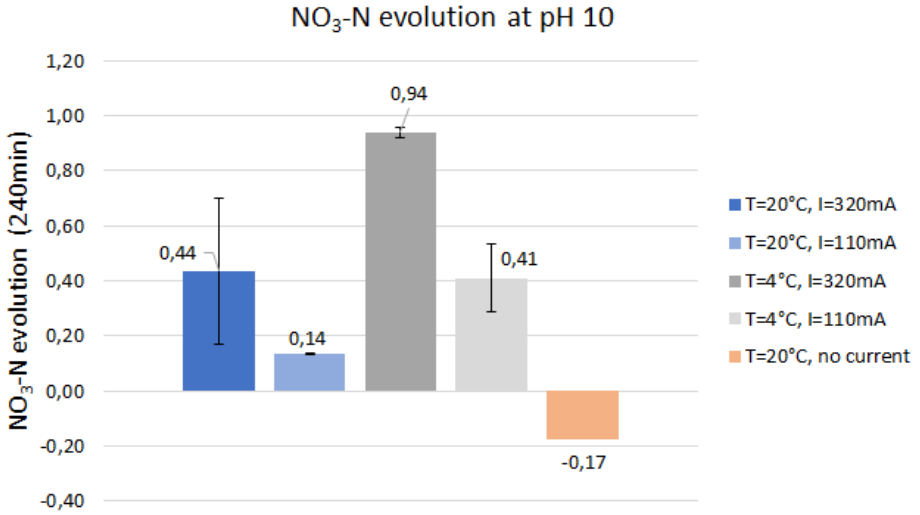

Figure 5.18.: Total evolution of nitrate during EO at pH 10 for different settings of temperature and current.

Figures 5.17 and 5.18 show the total NO_3-N evolution during 4 hours of oxidation at pH 5 and pH 10, respectively. The results show that in all runs nitrate is generated. The range of NO_3-N evolution for the different settings is remarkably high, reaching from 6 % at pH 5, T = 20 °C and I = 110 mA to 94 % at pH 10, T = 4 °C and I = 320 mA. For operating the reactor without applying a current, NO_3-N evolution reaches 17 %. 54 % NO_3-N is generated during the run at I = 7 A.

Normalized concentration profiles for the response factors TOC, COD, NH_4-N and NO_3-N as well as the evolution of free chlorine concentration during the 4 hours of EO treatment are depicted in 5.19 and 5.20. In contrast to the total degradation and evolution which are presented above and only relate the final concentrations to the initial ones, these graphs allow to discuss the transformation of parameters in the course of time. For each factor, the run without applied current and the run at 7 A are compared to each one run at 320 mA and 110 mA with the same settings for temperature and pH.

Figure 5.19 summarizes the concentration profiles for all factors at pH 10 and 20 °C for no applied current, I= 320 mA and I = 110 mA. For TOC, no remarkable difference can be constituted for the three profiles. The values range around one with only a slight decrease over treatment time. COD degradation similarly ranges around one with even a slight increase in COD/COD_0. For NH_4-N, almost no transformation can be seen in the course of EO when no current is applied. For the applied currents, NH_4-N concentration sinks gradually during the treatment with a slightly higher rate at I = 32 mA as compared to I = 110 mA. NO_3-N concentration rises slightly for the experiment at 110 mA and more distinct for the experiment at 320 mA. In contrast, when no current was applied, NO_3-N concentration first increases scarcely but then decreases in the second half of the experiment, especially during the last hour of the run.
The last subfigure depicts the evolution of free chlorine concentration during the 4 hours of EO. The concentration ranges from 0 to 0.2 mg/L for 110 mA and for 0 A. For 320 mA, free chlorine concentration shifts between 0 and 0.1 mg/L. No clear trend can be observed for free chlorine evolution.

Figure 5.20 summarizes the concentration profiles for all factors at pH 5 and T = 20 °C for I = 7A, I = 320 mA and I = 110 mA. The TOC profiles show a continuous decrease in TOC concentration for all applied currents, with a slightly higher degradation rate for 320 mA as compared to 110 mA. For 7A, TOC elimination is considerably faster and best described by an exponential trend. The rate constant is calculated according to Eq. 4.4, resulting in k = 0.00143 min^{-1}.

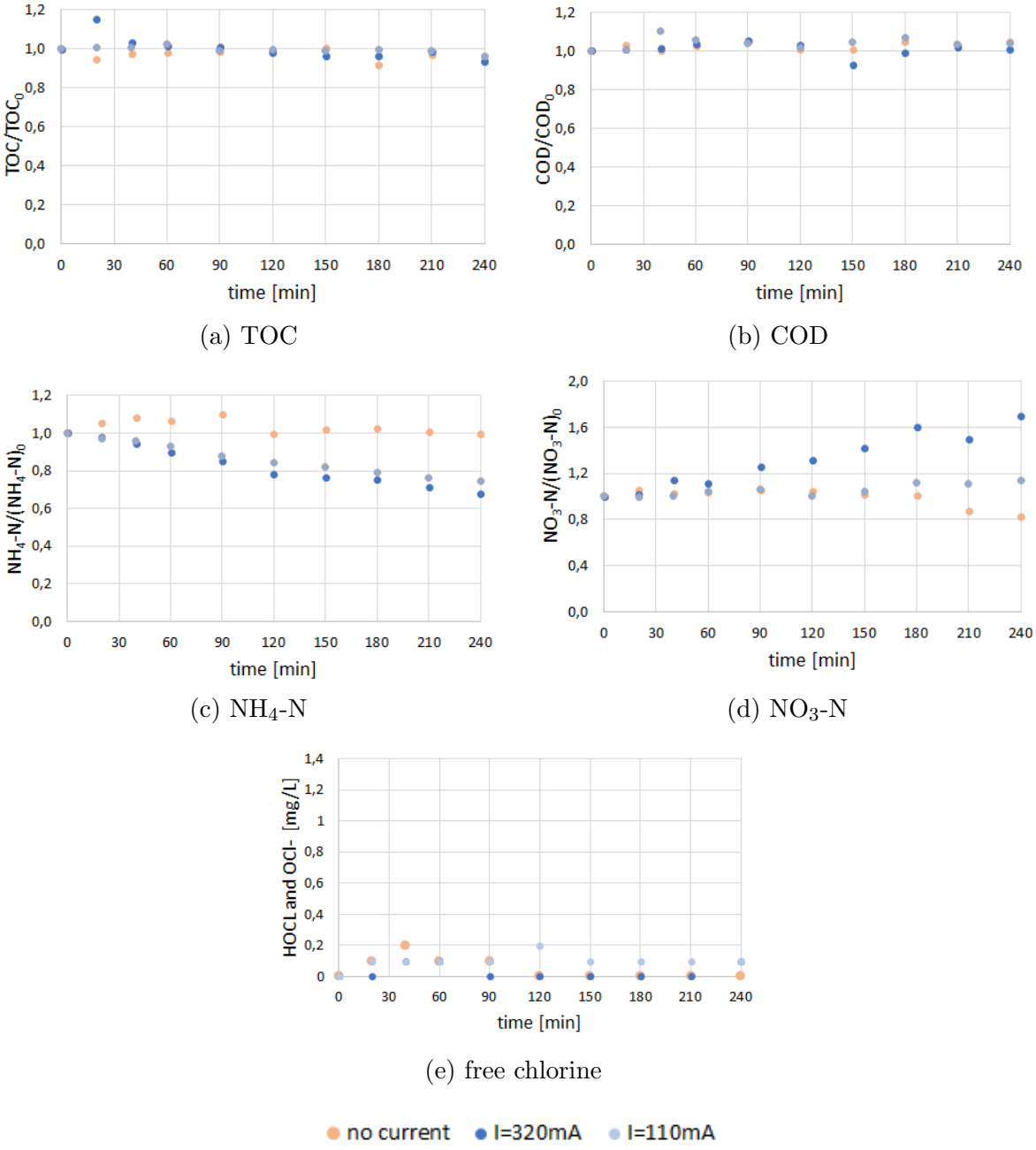

(a) TOC

(b) COD

(c) NH_4-N

(d) NO_3-N

(e) free chlorine

Figure 5.19.: Normalized concentration profiles for (a) TOC, (b) COD, (c) NH_4-N, (d) NO_3-N and (e) free chlorine at pH 10 and 20 °C for different current intensities and no applied current.

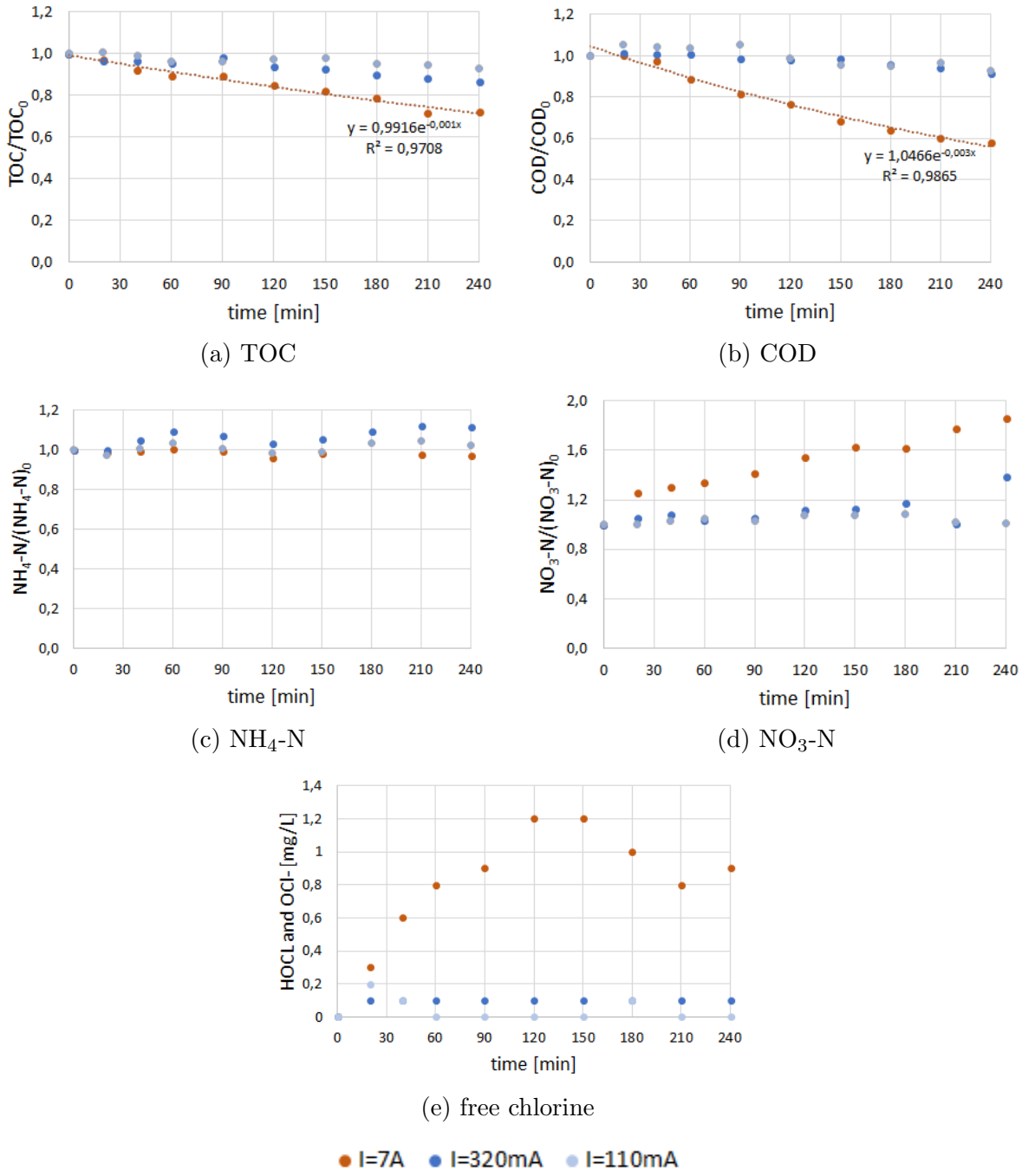

(a) TOC

(b) COD

(c) NH_4-N

(d) NO_3-N

(e) free chlorine

Figure 5.20.: Normalized concentration profiles for (a) TOC, (b) COD, (c) NH_4-N, (d) NO_3-N and (e) free chlorine at pH 5 and 20 °C for different current intensities.

The normalized COD profiles are similar for 320 mA and 110 mA. A slight decrease in the COD/COD_0 ratio can be observed after approximately 90 minutes of treatment. The profile at I = 7 A shows a significantly higher COD removal rate with a good exponential fit. The correspondent rate constant is k = 0.00251 min^{-1}.

No clear trend can be seen for NH_4-N concentration. The normalized concentration ranges around one for all currents with a slight increase for 320 mA and 110 mA and a slight decrease for 7 A.
NO_3-N concentration shows an approximately continuous rise for I = 7 A. At lower currents, no clear trend can be observed. However, all concentrations measured during EO are higher than the initial one.
The concentration of free chlorine shifts between 0 and 0.1 mg/L for I = 320 mA and between 0 and 0.2 mg/L for I = 110 mA. When applying a current of 7 A, a clear trend in free chlorine evolution can be observed. The concentration rises to 1.2 mg/L after 2 hours and then drops to 0.9 mg/L at the end of the experiment.

As accelerating chlorine concentrations have been reported to promote the formation of chlorinated byproducts, a random sample is taken and checked for trihalomethanes (THMs). High-performance liquid chromatography (HPLC) is applied to detect THMs. Samples were taken for I = 7 A and I = 320 mA at pH 5 and T = 20 °C. The corresponding chromatograms can be consulted in Appendix D. For I = 320 mA, no significant evolution of THMs is observed. In contrast, for I = 7 A, trichlormethane, bromodichlormethane and dibromochlormethane are detected in the leachate.

5.3.3. Energy Consumption

For the experimental run at 7 A, the cumulative energy consumption is presented as a function of COD removal. The plot is compared to the cumulative energy consumption for PI elimination at the same current intensity.
As can be seen, PI is eliminated completely with an energy consumption of 177.7 Wh. The treatment duration is 2 hours. In contrast, COD is eliminated by 42 % during 4 hours of EO with a total energy consumption of 303.8 Wh.

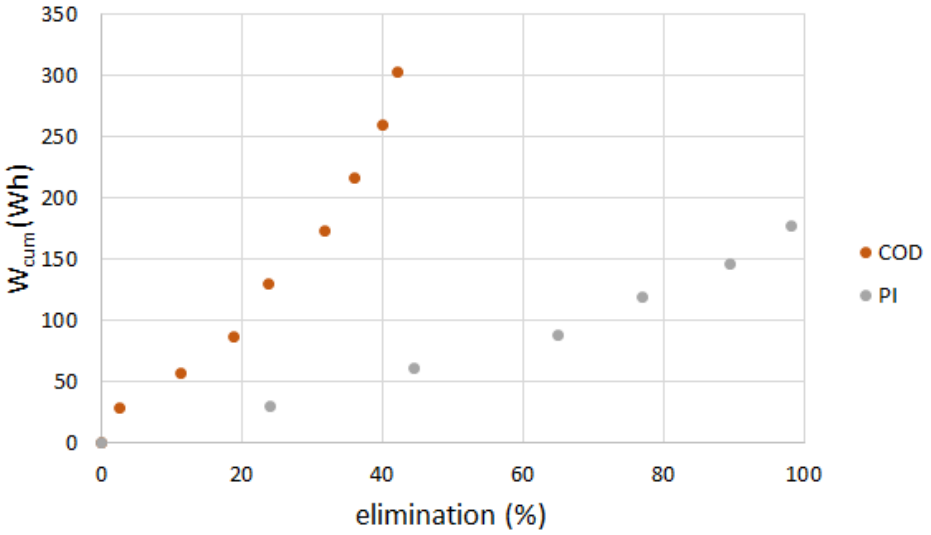

Figure 5.21.: Cumulative energy consumption as a function of COD and PI elimination at 7 A and 20 °C. For COD elimination, the flow rate is 600 L/h and the pH is 5. For PI elimination, the flow rate is 300 L/h and the pH is 10.

6. Discussion

In this chapter, the results reported in the previous chapter are discussed against the theoretical background and findings reported from similar applications of EO for waste water treatment presented throughout this thesis.

6.1. Preliminary Experiments

The first task for finding appropriate treatment settings was to identify the limiting current density for the given reactor design. The mathematical model proposed by Kapalka et al. (2010), introduced in Chapter 3.2.4.1, suggests a limiting current of 222 mA. This is in good agreement with the LSV experiments presented in chapter 5.1, that resulted in I_{lim} = 215 mA for Q = 600 L/h.
However, both methods have some limitations that need to be considered, being the most fatal one that they are mainly based on the reactor hydraulics, neglecting the molecular diffusivity and consequently the complex matrix of the landfill leachate. The mathematical model makes use of various empirically established equations to estimate k_m. These equations are built on assumptions and have a limited range of validity. In consequence, their application arises some uncertainties. One of the assumptions is that the molecular diffusivity, e.g. the diffusion coefficient (D), is equal for all compounds. As the exact composition of the leachate is unknown, D had to be estimated. In this work, the diffusion coefficient for BPA was employed, as BPA is a target compound found in the leachate. However, its concentration in the leachate is low (8 μg/L) and therefore, D_{BPA} might not be representative for the overall diffusivity of the leachate. Furthermore, the only transport mechanism taken into account with this model is diffusion; migration and convection are neglected.
The experimental determination of k_m with LSV is a common method, that has proven efficient in several papers published on EO of real waste waters (Chatzisymeon et al., 2009; Cañizares et al., 2006a). It is more reliable than the purely empirical determination, because the actual oxidative behavior in the reactor is evaluated and no assumptions are needed. On the other hand, the composition of the treated effluent is not considered at all.
Both methods neglect the complex composition of landfill leachate and can therefore only be seen as reference point.

Another series of preliminary experiments was conducted, wherein the degradation

of a test substance (potassium indigotrisulfonate) during EO in the pilot plant was recorded. The results are shown in Chapter 5.2. In the frame of this experimental series, the overall performance of the setup was validated, the electrolyte qualities of the leachate were tested against Na_2SO_4 as supporting electrolyte, the influence of the flow rate was evaluated and different currents were applied in order to validate the experimentally and mathematically obtained values for i_{lim}.

Figure 5.5 shows the concentration profiles for indigo trisulfonate in landfill leachate and in 0.05 M Na_2SO_4 solution for the applied currents of 100 mA and 7 A at a flow rate of 300 L/h. For 100 mA, the reaction shows zero order characteristics. The reaction constants are $1.60027{\cdot}10^{-7} M \cdot min^{-1}$ in Na_2SO_4 and $2.25763{\cdot}10^{-7} M \cdot min^{-1}$ in leachate. For I = 7A, first order kinetics are applied, resulting in k = 0.00553 min^{-1} for Na_2SO_4 and k = 0.03211 min^{-1} for leachate. As can be seen, for both applied currents, the elimination rate is higher in the real leachate than in Na_2SO_4 solution, even though the conductivity in Na_2SO_4 solution was about three times higher (8-10 mS/cm).
The faster degradation in leachate can be attributed to the presence of powerful oxidizing species like chlorine, that promote the indirect EO pathway.
In Figure 5.6, the cumulative energy is shown as a function of PI removal. At 100 mA, for the experiment in Na_2SO_4 solution 24 % PI elimination were achieved in 4 hours, consuming 1.5 Wh. The degradation was 12 % higher in leachate, for only 3 hours of treatment and nearly the same energy consumption.
At 7 A, PI was removed completely from the leachate after 2 hours. For the same treatment time, only have of the PI was eliminated in Na_2SO_4 solution. The energy consumption was 180 Wh and 120 Wh, respectively.
The plot suggests, that PI degradation in Na_2SO_4 solution at 7 A reaches a critical value were the elimination does not accelerate any further with the consumed energy. This can be attributed to competing chemical processes proceeding in the bulk solution.
It can be concluded, that the electrolyte properties of the leachate, like salinity and consequently conductivity, allow a treatment via EO without the addition of further electrolytes.

The model proposed by Cabeza et al. (2007c) for organic matter oxidation during landfill leachate on BDD anodes satisfactorily predicts the potassium indigotrisulfonate degradation at I = 100 mA in Na_2SO_4 solution. At increased intensities, however, the oxidation rate is higher than predicted by the model. This is ascribed to a change of oxidation mechanism at high current densities, were indirect oxidation processes gain more importance.

In order to evaluate the influence of the flow rate on the EO performance, LSV experiments were conducted at 300 L/h and at 600 L/h. The mass transfer coefficient and hence the limiting current density were enhanced significantly with the flow rate. For

Q = 300 L/h, k_m is 3.10 $\cdot 10^{-5}$ and i_{lim} is 127 mA. For Q = 600 /h, k_m is 5.26 $\cdot$ 10^{-5} and i_{lim} is 215 mA. The higher mass transfer at 600 L/h can be ascribed to higher turbulence. For 300 L/h the flow-through is laminar, whereas for 600 L/h it is turbulent. With increased convective mass transport, the thickness of the reaction layer decreases, which at its turn leads to a rise in k_m.
It was decided to work at a flow rate of 600 L/h, because a higher mass transfer is concomitant to faster organics degradation.

Subsequently, a series of experiments was run to identify the elimination rate of potassium indigotrisulfonate in real leachate at different current densities. This test aimed at validating the transferability of the experimentally and mathematically estimated values for i_{lim} to EO in the leachate. Figure 5.7 shows the concentration profiles of potassium indigotrisulfonate during electrochemical treatment in leachate, operating at 4 ° C and 600 L/h, at different currents (100 mA, 300 mA and 1 A). As expected, the elimination rate enhances with the current. All three curves are best fitted with first order kinetics, resulting in $k_{100mA} = 0.00239\ min^{-1}$, $k_{300mA} = 0.02315\ min^{-1}$ and $k_{1A} = 0.03017\ min^{-1}$.
k_{300mA} is about 10 times higher as compared to k_{100mA}. In contrast, the ratio of k_{1A} and k_{300mA} is 1.3. Therefore, a shift of the oxidation mechanism is concluded current intensity range between 100 mA and 300 mA.
In Figure 5.8, the correspondent energy consumption for the three experiment is depicted as a function of PI elimination. At 100 mA, 41 % removal were achieved after 200 minutes, consuming a total of 1.5 Wh. At both 300 mA and 1 A, total PI degradation was achieved. The treatment time was 3 hours at 300 mA and one hour less at 1 A. However, the energy consumption accelerates between these two current levels. At 300 mA, 4 Wh of energy were consumed, whereas energy consumption amounts to 14 Wh at 1 A. For 1 A, the ratio of energy consumption and removal rate rises quickly, showing a weak energy efficiency. This is due to secondary reactions, like oxygen evolution, arising at $i > i_{lim}$.
The great jump in the oxidation rate and the rising rate of energy consumption between 100 mA and 300 mA suggest that i_{lim} is settled in that range. However, according to the theory presented in Chapter 3.2.4, the concentration profile is expected to follow a linear trend for $i < i_{lim}$, whereas in this case, for 100 mA an exponential trend is the best fit. This deviance from the theory is believed to be a consequence of the complex leachate matrix, complicating the prediction of its behavior during EO.
In conclusion, the findings of this experimental series suggest a limiting current level between 100 mA and 300 mA, which is in good agreement with the estimation of i_{lim} discussed above. Therefore, it is assumed that the estimated i_{lim} can be applied to the EO of real leachate.

6.2. Electrochemical Oxidation of Landfill Leachate

Chapter 5.3 includes the statistical analysis of the designed experiments and detailed evaluations of the eight different settings tested. As the statistical analysis suggests that pH is the main influencing factor for EO of landfill leachate under the given conditions, the evaluation of the follow-up parameters concentrates on the comparison between the two pH levels.

6.2.1. Electrochemical Oxidation at pH 10

For TOC degradation at pH 10, the ratio of final and initial concentration is depicted in Figure 5.12 and concentration profiles at different currents are given in Figure 5.19. The total degradation ranges from 3 % to 7 % and yields 6 % even for no applied current. For three experimental runs of this series, the measured TOC values showed a strong oscillating behavior. These runs were excluded from the evaluation. The error bar for the repeated experiment indicates a high dispersion between the two runs. It can be concludes, that for pH 10 the TOC reduction is too small to allow reliable measurements.
The concentration profiles show no distinct trend for TOC degradation during the treatment. The behavior is similar for the applied currents as compared to no applied current. In conclusion, the electrochemical treatment cannot be found responsible for TOC removal at pH 10 under the tested conditions.

In accordance with the findings from TOC removal, the total COD degradation (see 5.14) as well as the COD concentration profiles (see Figure 5.19) show no elimination of organic matter for EO at pH 10. In fact, during all runs, COD increased. The extend of COD evolution is similar for no current and for the two applied currents (4 - 5 % COD evolution). The only exception are the experiments at 4 ° C and 320 mA, that yielded an average COD evolution of 14 %. As the standard deviation is relatively high for all settings, this exception is believed to be an outlier.
In other studies, similar behavior of COD during EO of landfill leachate (Anglada et al., 2011) and olive mill wastewaters (Chatzisymeon et al., 2009) on BDD anodes have been reported. Several explanations have been found for the increase in COD: (1) oxidative polymerization of certain landfill leachate constituents like phenols, (2) dissolution of unfiltered solids releasing organic matter in the liquid phase and (3) interference of unreacted compounds with the COD test. Oxidative polymerization of unreacted compounds can be rejected, because TOC measurement indicates that organic matter oxidation is inhibited. Dissolution of solids promoted by the recirculation during the treatment is a possible scenario. However, solubility of salts is higher at lower pH (Kurzweil, 2015). In consequence, this effect would be more distinct at pH 5. In contrast, a removal of TOC and COD concentration was observed at pH 5

(see Figure 5.11). Moreover, this effect would also present itself in rising TOC concentrations at pH 10 and does not deliver an explanation to why COD increases while TOC decreases.
Because of this discrepancy, interference of the COD test with inorganic compounds is suspected. The interference of chloride is prevented by complex formation with mercuric sulfate during COD measurement. Other inorganic compounds that can cause interference are ferrous ions, sulfides and nitrite (Gujer, 2007). As described in Chapter 2.3.1, $FeCl_3$ is added as a coagulant during the pre-treatment of the leachate, leading to the release of Fe^{2+} and Fe^{3+} ions. Most of the ions are flocculated, but a residual concentrations of 0.23 mg/L Fe^{2+} and 0.62 mg/L Fe^{3+} were detected in the pre-treated effluent. Fe^{2+} is easily oxidized in presence of abundant oxygen or other oxidizing agents (Kurzweil, 2015). For pH 10, however, TOC and COD measurements suggest that EO of organic matter is inhibited. Therefore, an explanation for the rise in COD is release of Fe^{2+} during the treatment and its subsequent oxidization by the COD test, resulting in an overestimation of organic matter concentration.

The presence of iron ions can furthermore give an explanation to the slight decrease in TOC, that was observed for all runs at pH 10, including at I = 0 A. These ions can build complexes with organic compounds, hence removing them from the leachate. This hypothesis is supported by a moderate amount of orange precipitate found in the filter and at the bottom of the tank after conducting experiments at pH 10. The turbulence induced by the recirculation of leachate is believed to promote the release of iron ions and subsequently the precipitation process. In addition, basic pH favors the precipitation.

In conclusion, as a possible scenario, Fe^{2+} and Fe^{3+} build complexes with organic matter, leading to organics precipitation, hence, elimination of TOC. Fe^{3+} has been reported to strongly promote flocculation, while precipitation with Fe^{2+} is relatively rare (Nierop et al., 2002). Released and unreacted Fe^{2+} interferes with the COD measurement, leading to values above the initial one.
This explanation demands the assumption that the effect of released Fe^{2+} interfering with the COD measurement superposes the effect of organic matter precipitation and that Fe^{2+} oxidation via indirect processes is not significant.

Another possible cause for interference is the generation of NO_2^- as intermediate of NH_4-N oxidation. NO_2^- is instable and quickly oxidized to NO_3^-. However, the rate of ammonium oxidation recorded is relatively low, supporting the assumption of intermediates presence. NH_3 is also an intermediate of NH_4 oxidation. In general, dichromate, the oxidizing agent used for COD determination, does not oxidize NH_3 into NO_2^-. However, Kim (1989) found, that in the presence of free chlorine ions, NH_3 can indeed cause interference with COD analysis and that the interference increases with NH_3 concentration.

In order to identify the cause of interference in COD measurement, more data from additional measurements are needed. First, a plausibility test of measured values by dilution and/or stocking of samples is suggested. If plausibility is given, concentrations of NO_2^-, Fe^{2+}, S^{2-} and NH_3 should be determined. When the cause of interference is found, the COD test results can be adjusted accordingly.

The inhibition of organics oxidation at pH 10 is ascribed to the presence of CO_2 in form of carbonate and hydrocarbonate at alkaline pH. As described in Chapter 3.3, CO_3^{2-} and HCO_3^- are effective •OH scavengers. Furthermore, according to the Nernst equation (3.17), the oxidative power of •OH lowers with the rise of pH.

NH_4-N concentration, conversely to COD, slightly decreases at pH 10. The total NH_4-N degradation at pH 10 is more pronounced for T = 20 ° C (23 - 25 %) than for T = 4 ° C (8 - 14 %, see Figure 5.16). For I = 0 A no elimination is recorded. Hence, the removal of NH_4-N at 110 mA and 320 mA is attributed to electrochemically induced oxidation processes. It is reported in literature, that organics removal is favored by direct oxidation mechanisms while NH_4-N removal is promoted through mediated oxidation and that chlorine species are particularly effective for the indirect oxidation of NH_4-N (Anglada et al., 2011; Cabeza et al., 2007c; Fernandes et al., 2015). It was already argued, that direct oxidation at pH 10 is inhibited due to the presence of •OH scavengers. Therefore, indirect oxidation by chlorine prevails, resulting in decreasing NH_4-N concentrations. The observation, that temperature seems to enhance the removal rate, supports this theory. Temperature has a greater affect on indirect oxidation than on the direct mechanism (Schmidt, 2003).

In agreement with the oxidation of NH_4-N, a rise in NO_3-N is detected for pH 10. Nitrate is the highest oxidized form of nitrogen and therefore expected to accumulate during EO. When no current is applied, a decrease in NO_3-N concentration is recorded (see Figure 5.18). The ratio TOC_{240min}/TOC_{0min} suggests a total NO_3-N degradation of 17 % for I = 0 A. When looking at the correspondent normalized concentration profile given in Figure 5.19, it can be seen that NO_3-N concentration is nearly constant during the first three hours of treatment, and only drops in the last hour.
NO_3-N is the only response factor, that according to the statistical evaluation, is not only influenced by pH, but also by current intensity and the interaction of pH and temperature. NO_3-N evolution is more pronounced at higher current intensities. This is in line with the expectation, that EO accelerates with rising current density. However, enhanced oxidation through higher current densities would have an impact on all response factors, not only on NO_3-N.

6.2.2. Electrochemical Oxidation at pH 5

The values for total TOC removal obtained for the experiments at pH 5 can be consulted in Figure 5.11. They range between 9 % and 13 % and are holistically higher than the respective values at pH 10. At 7 A, a total TOC removal of 28 % is recorded. No experiment was run at pH 5 without applying a current, therefore, no random noise can be applied to these results. Concentration profiles for TOC removal are shown in Figure 5.20. They show, that TOC degraded continuously during the EO treatment.
The evaluation of COD degradation at pH 5 leads to a similar conclusion. Total COD elimination varies between 5 % and 11 % for the different settings, as seen in Figure 5.13. The experiment at 7 A yields a considerably higher removal rate of 42 %.
From the decrease in TOC and COD, it can be concluded that at pH 5, EO leads to organic matter elimination. However, the elimination rate is low.
The statistical analysis shows, that the applied current does not have a significant influence on elimination in the range of the two current levels tested. For the additional experiment at 7 A, the removal rates are considerably higher and are well fitted with an exponential trend, yielding $k_{TOC} = 0.00143\ min^{-1}$ and $k_{COD} = 0.00252\ min^{-1}$. Therefore, it is assumed, that the current has a significant influence on organic matter removal when higher intensities are applied and/or when the gap between the tested values is greater.

As can be derived from the rate constants at 7 A, TOC degrades faster as compared to COD. Similar findings have been reported previously in literature and are explained in terms of accumulation of resistant compounds as final products of the EO (Anglada et al., 2009b; Cañizares et al., 2006b).

The normalized profiles of COD concentration (see Figure 5.20) show, that for both 110 mA and 320 mA COD degradation initiates after around 90 minutes of EO. Likewise, for the correspondent NH_4-N profiles obtained during the same experimental runs a slight increase can be seen during the first hour of treatment, followed by a drop between minute 60 and 90. For the run at 320 mA, TOC was removed by 2 % during the first 90 minutes of EO and degraded by another 12 % during the further course of treatment. Therefore, a change in the oxidizing mechanism is assumed to occur after approx. 60 to 90 minutes of treatment, enhancing the removal efficiency. Formation of mediators, that induce indirect oxidation processes, is thought to be responsible for this behavior.

NH_4-N concentration, conversely to COD, slightly increases at pH 5. The total NH_4-N evolution is similar for all settings (6 - 9%, see Figure 5.15). Only for 7 A, a marginal removal of 3 % can be observed. This is attributed to the fact, that at higher current intensities, the extend of indirect oxidation increases and therefore NH_4-N is oxidized. According to the literature (Chiang et al., 1995; Deng and Englehardt, 2007), NH_4-N

removal is mainly driven by indirect oxidation mediated through in-site electrochemically produced hypochlorite. The concentration profiles for free chlorine evolution at pH 5 are depicted in Figure 5.20. As can be seen, free chlorine generation accelerates during the run at 7 A, reaching a maximum of 1.2 mg/L, while at lower currents HOCl and OCL^{-1} concentrations stay nearly constant at low levels (0 - 0.2 mg/L). In consequence, the NH_4-N removal observed at 7 A can be attributed to higher hypochlorite availability and better kinetics at higher current densities.
However, at acidic pH a part of the chloride ions forms gaseous chlorine, which manifests itself in a characteristic smell. It has been reported, that in order to efficiently eliminate NH_4-N and organic compounds at the same time, current densities significantly higher than i_{lim} have to be applied (Fernandes et al., 2015; Anglada et al., 2011) studied EO of landfill leachate on BDD anodes and found that NH_4-N removal was low during the first four hours of treatment and then accelerated. They explain this behavior with the dominance of direct oxidation during the initial stages of EO. Similarly, Cabeza et al. (2007c) observed that during EO of landfill leachate on BDD anodes NH_4-N removal accelerated when most of the COD had been degraded. As COD is removed by only 42 % during the four hours of treatment at 7 A, the small extend of NH_4-N oxidation is in agreement with the cited literature.

Even though no removal of NH_4-N was recorded, NO_3-N was generated during all runs (see Figure 5.17). NO_3-N evolution ranged from 6 % to 29 % at 110 mA and 320 mA and yielded 54 % at 7 A. In accordance with the observation that more NH_4-N is oxidized at alkaline conditions, NO_3-N evolution is more pronounced at pH 10 as compared to pH 5. Similarly to the findings for pH 10, NO_3-N evolution accelerates with increasing current intensity.

Further studies are needed to identify the cause for the rising NH_4-N concentrations and the contradictory evolution of NO_3-N.

6.2.3. Evaluation of Influencing Factors

Applied Current
From the low removal rates for organic matter and ammonium obtained for EO at 110 mA and 320 mA it can be concluded, that the range of applied currents is too low for an effective treatment of the leachate. The evaluation of experiments with real leachate suggest that the experimentally determined k_m-value and hence the estimated i_{lim} underrate the k_m of the leachate. The discrepancy can be attributed to the fact, that the matrix (ferro/ferri-cyanide) employed to determine the coefficient is substantially different from the actual leachate. To evaluate the transferability of the estimated i_{lim} to the leachate matrix, preliminary experiments have been conducted on EO performance in leachate. The results are in good agreement with the experimentally determined i_{lim}. However, the evaluation is based on the degradation of

potassium indigotrisulfonate, a dye that was added to the leachate and traced via UV-Vis spectrophotometry. It is suspected, that the behavior of PI is not representative for the organic matter found in the leachate.
The UV-Vis measurement is based on the degradation of color intensity. The deep blue color of PI is easily removed by breaking a double bond it its structure (see Figure 4.3). However, the educts of this reaction are intermediates that still contribute to the COD concentration and might be more recalcitrant to further oxidation. Therefore, recording the degradation of PI does not permit direct conclusions on the removal efficiency concerning COD.
To gain more insights on the correlation between PI and COD elimination, rate constants and energy consumption during EO were compared for PI and COD. PI degradation at 7 A (at 300 L/h, 4 ° C and pH 10) proceeded with a rate constant of 0.03211 min^{-1}. In comparison, the rate constant for COD degradation at 7 A (at 600 L/h, 20 ° C and pH 5) is 0.00251 min^{-1}. Higher flow rates and an acidic pH have shown to favor organics oxidation. Nevertheless, k is over ten times lower for COD than for PI, supporting the assumption that PI is degraded significantly faster than the organic matter inherently present in the leachate.
Figure 5.21 shows the cumulative energy consumption against the elimination of COD and PI, respectively. PI is degraded completely from the leachate matrix after 2 hours of treatment, consuming 180 Wh. COD elimination yielded 42 % during 4 hours of EO with a total energy consumption of 300 Wh. It can be seen, that COD elimination tends to a critical level, where it does not increase with further rise of the energy consumption anymore. This observation indicates, that higher intensities have to be applied in order to achieve complete removal of organic matter.
In conclusion, i_{lim} needs to be reevaluated for the EO of SHMIL Åremma Landfill Leachate, for example through COD measurements at varying current levels, that are higher than the ones applied in this study.

In several other studies, the applied current has been found to have a significant effect on EO performance on BDD anodes. It is believed, that the intensity did not show significance in this study, because the applied currents were below the limiting current and the overall oxidation rates were low. Several observations concerning the behavior of response factors are ascribed to chemical properties that depend on pH, independently from oxidation processes. Therefore, it is proposed to reevaluate the significance of I at higher current densities.

Higher currents lead to a decline of current efficiency when working under mass transport control, as described in Chapter 3.2.4. Therefore, the instantaneous energy efficiency should be considered when working with $i > i_{lim}$ to safeguard a reasonable ratio of elimination rates and energy consumption.

Another affect of applying currents densities above i_{lim} is the accelerating evolution

of free chlorine. This effect has been observed for the experiment at 7 A (see Figure 5.20). Apart from having a positive influence on NH_4-N removal, free chlorine has been found to promote the formation of chlorinated byproducts. Therefore, EO at higher current densities should be accompanied by the evaluation of chlorinated byproducts formation.
The formation of Trihalomethanes (THM) was measured via high-performance liquid chromatography (HPLC) for each one random sample at 7 A and 320 mA. The corresponding chromatograms can be consulted in Appendix D. For 320 mA, no significant evolution of THMs was observed. In contrast, for 7 A, trichlormethane, bromodichlormethane and dibromochlormethane were detected in the leachate. The formation of those compounds is problematic, as they are considered to be environmental pollutants and have carcinogenic properties (Hood, 2005).

Temperature
The preliminary experiments with potassium indigotrisulfonate show good elimination rates for EO at 4 °C. Concerning the factorial design experiments, no significant influence of temperature was detected on the removal rates of organic matter and NH_4-N. Therefore, it is believed that EO can successfully be applied at low temperatures and further experiments with this setting are encouraged.

pH
The evaluation of the effect of pH on the oxidation performance provides ambiguous findings. At alkaline pH, COD is not removed from the leachate, whereas a low removal of NH_4-N can be observed at 110 mA and 320 mA. In contrast, at acidic pH, COD is removed slightly, whereas no NH_4-N removal is yielded. Further studies at more intense conditions, specifically higher current densities, are suggested to reevaluate the influence of pH on the EO performance.

Further Influencing Factors
Chatzisymeon et al. (2009) report that higher **initial COD concentrations** lead to higher removal rates for the EO of olive mill wastewaters on BDD anodes. The initial COD concentration of 53 mg/L of the pre-treated leachate from SHMIL Åremma Landfill is remarkably low in comparison with leachates that were used in other studies on EO on BDD anodes. The initial COD concentrations reported range from 380 mg/L to 4000 mg/L (Anglada et al., 2011; Urtiaga et al., 2009; Anglada et al., 2009b, 2010b; Cabeza et al., 2007b; Pérez et al., 2012; Cabeza et al., 2007c). The COD of SHMIL Åremma Landfill Leachate varies strongly and is highly dependent on the season, as the dilution index is significantly higher during winter time. The average COD concentration is 211.5 mg/L (see Table 2.3). Further studies with leachate samples that are taken in summer and therefore have a COD concentration above the average, can give insight on the effect of higher initial COD concentrations on the EO efficiency.

Apart from the mass transport coefficient, the **specific electrode area** (ratio of electrode area to feed volume) plays an important role for achieving high space-time yields (Jüttner et al., 2000). In accordance, the kinetic model proposed by Cabeza et al. (2007c) presented in Chapter 5.2 suggests an increase in removal efficiency of organic matter with a rise in A/V ratio (see Equation 4.5).
Cabeza et al. (2007c) report complete COD removal during the EO of landfill leachate on BDD anodes at 6.3 A after 6 hours of treatment. The feed stream was 1 L and the electrode area was 70 cm^2, yielding an specific electrode area of 7 m^{-1}. In contrast, a feed stream of 15 L was applied in this study, for the same electrode area. The resulting specific electrode area is 0.05 m^{-1}. Subsequently, the low A/V ratio is thought to be responsible for the lower COD oxidation achieved in this study.
In agreement, Anglada et al. (2011) report COD removal rates below 20 % for oxidation of landfill leachate on BDD anodes at 8.4 A with a specific electrode area of 0.7 m^{-1}. In consequence, it is believed that significantly higher removal rates can be achieved by lowering the feed stream.

In other studies on wastewater treatment on BDD anodes, the **treatment time** has shown to have a significant effect on removal efficiencies (Anglada et al., 2011; Chatzisymeon et al., 2009). Especially if both organic matter and ammonium are to be removed, higher treatment times need to be applied, as the degradation mechanisms responsible for COD and NH_4-N degradation compete with each other. NH_4-N removal has been reported to accelerate once most of the COD is degraded.

6.3. Evaluation of Error Sources

In this section, some error sources are discussed, that might bias the measurements conducted in this study.

Concerning the exhaustion of the reactor, it is not possible to clear all liquids from the setup. A small volume remains at the bottom of the tank and in the pipes. In order to minimize the impact from one experimental run on the following one, the reactor was flushed three times with 15 L of Milli-Q after each run. In consequence, slight dilution of the treated effluent occurs.
In addition, the adjustment of the flow rate with the flow-meter is not exact. A valve is adjusted until the floater indicating the flow rate meets the corresponding tic on the scale satisfactorily. Slight deviations in the flow rate are expected for the different runs.
In some experiments, precipitate built during the EO and was restrained by the filter. In this case, the filter resistance rises. This has an impact on energy consumption and can also increase the heat generated during the treatment.
Temperature deviation was observed in a range of +/- 2 ° C with respect to the setpoint.

In the factorial design experiments, 58.2 mL of sample volume per data point was needed for the analyses. Ten samples were taken in each experimental run. Consequently, in the course of the experiment a volume of almost 600 mL is removed from the reactor. As discussed above, the A/V ratio plays a significant role on EO efficiency. The decrease in volume positively influences the elimination efficiency. However, as the removed effluent volume is the same for all runs, no significant interference of the evaluation is attributed to this.

For the runs at pH 5, the appropriate amount of ortho-phosphoric acid was added to the effluent to lower the pH. This acid was chosen, because no major interference is associated to it. However, as already stated above, the leachate matrix is complex and not entirely known. The addition of external substances can lead to undetected side-effects.

The leachate was collected in October 2018 at SHMIL Åremma Landfill in Mosjøen and carried to the laboratory facilities in Trondheim in a 1 m3 tank. It was than bottled immediately in 10 and 20 L containers and put into the cooling chamber. As the tank was carried on a trailer, circulation was given. However, the discharge of the leachate into containers demanded some time during which sedimentation of solids could have occurred. Therefore, slight variations are given in the exact composition for the different containers. This effect is manifested in the deviation of initial pH measured at different experimental runs, ranging from 10,19 to 10,99.
The pH appeared to be decreasing with the storing time. Experiments were performed from October 2018 to March 2019. The change of pH indicates that the effluent is not entirely stable during the storage.
However, initial concentration of NH_4-N, NO_3-N, COD and TOC are distributed randomly, without showing a trend.

The statistical analysis of the factorial desing experiments revealed some outliers in the residual plots. It can be argued, that the data set is rather small for conducting robust statistical analysis. In addition, for various experiments no distinct trend was shown in the behavior of response factors. Therefore, a greater set of experiments under more intense conditions needs to be conducted to generate reliable and robust predictions of the system behavior.

7. Conclusion

The aim of this study is to assess the viability of EO treatment for organic matter removal from a physio-chemically pre-treated municipal landfill leachate on BDD anodes. EO is a popular method in the treatment of complex effluents as it versatile in terms of the nature and concentration of compounds to be treated as well as operating setting like pH and temperature. For EO on BDD anodes, high effectiveness in the removal of recalcitrant compounds has been reported.
The subject of this work is landfill leachate, a real waste water with a complex composition. In contrast to synthetic effluents, the exact matrix of compounds is not known. Therefore, assumptions for the system's behavior under EO are speculative. The main focus is on the characteristics of species known to be present in the leachate. In order to achieve a broad understanding of the entirety of chemical and physical processes during EO, extensive analysis are needed that extend the scope of this thesis. In this section, the main results of the performed studies are summarized and recommendation on further in-depth studies to broaden the understanding of the EO process are given.

Preliminary experiments showed that the electrolyte properties of the leachate are sufficient to allow EO treatment without further addition of electrolytes like chlorine. Furthermore, the experiments suggest that a good performance is given at a flow rate of 600 L/h.

A main task was to find appropriate treatment conditions regarding pH, temperature and current density. Levels for pH and T were given by the inherent characteristics of the leachate and extracted from literature research. In order to find appropriate settings for the applied current, preliminary experiments were conducted to determine i_{lim} for the given reactor hydraulics. An empirical model and a practical experiment using linear sweep voltammetry provided consistent results for the value of i_{lim}, being 31.68 Am^{-2} and 30.72 Am^{-2}, respectively. Relating to the electrode area of 70 cm^2, a limiting current of 215 mA was estimated.

The performance of the setup was further investigated by conducting preliminary experiments with potassium indigotrisulfonate as a model substance. The leachate was spiked with PI and normalized concentration profiles as well as energy consumption were recorded at different current intensities. PI was successfully removed from the leachate at pH 10 and 4°C after 2 hours of treatment at 1 A and 3 hours of treatment at 300 mA. However, energy consumption was about 3.5 times higher for the treatment

at 1 A.

A factorial design experimental series was established to evaluate the treatment efficiency of EO for real leachate on the basis of the evolution of the factors nitrate, ammonium, COD and TOC. With the attempt of testing one level of applied current intensity above and one below the limiting current, 110 mA and 320 mA were chosen for the factorial design experiment. However, overall removal efficiencies were low and the statistical analysis indicated no effect of the applied current. Only the pH was identified as an influencing factor of statistical importance. At pH 10, no reduction of organic matter could be ascribed to EO processes. The presence of carbonate and hydrocarbonate as effective scavengers of hydroxyl radicals in alkaline solutions is thought to be responsible for the inhibition of COD reduction. For NH_4-N, elimination of up to 25 % proceeded during EO treatment at pH 10. Conversely, at pH 5 no removal of NH_4-N could be attributed to electrochemically induced processes, whereas up to 11 % of COD was removed. The results suggest, that when no inhibition of COD removal occurs, the elimination of organic matter dominates over the removal of NH_4-N. COD degradation is believed to mainly be driven by direct oxidation, whereas NH_4-N removal is promoted by indirect oxidation mechanisms.

As a result of NH_4-N oxidation, the concentration of nitrate ions increased during the treatment. A post-treatment has to be considered to compensate the NO_3-N accumulation in the final effluent. In previous studies, ion exchange for reverse osmosis was proposed as a possible post-treatment step (Cabeza et al., 2007a).

Due to the poor removal efficiencies achieved with the chosen settings of current intensity, an additional experimental run was performed at 7 A, pH 5 and 20 °C. 42 % of COD and 3 % of NH_4-N were eliminated during four hours of treatment. Energy consumption amounted to approximately 300 Wh. The ratio of consumed energy to COD elimination accelerated quickly during the treatment, suggesting that under the tested conditions complete removal of organic matter can not be achieved with a proportionate consumption of energy.

During the treatment at 7 A, the amount of in-situ generated free chlorine accelerated, leading to the generation of THMs. In consequence, a continuous measurement of chlorinated byproducts is recommended when working at high current densities. To assess if the chlorinated byproduct formation increases the ecotoxicity of the effluent, acute ecotoxicity can be determined before and after the treatment. If the formation of chlorinated byproducts turns out to be critical, the usage of BDD anodes has to be reevaluated, as they have been reported to especially promote chlorinated byproducts formation for chloride containing wastewaters (Wu et al., 2016).

A rise in the COD/TOC ratio for the experimental run at 7 A and the great deviance

between the removal rate for PI and COD suggest that recalcitrant compounds accumulate in the leachate. In consequence, removal rates slow down and energy consumption increases in the course of the treatment.

The goal for the treatment of SHMIL Åremma Landfill Leachate is to significantly decrease the overall organic load with special regard to recalcitrant, ecotoxic compounds. Therefore, an objective at the beginning of this study was to trace the removal of BPA, a recalcitrant compound which is detected in the leachate and named in the Norwegian List of Priority Substances. However, the BPA concentration in the pre-treated leachate is low (8 μg/L) and no method could be developed in the scope of this study to reliably determine such small concentrations in the leachate samples taken during the EO treatment. Therefore, a promising approach for further studies is to spike the feed stream of leachate with a pre-defined concentration of BPA to ensure concentrations high enough for tracing degradation effects in the course of time. Additionally, degradation mechanisms could be studied in detail by means of HPLC analyses. However, it is of special interest to study the degradation mechanism for the actual concentration found in the leachate. Therefore, efforts are still made to establish a method for reliably determining low BPA concentrations.

The assessment of EO performance under the given conditions revealed that further treatment optimization is needed in terms of removal efficiency and energy consumption. The elimination of organic matter was enhanced by applying a current intensity of 7 A. However, energy consumption rose unproportional and chlorinated by-products were produces. Therefore, the application of higher current densities needs to be accompanied by further modifications of the treatment scheme.
Several approaches for optimizing the reactor design can be realized. Two essential factors for obtaining high space-time yields are the mass transport coefficient and the specific electrode area. Different types of cell constructions have been designed to optimize these factors: (1) circulating electrodes and turbulence promoters, to enhance mass transport, (2) multiple-anode cells to accommodate large electrode areas in small cell volumes and (3) three-dimensional electrodes to improve the mass transport coefficient and enlarge the specific electrode area (Jüttner et al., 2000). A first approach for enhancing the specific electrode area for the given reactor is to apply lower feed volumes of leachate. It is recommended to reevaluate the batch volume as an initial step of treatment optimization.

Another measure for maximizing the current efficiency is the application of multi-step electro-oxidation, as proposed by Panizza et al. (2008). Furthermore, an extension of treatment time promises higher removal efficiencies.

Bibliography

Anglada, A., Ortiz, D., Urtiaga, A. M., and Ortiz, I. (2010a). Electrochemical oxidation of landfill leachates at pilot scale: evaluation of energy needs. *Water science and technology : a journal of the International Association on Water Pollution Research*, 61(9):2211–2217.

Anglada, A., Urtiaga, A., and Ortiz, I. (2009a). Contributions of electrochemical oxidation to waste-water treatment: fundamentals and review of applications. *Journal of Chemical Technology & Biotechnology*, 84(12):1747–1755.

Anglada, A., Urtiaga, A., and Ortiz, I. (2009b). Pilot scale performance of the electrooxidation of landfill leachate at boron-doped diamond anodes. *Environmental Science & Technology*, 43(6):2035–2040.

Anglada, A., Urtiaga, A., Ortiz, I., Mantzavinos, D., and Diamadopoulos, E. (2011). Boron-doped diamond anodic treatment of landfill leachate: evaluation of operating variables and formation of oxidation by-products. *Water research*, 45(2):828–838.

Anglada, A., Urtiaga, A. M., and Ortiz, I. (2010b). Laboratory and pilot plant scale study on the electrochemical oxidation of landfill leachate. *Journal of hazardous materials*, 181(1-3):729–735.

Cabeza, A., Primo, Ó., Urtiaga, A. M., and Ortiz, I. (2007a). Definition of a clean process for the treatment of landfill leachates integration of electrooxidation and ion exchange technologies. *Separation Science and Technology*, 42(7):1585–1596.

Cabeza, A., Urtiaga, A., Rivero, M.-J., and Ortiz, I. (2007b). Ammonium removal from landfill leachate by anodic oxidation. *Journal of hazardous materials*, 144(3):715–719.

Cabeza, A., Urtiaga, A. M., and Ortiz, I. (2007c). Electrochemical treatment of landfill leachates using a boron-doped diamond anode. *Industrial & Engineering Chemistry Research*, 46(5):1439–1446.

Cañizares, P., García-Gómez, J., Fernández de Marcos, I., Rodrigo, M. A., and Lobato, J. (2006a). Measurement of mass-transfer coefficients by an electrochemical technique. *Journal of Chemical Education*, 83(8):1204.

Cañizares, P., Lobato, J., Paz, R., Rodrigo, M. A., and Sáez, C. (2005). Electrochemical oxidation of phenolic wastes with boron-doped diamond anodes. *Water research*, 39(12):2687–2703.

Cañizares, P., Paz, R., Lobato, J., Sáez, C., and Rodrigo, M. A. (2006b). Electrochemical treatment of the effluent of a fine chemical manufacturing plant. *Journal of hazardous materials*, 138(1):173–181.

Cañizares, P., Sáez, C., Lobato, J., and Rodrigo, M. A. (2004). Electrochemical treatment of 4-nitrophenol-containing aqueous wastes using boron-doped diamond anodes. *Industrial & Engineering Chemistry Research*, 43(9):1944–1951.

Chatzisymeon, E., Xekoukoulotakis, N. P., Diamadopoulos, E., Katsaounis, A., and Mantzavinos, D. (2009). Boron-doped diamond anodic treatment of olive mill wastewaters: statistical analysis, kinetic modeling and biodegradability. *Water research*, 43(16):3999–4009.

Chiang, L.-C., Chang, J.-E., and Wen, T.-C. (1995). Indirect oxidation effect in electrochemical oxidation treatment of landfill leachate. *Water research*, 29(2):671–678.

Comninellis, C. (1994). Electrocatalysis in the electrochemical conversion/combustion of organic pollutants for waste water treatment. *Electrochimica Acta*, 39(11-12):1857–1862.

de Oliveira Campos, V. (2018). Electrochemical treatment of produced water using Ti/Pt and BDD anode. *International Journal of Electrochemical Science*, pages 7894–7906.

Deng, Y. and Englehardt, J. D. (2007). Electrochemical oxidation for landfill leachate treatment. *Waste management (New York, N.Y.)*, 27(3):380–388.

Donaghue, A. and Chaplin, B. P. (2013). Effect of select organic compounds on perchlorate formation at boron-doped diamond film anodes. *Environmental science & technology*, 47(21):12391–12399.

European Council (1999). Council directive 1999/31/ec of 16 april 1999 on the landfill of waste.

European Parliament and Council of the European Union (2012). Directive 2008/105/ec of the european parliament and of the council of 16 december 2008 on environmental quality standards in the field of water policy, amending and subsequentlyrepealing council directives 82/176/eec, 83/513/eec, 84/156/eec, 84/491/eec, 86/280/eec andamending directive 2000/60/ec of the european parliament and of the council.

Fernandes, A., Pacheco, M. J., Ciríaco, L., and Lopes, A. (2015). Review on the electrochemical processes for the treatment of sanitary landfill leachates: Present and future. *Applied Catalysis B: Environmental*, 176-177:183–200.

Google Maps (2019). Location of SHMIL Aremma Landfill. Website, last visited on 09.05.2019. Online available on:. https://www.google.com/maps/place/SHMIL+-+%C3%85remma+avfallsanlegg/@65.8734134,13.1581578,13.25z/data=!4m5!3m4!1s0x467450c3d9da8c9b:0xf47a9ee6e29a12e6!8m2!3d65.8804264!4d13.2060503?hl=en.

Gröhlich, A. (2015). *Evaluation of landfill leachate treatment, considering water quality, legal aspects and site specifics*. PhD thesis, Technical University Hamburg-Harburg, Hamburg.

Gujer, W. (2007). *Siedlungswasserwirtschaft: Mit 84 Tabellen*. Springer, Berlin and Heidelberg, 3., bearb. aufl. edition.

Hach Lange GmbH (1995). Cuvette Test LCK 339 for Determination of NO3-N. Website, last visited on 20.05.2019. Online available on:. https://www.ethz.ch/content/dam/ethz/special-interest/baug/luiw-dam/documents/LUIW_Kurzbeschriebe/lck339.pdf.

Hach Lange GmbH (2014). Wasseranalytik für das Labor: Photometrische und elektrochemische Geräte, Reagenzien und Services. Website, last visited on 20.05.2019. Online available on:. https://de.hach.com/cms/documents/lab-catalogue-de-DOC032.72.20121.Feb14.pdf.

Hach Lange GmbH (2018). Chlorine, Free and Total, High Range: USEPA DPD Method. Website, last visited on 20.05.2019. Online available on:. https://www.google.com/url?sa=t&rct=j&q=&esrc=s&source=web&cd=6&ved=2ahUKEwitwK-0mqriAhVIsaQKHR-AAxAQFjAFegQIAxAC&url=https%3A%2F%2Fwww.hach.com%2Fasset-get.download-en.jsa%3Fid%3D31948984021&usg=AOvVaw2tgR3e8itPKJI5AQ4A6OAM.

Hach Lange GmbH (2019). Ammonium Küvetten-Test 2,0-47,0 mg/L NH4-N. Website, last visited on 20.05.2019. Online available on:. https://de.hach.com/ammonium-kuvetten-test-2-0-47-0-mg-l-nh-sub-4-sub-n/product?id=26370260971.

Harstad, K. (2006). *Handling and Assessment of Leachates from Municipal Solid Waste Landfills in the Nordic Countries*. Nordic Council of Ministers.

Hood, E. (2005). Tap water and trihalomethanes: Flow of concerns continues. *Environmental Health Perspectives*, 113(7):A474.

Jüttner, K., Galla, U., and Schmieder, H. (2000). Electrochemical approaches to environmental problems in the process industry. *Electrochimica Acta*, 45(15-16):2575–2594.

Kapalka, A., Fóti, G., and Comninellis, C. (2010). Basic principles of the electrochemical mineralization of organic pollutants for wastewater treatment. In Comninellis, C., editor, *Electrochemistry for the Environment*, pages 1–23. Springer-Verlag New York, New York, NY.

Kim, B. R. (1989). Effect of ammonia on COD analysis. *Water Pollution Control Federation*, (Vol. 61, No. 5 (May, 1989)):614–617.

Kjeldsen, P., Barlaz, M. A., Rooker, A. P., Baun, A., Ledin, A., and Christensen, T. H. (2002). Present and long-Term composition of MSW landfill leachate: A review. *Critical Reviews in Environmental Science and Technology*, 32(4):297–336.

Koppe, P. and Stozek, A. (1990). *Kommunales Abwasser: Seine Inhaltsstoffe nach Herkunft, Zusammensetzung und Reaktionen im Reinigungsprozeß einschließlich Klärschlämme*. Vulkan Verlag, Essen, 2. auflage edition.

Kurniawan, T. A. (2012). *Landfill leachate treatment: Laboratory studies*. Lap Lambert Academic Publ, [Place of publication not identified].

Kurzweil, P. (2015). *Chemie*. Springer Fachmedien Wiesbaden, Wiesbaden.

Li, H. and Ni, J. (2012). Electrogeneration of disinfection byproducts at a boron-doped diamond anode with resorcinol as a model substance. *Electrochimica Acta*, 69:268–274.

Martínez-Huitle, C. A. and Ferro, S. (2006). Electrochemical oxidation of organic pollutants for the wastewater treatment: direct and indirect processes. *Chemical Society reviews*, 35(12):1324–1340.

Martínez-Huitle, C. A. and Panizza, M. (2018). Electrochemical oxidation of organic pollutants for wastewater treatment. *Current Opinion in Electrochemistry*, 11:62–71.

Martínez-Huitle, C. A., Quiroz, M. A., Comninellis, C., Ferro, S., and de Battisti, A. (2004). Electrochemical incineration of chloranilic acid using Ti/IrO2, Pb/PbO2 and Si/BDD electrodes. *Electrochimica Acta*, 50(4):949–956.

Merkel, A. (2013). Climate Data Mosjoen 1982-2012. Website, last visited on 09.05.2019. Online available on:. `https://de.climate-data.org/europa/norwegen/nordland/mosj%C3%B8en-9908/`.

Michael, T. and Munt, I. (2012). Diercke - Weltatlas.

Minitab Inc. (2017). Getting Started with Minitab 18. Website, last visited on 09.05.2019. Online available on:. `https://www.minitab.com/uploadedFiles/Documents/getting-started/MinitabGettingStarted_EN.pdf`.

Moreira, F. C., Boaventura, R. A., Brillas, E., and Vilar, V. J. (2017). Electrochemical advanced oxidation processes: A review on their application to synthetic and real wastewaters. *Applied Catalysis B: Environmental*, 202:217–261.

Moreira, F. C., Soler, J., Fonseca, A., Saraiva, I., Boaventura, R. A. R., Brillas, E., and Vilar, V. J. P. (2015). Incorporation of electrochemical advanced oxidation processes in a multistage treatment system for sanitary landfill leachate. *Water research*, 81:375–387.

Murugananthan, M., Yoshihara, S., Rakuma, T., and Shirakashi, T. (2008). Mineralization of bisphenol A (BPA) by anodic oxidation with boron-doped diamond (BDD) electrode. *Journal of hazardous materials*, 154(1-3):213–220.

Nierop, K. G. J., Jansen, B., and Verstraten, J. M. (2002). Dissolved organic matter, aluminium and iron interactions: precipitation induced by metal/carbon ratio, pH and competition. *The Science of the total environment*, 300(1-3):201–211.

Ozkaya, B. (2005). Chlorophenols in leachates originating from different landfills and aerobic composting plants. *Journal of hazardous materials*, 124(1-3):107–112.

Panizza, M. (2010). Importance of electrode material in the electrochemical treatment of wastewater containing organic pollutants. In Comninellis, C., editor, *Electrochemistry for the Environment*, volume 44, pages 25–54. Springer-Verlag New York, New York, NY.

Panizza, M., Kapalka, A., and Comninellis, C. (2008). Oxidation of organic pollutants on BDD anodes using modulated current electrolysis. *Electrochimica Acta*, 53(5):2289–2295.

Panizza, M. and Martinez-Huitle, C. A. (2013). Role of electrode materials for the anodic oxidation of a real landfill leachate – Comparison between Ti–Ru–Sn ternary oxide, PbO2 and boron-doped diamond anode. *Chemosphere*, 90(4):1455–1460.

Panizza, M., Michaud, P. A., Cerisola, G., and Comninellis, C. (2001a). Anodic oxidation of 2-naphthol at boron-doped diamond electrodes. *Journal of Electroanalytical Chemistry*, 507(1-2):206–214.

Panizza, M., Michaud, P. A., Cerisola, G., and Comninellis, C. (2001b). Electrochemical treatment of wastewaters containing organic pollutants on boron-doped diamond electrodes: Prediction of specific energy consumption and required electrode area. *Electrochemistry Communications*, 3(7):336–339.

Pereira, G. F., Rocha-Filho, R. C., Bocchi, N., and Biaggio, S. R. (2012). Electrochemical degradation of bisphenol A using a flow reactor with a boron-doped diamond anode. *Chemical Engineering Journal*, 198-199:282–288.

Pérez, G., Saiz, J., Ibañez, R., Urtiaga, A. M., and Ortiz, I. (2012). Assessment of the formation of inorganic oxidation by-products during the electrocatalytic treatment of ammonium from landfill leachates. *Water research*, 46(8):2579–2590.

Polcaro, A. M., Vacca, A., Palmas, S., and Mascia, M. (2003). Electrochemical treatment of wastewater containing phenolic compounds: oxidation at boron-doped diamond electrodes. *Journal of Applied Electrochemistry*, 33(10):885–892.

Rabaaoui, N., Saad, M. E. K., Moussaoui, Y., Allagui, M. S., Bedoui, A., and Elaloui, E. (2013). Anodic oxidation of o-nitrophenol on BDD electrode: variable effects and mechanisms of degradation. *Journal of hazardous materials*, 250-251:447–453.

Rodrigo, M. A., Michaud, P. A., Duo, I., Panizza, M., Cerisola, G., and Comninellis, C. (2001). Oxidation of 4-chlorophenol at boron-doped diamond electrode for wastewater treatment. *Journal of Applied Electrochemistry*, 148(5):D60.

Sahiri, T. (1995). *Optimierung einer elektrochemischen Anlage zum Abbau von Nitrophenolen in industriellen Abwässern*. PhD thesis, TU Berlin, Berlin.

Schmidt, V. M. (2003). *Elektrochemische Verfahrenstechnik*. Wiley-VCH Verlag GmbH & Co. KGaA, Weinheim, FRG.

SHMIL IKS (2019). Homepage Landfill Aremma SHMIL. Website, last visited on 09.05.2019. Online available on:. `https://shmil.no/om-shmil/`.

Sigma-Aldrich (2019). Potassium indigotrisulfonate. Website, last visited on 20.05.2019. Online available on:. `https://www.sigmaaldrich.com/catalog/product/sial/234087?lang=en&region=NO&gclid=EAIaIQobChMIq-PWzqSq4gIVSCjTCh1GXQnKEAAYASAAEgJLBPD_BwE`.

STEP Systems GmbH (2000). LCK 303 2-47 mg/L NH4-N. Website, last visited on 09.05.2019. Online available on:. `https://www.google.com/url?sa=t&rct=j&q=&esrc=s&source=web&cd=1&ved=2ahUKEwiY49S84aniAhXLy6QKHUAMD-YQFjAAegQIBBAC&url=https%3A%2F%2Fwww.stepsystems.de%2Ffiles%2Flck-303-ammonium.pdf&usg=AOvVaw3NDY0BGUKWx467Fk_Jq5Ee`.

Sun, J., Lu, H., Lin, H., Du, L., Huang, W., Li, H., and Cui, T. (2012). Electrochemical oxidation of aqueous phenol at low concentration using Ti/BDD electrode. *Separation and Purification Technology*, 88:116–120.

The Norwegian Environment Agency (2018). List of Priority Substances. https://www.environment.no/topics/hazardous-chemicals/list-of-priority-substances/.

Upadhyay, S. K. (2006). *Chemical Kinetics and Reaction Dynamics*. Springer-Verlag, s.l., 1. aufl. edition.

Urbansky, E. T. (2002). Perchlorate as an environmental contaminant. *Environmental Science and Pollution Research*, 9(3):187–192.

Urbansky, E. T. and Schock, M. R. (1999). Issues in managing the risks associated with perchlorate in drinking water. *Journal of Environmental Management*, 56(2):79–95.

Urtiaga, A., Rueda, A., Anglada, A., and Ortiz, I. (2009). Integrated treatment of landfill leachates including electrooxidation at pilot plant scale. *Journal of hazardous materials*, 166(2-3):1530–1534.

Vlyssides, A. G. (2003). Influence of various parameters on the electrochemical treatment of landfill leachates. *Journal of Applied Electrochemistry*, 33(2):155–159.

WaterDiam (2015). Water treatment by electro-oxidation: Instructions for follow-up and set up of treatment tests (case of wastewater containing organics): Instruction manual on waste water treatment by diaclean unit.

Wu, W., Huang, Z.-H., and Lim, T.-T. (2016). A comparative study on electrochemical oxidation of bisphenol A by boron-doped diamond anode and modified SnO 2 -Sb anodes: Influencing parameters and reaction pathways. *Journal of Environmental Chemical Engineering*, 4(3):2807–2815.

A. Quality Data for SHMIL Åremma Landfill Leachate

Parameter	Unit	No. of measured values	Max.	Min.	Mean	Medi-an	Std. Dev.
pH	-	46	7,4	6,4	6,82	6,8	0,29
conductivity	mS/m	46	420	122	257,13	265	70,4
suspended solids	mg/l	46	360	27	86,56	80,5	56,3
COD	mg/l	50	643	72	211,5	187	108,85
BOD5	mg/l	50	160	4	20,7	11	28,6
TOC	mg/l	46	135	3	59,5	53,85	29,76
Total-P	mg/l	46	2,3	0,12	0,55	0,41	0,40
Total-N	mg/l	46	200	22	102,2	98,5	41,3
NH_4-N	mg/l	46	210	20	95,15	93	39,45

Figure A.1.: Characterizing parameters for SHMIL Åremma Landfill Leachate (2006-2015)(Gröhlich, 2015).

Parameter	Unit	No. of measured values	Max.	Min.	Mean	Median	Std. Dev.
Ca	mg/l	19	184	32	127,6	122	36,3
K	mg/l	19	187	35,5	76,5	56,9	37,8
Mg	mg/l	19	42,9	14,2	26,35	25,9	7,03
Na	mg/l	49	514	84,9	198,55	192	72,43

Figure A.2.: Concentrations of alkaline earth metals for SHMIL Åremma Landfill Leachate (2006-2015)(Gröhlich, 2015).

Parameter	Unit	No. of measured values	Max.	Min.	Mean	Median	Std. Dev.
Fe	mg/l	50	101,9	0,097	32,27	29,65	18,60
Al	µg/l	19	1740	22,6	393,77	237	415,6
As	µg/l	49	9,97	1,73	4,15	3,77	1,77
Ba	µg/l	19	243	59,3	121,7	125	44,87
Cd	µg/l	43	0,521	0,01	0,089	0,05	0,09
Co	µg/l	19	12,2	3,28	5,15	4,7	1,86
Cr	µg/l	50	48,4	1,84	15,36	11,7	11,29
Cu	µg/l	50	248	1	15,36	4,73	40,11
Hg	µg/l	50	0,094	0,0005	0,023	0,02	0,013
Mn	µg/l	50	1990	513	1385,4	1475	385,74
Mo	µg/l	8	1,92	0,63	1,47	1,72	0,47
Ni	µg/l	50	71,9	7,88	18,76	16,1	11,08
Pb	µg/l	50	5,5	0,5	1,57	1,2	1,08
Zn	µg/l	50	440	9,66	74,02	57,25	76,69
V	µg/l	8	4,39	0,388	1,92	1,89	1,22

Figure A.3.: Concentrations of (heavy) metals for SHMIL Åremma Landfill Leachate (2006-2015)(Gröhlich, 2015).

Parameter	Unit	No. of measured values	Max.	Min.	Mean	Median	Std. Dev.
Naphthalene	µg/l	45	6,49	0,01	1,94	1,61	1,73
Acenaphtylene	µg/l	45	0,25	0,01	0,026	0,011	0,044
Acenaphtene	µg/l	46	1,03	0,01	0,436	0,445	0,23
Flourene	µg/l	46	0,61	0,01	0,29	0,32	0,16
Phenanthrene	µg/l	46	0,77	0,02	0,28	0,33	0,18
Anthracene	µg/l	46	0,47	0,01	0,047	0,03	0,08
Flouranthene	µg/l	46	0,16	0,01	0,065	0,056	0,032
Pyrene	µg/l	46	0,3	0,017	0,061	0,06	0,04
Benz(a)anthracene	µg/l	45	0,1	0,01	0,014	0,01	0,0146
Chrysene	µg/l	46	0,1	0,01	0,015	0,01	0,0149
Benzo(b)flouranthene	µg/l	46	0,1	0,01	0,0151	0,01	0,0154
Benzo(k)flouranthene	µg/l	42	0,1	0,01	0,013	0,01	0,015
Benzo(a)pyrene	µg/l	46	0,1	0,005	0,019	0,02	0,013
Dibenz(a,h)anthracene	µg/l	46	0,1	0,01	0,013	0,01	0,014
Benzo(ghi)perylene	µg/l	46	0,1	0,01	0,013	0,01	0,0144
Indeno (123cd) pyrene	µg/l	46	0,1	0,01	0,015	0,01	0,019
Sum PAH-16	µg/l	45	8,63	0,02	3,04	2,8	2,27
Sum PAH carcinogenic	µg/l	12	0,4	0,011	0,069	0,035	0,11

Figure A.4.: Concentrations of PAHs for SHMIL Åremma Landfill Leachate (2006-2015)(Gröhlich, 2015).

Parameter	Unit	No. of measured values	Max.	Min.	Mean	Median	Std. Dev.
Benzene	µg/l	46	84	0,2	2,57	0,2	12,31
Toluene	µg/l	46	40	0,16	3,15	1	6,64
Ethylbenzene	µg/l	46	31	0,04	2,89	0,1	6,45
o-Xylene	µg/l	46	15	0,1	3,15	1,47	3,78
m-/p-Xylene	µg/l	46	57	0,02	8,2	2,11	13,20
Sum BTEX	µg/l	42	230	0,17	20,36	5,05	40,22

Figure A.5.: Concentrations of BTEX for SHMIL Åremma Landfill Leachate (2006-2015)(Gröhlich, 2015).

Parameter	Unit	No. of measured values	Max.	Min.	Mean	Median	Std. Dev.
Fraction >C10-C12	µg/l	46	150	5	34,06	27,5	27,78
Fraction >C12-C16	µg/l	46	7890	5	220,63	24,2	1160,72
Fraction >C16-C35	µg/l	46	6390	30	217,5	60	934,2
Fraction >C35-C40	µg/l	26	736	10	39,04	10	142,2
Fraction >C10-C40	µg/l	40	15100	50	552,70	118	2386,2
Sum >C12-C35	µg/l	4	35	8,2	28,3	35	13,4

Figure A.6.: Concentrations of hydrocarbons for SHMIL Åremma Landfill Leachate (2006-2015)(Gröhlich, 2015).

Parameter	Unit	No. of measured values	Max.	Min.	Mean	Median	Std. Dev.
2,4-D	µg/l	18	0,2	0,05	0,07	0,05	0,04
MCPA	µg/l	18	0,1	0,05	0,06	0,05	0,02
MCPP	µg/l	18	3,7	0,68	2,1	2,1	0,91
2,4,5-T	µg/l	18	0,1	0,05	0,06	0,05	0,02
2,4,5-TP	µg/l	18	0,1	0,05	0,06	0,05	0,02
MCPB	µg/l	18	0,1	0,05	0,06	0,05	0,02
2,4-DB	µg/l	18	0,4	0,05	0,08	0,05	0,09
2,4-DP	µg/l	18	1,4	0,083	0,34	0,199	0,37

Figure A.7.: Concentrations of herbicides for SHMIL Åremma Landfill Leachate (2006-2015)(Gröhlich, 2015).

Parameter	Unit	No. of measured values	Max.	Min.	Mean	Median	Std. Dev.
acute toxicity	TU	30	47	1	5,27	1	9,99
EC50 (15:15)	ml/l	1	754	754	754	754	0
EC20 (15:15)	ml/l	3	382	148	269	277	117,21
CN free	mg/l	9	0,041	0,005	0,014	0,005	0,014
CN total	mg/l	8	14	0,031	2,27	0,46	4,79

Figure A.8.: Other parameters for SHMIL Åremma Landfill Leachate (2006-2015)(Gröhlich, 2015).

Priority substance	Unit	Median (from 2006-2015)
Anthracene	µg/l	0,031
PBDE-99	µg/l	0,001
PBDE-203	µg/l	0,002
Naphthalene	µg/l	1,7350
Octylphenole	µg/l	0,3180
Trichlorobenzene	µg/l	0,02
Cadmium and org. Cadmium compounds	µg/l	0,0916
Lead and org. Lead compounds	µg/l	1,38
Mercury and org. Mercury compounds	µg/l	0,0258
Nickel and org. Nickel compounds	µg/l	16,1
Tributyltin [-cation]	µg/l	0,002
Benzene	µg/l	0,2
Terbutryn	µg/l	0,237
PFOS	µg/l	0,09
Nonylphenol	µg/l	1,05
PAH (Benzo(a)pyrene, Benzo(b)flouranthene, Benzo(k)flouranthene, Benzo(g,h,i)perylene, Indeno(1,2,3-cd)pyrene)	µg/l	0,06

Figure A.9.: Substances from the EU-LoPS that have been detected in SHMIL Åremma Landfill Leachate (Gröhlich, 2015).

Norwegian priority substance	Unit	Median (from 2006-2015)
Arsenic	µg/l	3,79
Bisphenol A	µg/l	15
Chromium	µg/l	11,7

Figure A.10.: Substances from the N-LoPS that have been detected in SHMIL Åremma Landfill Leachate (Gröhlich, 2015).

AA: annual average;

MAC: maximum allowable concentration.

Unit: [µg/l]

(1)	(2)	(3)	(4)	(5)	(6)	(7)
No	Name of substance	CAS number (1)	AA-EQS (2) Inland surface waters (3)	AA-EQS (2) Other surface waters	MAC-EQS (4) Inland surface waters (3)	MAC-EQS (4) Other surface waters
(1)	Alachlor	15972-60-8	0,3	0,3	0,7	0,7
(2)	Anthracene	120-12-7	0,1	0,1	0,4	0,4
(3)	Atrazine	1912-24-9	0,6	0,6	2,0	2,0
(4)	Benzene	71-43-2	10	8	50	50
(5)	Brominated diphenylether (5)	32534-81-9	0,0005	0,0002	not applicable	not applicable
(6)	Cadmium and its compounds (depending on water hardness classes) (6)	7440-43-9	≤ 0,08 (Class 1) 0,08 (Class 2) 0,09 (Class 3) 0,15 (Class 4) 0,25 (Class 5)	0,2	≤ 0,45 (Class 1) 0,45 (Class 2) 0,6 (Class 3) 0,9 (Class 4) 1,5 (Class 5)	≤ 0,45 (Class 1) 0,45 (Class 2) 0,6 (Class 3) 0,9 (Class 4) 1,5 (Class 5)
(6a)	Carbon-tetrachloride (7)	56-23-5	12	12	not applicable	not applicable
(7)	C10-13 Chloroalkanes	85535-84-8	0,4	0,4	1,4	1,4
(8)	Chlorfenvinphos	470-90-6	0,1	0,1	0,3	0,3
(9)	Chlorpyrifos (Chlorpyrifos-ethyl)	2921-88-2	0,03	0,03	0,1	0,1
(9a)	Cyclodiene pesticides: Aldrin (7) Dieldrin (7) Endrin (7) Isodrin (7)	 309-00-2 60-57-1 72-20-8 465-73-6	Σ = 0,01	Σ = 0,005	not applicable	not applicable
(9b)	DDT total (7) (8)	not applicable	0,025	0,025	not applicable	not applicable
	para-para-DDT (7)	50-29-3	0,01	0,01	not applicable	not applicable
(10)	1,2-Dichloroethane	107-06-2	10	10	not applicable	not applicable
(11)	Dichloromethane	75-09-2	20	20	not applicable	not applicable
(12)	Di(2-ethylhexyl)-phthalate (DEHP)	117-81-7	1,3	1,3	not applicable	not applicable
(13)	Diuron	330-54-1	0,2	0,2	1,8	1,8
(14)	Endosulfan	115-29-7	0,005	0,0005	0,01	0,004
(15)	Fluoranthene	206-44-0	0,1	0,1	1	1
(16)	Hexachloro-benzene	118-74-1	0,01 (9)	0,01 (9)	0,05	0,05
(17)	Hexachloro-butadiene	87-68-3	0,1 (9)	0,1 (9)	0,6	0,6
(18)	Hexachloro-cyclohexane	608-73-1	0,02	0,002	0,04	0,02

Figure A.11.: EU List of Priority Substances, Part 1 (European Parliament and Council of the European Union, 2012).

(1)	(2)	(3)	(4)	(5)	(6)	(7)
No	Name of substance	CAS number (1)	AA-EQS (2) Inland surface waters (3)	AA-EQS (2) Other surface waters	MAC-EQS (4) Inland surface waters (3)	MAC-EQS (4) Other surface waters
(19)	Isoproturon	34123-59-6	0,3	0,3	1,0	1,0
(20)	Lead and its compounds	7439-92-1	7,2	7,2	not applicable	not applicable
(21)	Mercury and its compounds	7439-97-6	0,05 (9)	0,05 (9)	0,07	0,07
(22)	Naphthalene	91-20-3	2,4	1,2	not applicable	not applicable
(23)	Nickel and its compounds	7440-02-0	20	20	not applicable	not applicable
(24)	Nonylphenol (4-Nonylphenol)	104-40-5	0,3	0,3	2,0	2,0
(25)	Octylphenol ((4-(1,1′,3,3′-tetramethylbutyl)-phenol))	140-66-9	0,1	0,01	not applicable	not applicable
(26)	Pentachloro-benzene	608-93-5	0,007	0,0007	not applicable	not applicable
(27)	Pentachloro-phenol	87-86-5	0,4	0,4	1	1
(28)	Polyaromatic hydrocarbons (PAH) (10)	not applicable	not applicable	not applicable	not applicable	not applicable
	Benzo(a)pyrene	50-32-8	0,05	0,05	0,1	0,1
	Benzo(b)fluor-anthene	205-99-2	Σ = 0,03	Σ = 0,03	not applicable	not applicable
	Benzo(k)fluor-anthene	207-08-9				
	Benzo(g,h,i)-perylene	191-24-2	Σ = 0,002	Σ = 0,002	not applicable	not applicable
	Indeno(1,2,3-cd)-pyrene	193-39-5				
(29)	Simazine	122-34-9	1	1	4	4
(29a)	Tetrachloro-ethylene (7)	127-18-4	10	10	not applicable	not applicable
(29b)	Trichloro-ethylene (7)	79-01-6	10	10	not applicable	not applicable
(30)	Tributyltin compounds (Tributhyltin-cation)	36643-28-4	0,0002	0,0002	0,0015	0,0015
(31)	Trichloro-benzenes	12002-48-1	0,4	0,4	not applicable	not applicable
(32)	Trichloro-methane	67-66-3	2,5	2,5	not applicable	not applicable
(33)	Trifluralin	1582-09-8	0,03	0,03	not applicable	not applicable

(1) CAS: Chemical Abstracts Service.
(2) This parameter is the EQS expressed as an annual average value (AA-EQS). Unless otherwise specified, it applies to the total concentration of all isomers.
(3) Inland surface waters encompass rivers and lakes and related artificial or heavily modified water bodies.
(4) This parameter is the EQS expressed as a maximum allowable concentration (MAC-EQS). Where the MAC-EQS are marked as 'not applicable', the AA-EQS values are considered protective against short-term pollution peaks in continuous discharges since they are significantly lower than the values derived on the basis of acute toxicity.
(5) For the group of priority substances covered by brominated diphenylethers (No 5) listed in Decision No 2455/2001/EC, an EQS is established only for congener numbers 28, 47, 99, 100, 153 and 154.
(6) For cadmium and its compounds (No 6) the EQS values vary depending on the hardness of the water as specified in five class categories (Class 1: < 40 mg $CaCO_3$/l, Class 2: 40 to < 50 mg $CaCO_3$/l, Class 3: 50 to < 100 mg $CaCO_3$/l, Class 4: 100 to < 200 mg $CaCO_3$/l and Class 5: ≥ 200 mg $CaCO_3$/l).
(7) This substance is not a priority substance but one of the other pollutants for which the EQS are identical to those laid down in the legislation that applied prior to 13 January 2009.
(8) DDT total comprises the sum of the isomers 1,1,1-trichloro-2,2 bis (p-chlorophenyl) ethane (CAS number 50-29-3; EU number 200-024-3); 1,1,1-trichloro-2 (o-chlorophenyl)-2-(p-chlorophenyl) ethane (CAS number 789-02-6; EU number 212-332-5); 1,1-dichloro-2,2 bis (p-chlorophenyl) ethylene (CAS number 72-55-9; EU number 200-784-6); and 1,1-dichloro-2,2 bis (p-chlorophenyl) ethane (CAS number 72-54-8; EU number 200-783-0).
(9) If Member States do not apply EQS for biota they shall introduce stricter EQS for water in order to achieve the same level of protection as the EQS for biota set out in Article 3(2) of this Directive. They shall notify the Commission and other Member States, through the Committee referred to in Article 21 of Directive 2000/60/EC, of the reasons and basis for using this approach, the alternative EQS for water established, including the data and the methodology by which the alternative EQS were derived, and the categories of surface water to which they would apply.
(10) For the group of priority substances of polyaromatic hydrocarbons (PAH) (No 28), each individual EQS is applicable, i.e. the EQS for Benzo(a)pyrene, the EQS for the sum of Benzo(b)fluoranthene and Benzo(k)fluoranthene and the EQS for the sum of Benzo(g,h,i)perylene and Indeno(1,2,3-cd)pyrene must be met.

Figure A.12.: EU List of Priority Substances, Part 2 (European Parliament and Council of the European Union, 2012).

(Miljødirektoratet, 2018)

	Substance (short)
1)	Arsenic
2)	Bisphenol A
3)	Brominated flame retardants
4)	DEHP
5)	Certain surfactants (DTDMAC, DSDMAC, DHTDMAC)
6)	1,2-Dichlorethane (EDC)
7)	Dioxins and furans
8)	Cadmium
9)	Chlorinated alkyl benzenes (CABs)
10)	Chromium
11)	Hexachlorbenzene
12)	Lead
13)	Medium-chain chlorinated paraffins
14)	Mercury
15)	Musk xylenes
16)	Nonylphenol and its ethoxylates
17)	Octylphenol and its ethoxylates
18)	PAHs
19)	Pentachlorphenol (PCP)
20)	Polychlorinated biphenyls (PCBs)
21)	PFOA
22)	PFOS
23)	Short-chain chlorinated paraffins
24)	Siloxane-D4
25)	Siloxane-D5
26)	TCEP (tris(2-chloroethyl)phosphate)
27)	Tetrachloroethene (PER)
28)	Tributyl tin compounds
29)	Trichlorobenzene
30)	Trichloroethene (TRI)
31)	Triclosan
32)	2.4.6 Tri-tert-butylphenol

Figure A.13.: Norwegian List of Priority Substances (The Norwegian Environment Agency, 2018).

B. Run Order for DoE

	pH	T (°C)	Current (mA)
1	10	20	110
2	10	4	110
3	10	4	320
4	10	20	110
5	5	20	110
6	5	4	320
7	5	20	320
8	5	20	110
9	10	20	320
10	5	4	320
11	10	20	320
12	10	4	320
13	5	20	320
14	5	4	110
15	5	4	110
16	10	4	110

Figure B.1.: Run order of the factorial design of experiments.

C. Pareto Charts and Residual Plots for DoE

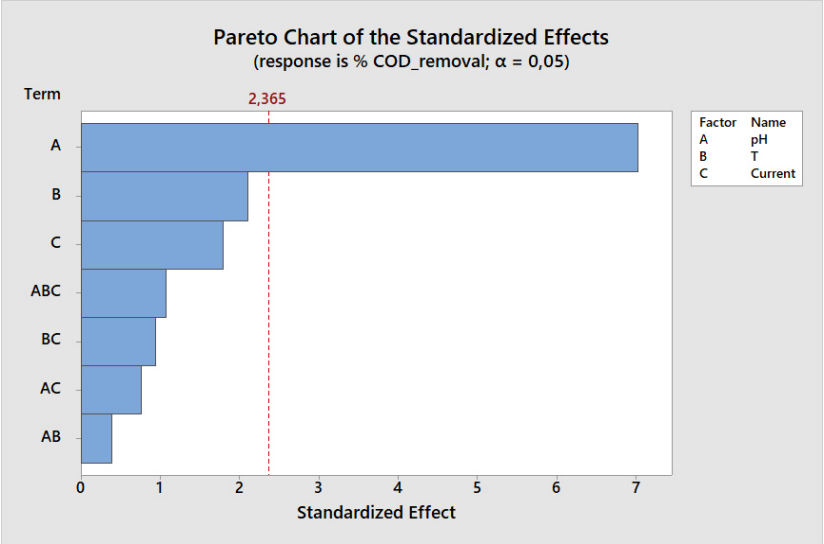

Figure C.1.: Pareto chart for COD removal.

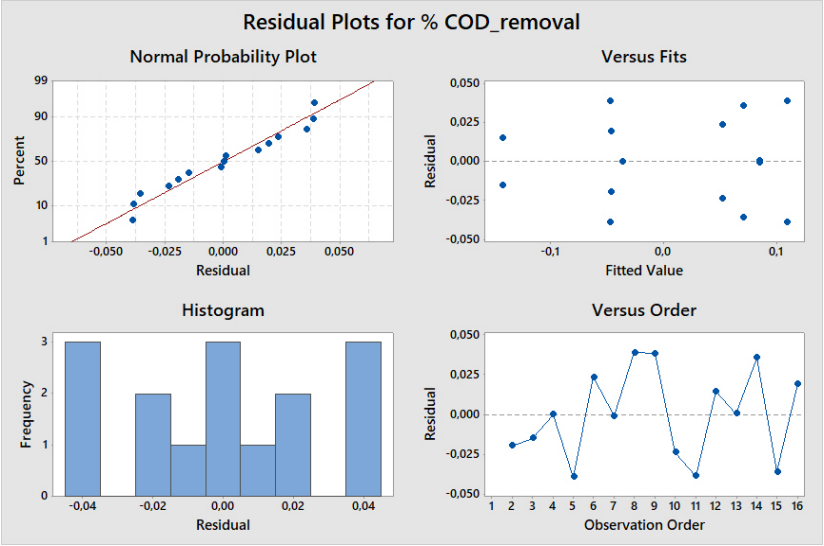

Figure C.2.: Residuals for COD removal.

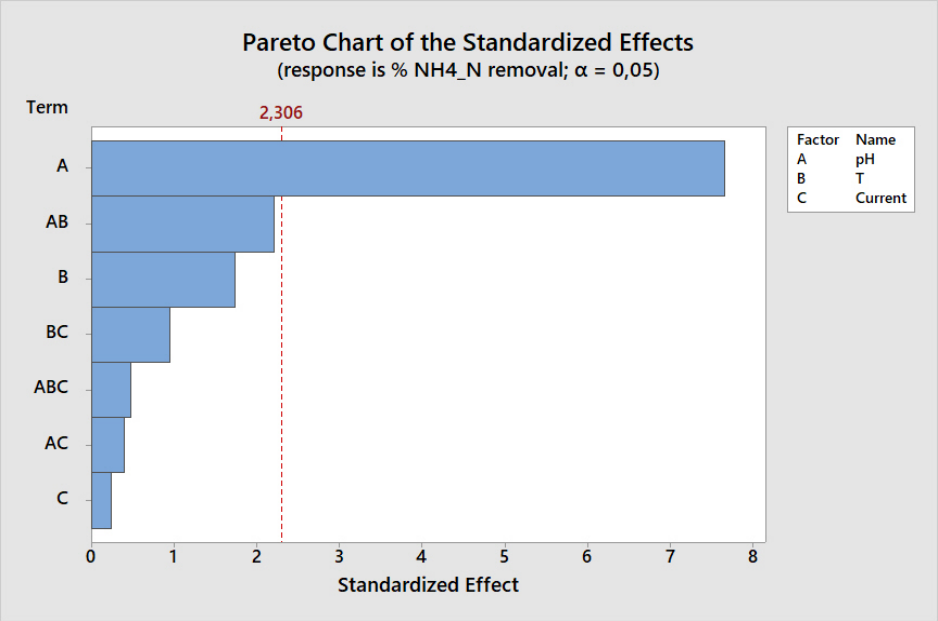

Figure C.3.: Pareto chart for $NH_4 - N$ removal.

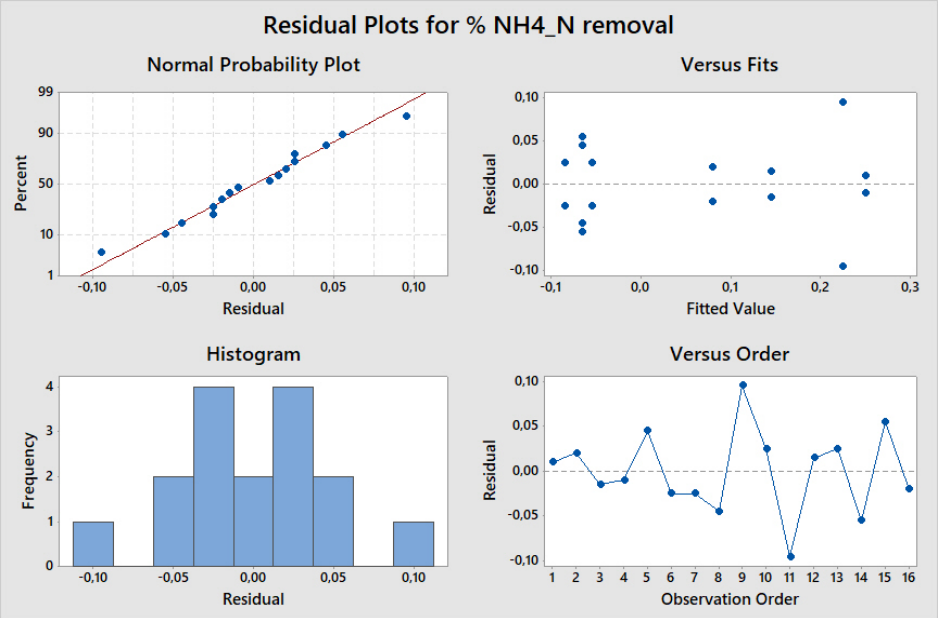

Figure C.4.: Residuals for $NH_4 - N$ removal.

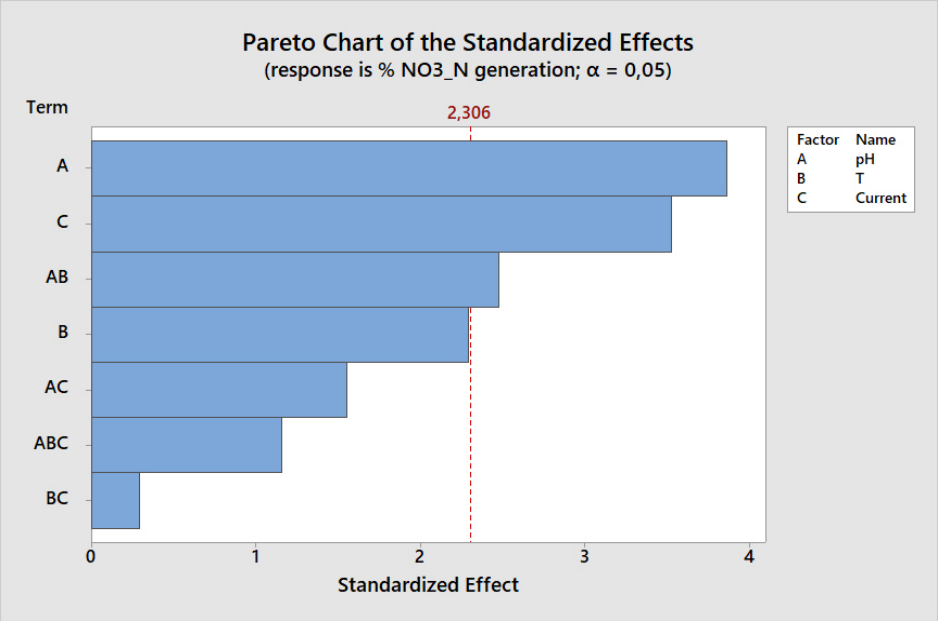

Figure C.5.: Pareto chart for $NO_3 - N$ removal.

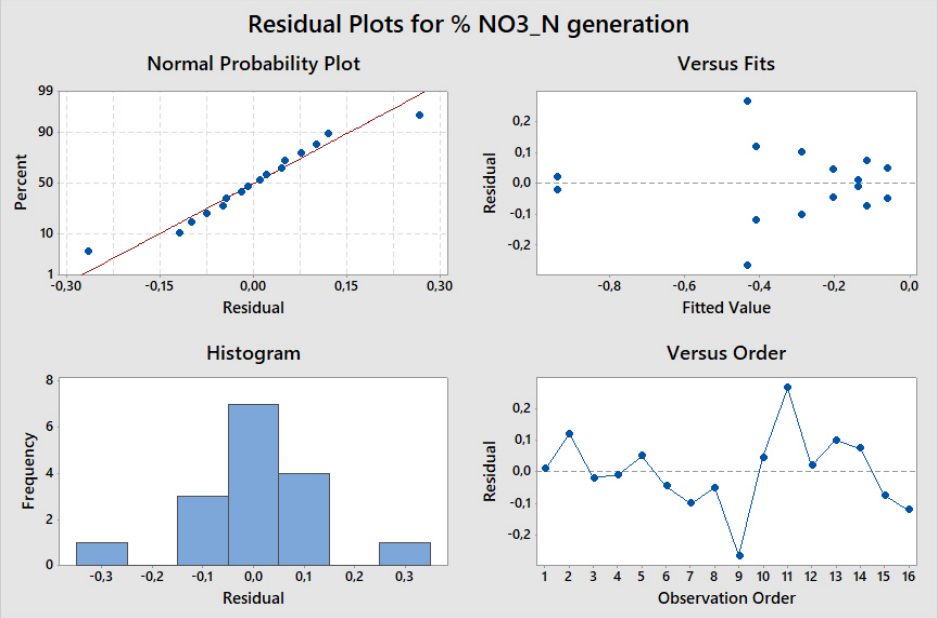

Figure C.6.: Residuals for $NO_3 - N$ removal.

D. Chromatogram THMs

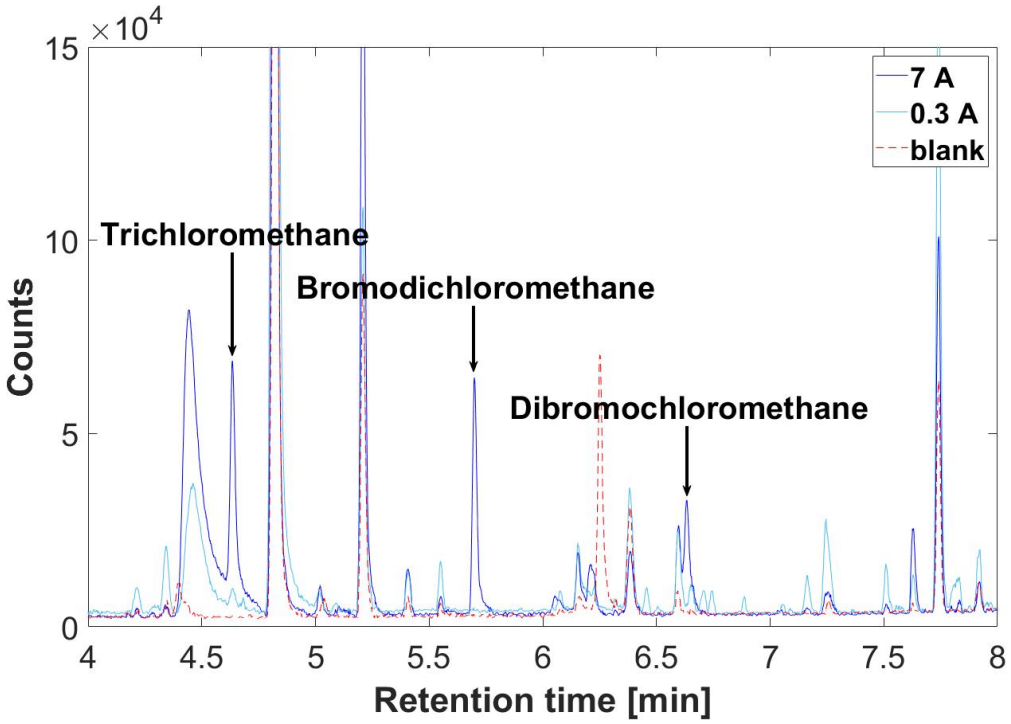

Figure D.1.: Chromatogram detecting THMs for random samples taken during EO of landfill lechate at 20 °C and pH 5 for 7 A and 320 mA.

Pauline Zimmermann

Electrochemical Oxidation of Landfill Leachate on Boron-Doped Diamond Anodes

NTNU
Norwegian University of
Science and Technology

University of Stuttgart
Germany